(2)

EFFECTS OF AEROELASTIC TAILORING ON ANISOTROPIC COMPOSITE MATERIAL BEAM MODELS OF HELICOPTER BLADES

A Thesis

Presented to

the faculty of the School of Engineering and Applied Science

University of Virginia

In Partial Fulfillment

of the requirements for the Degree

Master of Science (Mechanical and Aerospace Engineering)

by

Patrick Graham Forrester

May 1989

AD-A213478

SECURITY CLASSIFICATION OF THIS PAGE

REPORT DOCUMENTATION PAGE

Form Approved OMB No. 0704-0188

1a. REPORT SECURITY CLASSIFICATION: Unclassified	1b. RESTRICTIVE MARKINGS
2a. SECURITY CLASSIFICATION AUTHORITY	3. DISTRIBUTION/AVAILABILITY OF REPORT: Unlimited/May 1989
2b. DECLASSIFICATION/DOWNGRADING SCHEDULE	
4. PERFORMING ORGANIZATION REPORT NUMBER(S)	5. MONITORING ORGANIZATION REPORT NUMBER(S)
6a. NAME OF PERFORMING ORGANIZATION / 6b. OFFICE SYMBOL (If applicable)	7a. NAME OF MONITORING ORGANIZATION
6c. ADDRESS (City, State, and ZIP Code)	7b. ADDRESS (City, State, and ZIP Code)
8a. NAME OF FUNDING/SPONSORING ORGANIZATION / 8b. OFFICE SYMBOL (If applicable)	9. PROCUREMENT INSTRUMENT IDENTIFICATION NUMBER
8c. ADDRESS (City, State, and ZIP Code)	10. SOURCE OF FUNDING NUMBERS: PROGRAM ELEMENT NO. / PROJECT NO. / TASK NO. / WORK UNIT ACCESSION NO.

11. TITLE (Include Security Classification): Effects of Aeroelastic Tailoring on Anisotropic Composite Material Beam Models of Helicopter Blades UNCLASSIFIED

12. PERSONAL AUTHOR(S): Patrick Graham Forrester

13a. TYPE OF REPORT	13b. TIME COVERED	14. DATE OF REPORT (Year, Month, Day)	15. PAGE COUNT
MS Thesis	FROM _____ TO _____	89/05	165

16. SUPPLEMENTARY NOTATION: Prepared as partial degree requirement at the University of Virginia for a Master of Science Degree in Aerospace Engineering.

17. COSATI CODES			18. SUBJECT TERMS (Continue on reverse if necessary and identify by block number)
FIELD	GROUP	SUB-GROUP	Aeroelastic Tailoring Composite Materials Helicopter Blades

19. ABSTRACT (Continue on reverse if necessary and identify by block number)

The role of composite materials in modern helicopter blade design has become most important during recent years. By exploiting the directional stiffness properties of these cmposites, favorable torsion modes or "twisting" can be achieved. The capability to apply this potential as a design parameter is generally known as aeroelastic tailoring. The bending-torsional coupling of static, hingeless composite rotor blades is investigated using finite element theory. The hingeless blade is treated as a single cell laminated shell beam. Each laminate is composed of different lay-ups of graphite-epoxy composite plies and is categorized as isotropic or anisotropic based upon this lay-up. A systematic study is made to identify the effects of ply orientation and lamina thickness on blade section properties. The results of this study are used to solve the beam equations for composite materials. First, the beam is modeled and the fiber orientation and thickness variations are selected. This is done using PATRAN by PDA Engineering as both a solid modeler and as a pre-processor. The model then undergoes finite element analysis and post-processing using ANSYS by Swanson Analysis Systems Inc.

20. DISTRIBUTION/AVAILABILITY OF ABSTRACT	21. ABSTRACT SECURITY CLASSIFICATION
☒ UNCLASSIFIED/UNLIMITED ☐ SAME AS RPT. ☐ DTIC USERS	UNCLASSIFIED

22a. NAME OF RESPONSIBLE INDIVIDUAL	22b. TELEPHONE (Include Area Code)	22c. OFFICE SYMBOL
Captain Patrick Graham Forrester	(804) 978-3601	N/A

DD Form 1473, JUN 86 — Previous editions are obsolete. — SECURITY CLASSIFICATION OF THIS PAGE

(2)

APPROVAL SHEET

This thesis is submitted in partial fulfillment of the

requirements for the degree of

Master of Science (Mechanical and Aerospace Engineering)

Patrick G. Forester
AUTHOR

This thesis has been read and approved by the examining Committee:

John Kennett Haviland
Thesis Advisor

Edgar J. Hunter

Frank Jay Lane

Accepted for the School of Engineering and Applied Science:

Edgar A. Mantle, Jr.
Dean, School of Engineering and
Applied Science

May 1989

Abstract

The role of composite materials in modern helicopter blade design has become most important during recent years. By exploiting the directional stiffness properties of these composites, favorable torsion modes or "twisting" can be achieved. The capability to apply this potential as a design parameter is generally known as aeroelastic tailoring.

The bending-torsional coupling of static, hingeless composite rotor blades is investigated using finite element theory. The hingeless blade is treated as a single cell laminated shell beam. Each laminate is composed of different lay-ups of graphite-epoxy composite plies and is categorized as isotropic or anisotropic based upon this lay-up.

A systematic study is made to identify the effects of ply orientation and lamina thickness on blade section properties. The results of this study are used to solve the beam equations for composite materials. First, the beam is modeled and the fiber orientation and thickness variations are selected. This is done using **PATRAN®** by PDA Engineering as both a solid modeler and as a pre-processor. The model then undergoes finite element analysis and post-processing using **ANSYS®** version *4.3A* by Swanson Analysis Systems Inc. The results are displayed both graphically and in numerical form. It is concluded that this is an effective method of tailoring and analysis.

Acknowledgements

The author is indebted to Dr. J. K. Haviland for his guidance and direction throughout the entirety of this thesis project. The author is also greatly indebted to Dr. E. J. Gunter and Dr. M. J. Pindera. Although they were extremely busy, they always found time to answer questions and help solve problems. Dr. Gunter helped immensely on the problems that developed with the ANSYS program and Dr. Pindera helped continuously with the composite modeling.

Special appreciation is extended to several other individuals for their help, support and friendship. Thanks to Miss Cheryl A. Rose for her help with laminate analysis. Thanks to Mr. Brett Averick for his help with the computer programming and Mr. David Baldwin for his help with the equation formulation. Thanks to Mr. Inderdeep Huja and Mr. Ed Williams for all their help on the computers. Also a special thanks to Mr. Rohn England for his guidance, encouragement and friendship throughout all of my graduate work.

Last, but certainly not least, thank you to Diana, Patrick and Andrew for your love and understanding during the long hours and uncertain times which came along with this degree.

Table of Contents

Table of Contents (Continued)

List of Figures

List of Figures (Continued)

List of Figures (Continued)

List of Figures (Continued)

List of Tables

List of Symbols

A	Cross Sectional Area
A_{ij}	Extensional Stiffness Matrix
A_m	Median Area
B_{ij}	Extensional Bending Matrix
b	Beam Width
C_{ij}	Stiffness Matrix
D_{ij}	Bending Stiffness Matrix
D^*_{ij}	Inverse Bending Stiffness Matrix
E_x	Young's Modulus in x-direction
E^b_x	Effective Bending Modulus
E^k_l	Modulus of kth Layer
G	Shear Modulus
H	One Half Laminate Thickness
I_y	Moment of Inertia About y-axis
I_p	Polar Moment of Inertia
J	Torsion Constant
K	Lamina Thickness
k	Lamina Number
L	Beam Length
L_m	Median Line
M	Bending Moment
M_x	In-Plane Moment Resultant
N	Number of Layers

List of Symbols (Continued)

N_x	In-Plane Force Resultant
O'	Center of Curvature
P	Force (Axial or Normal)
Q_{ij}	Reduced Stiffness Matrix
$\overline{Q}_{ij}$	Reduced Stiffness Matrix For Rotation
r	Radius
S_{ij}	Compliance Matrix
$\overline{S}$	Compliance Matrix For Rotation
s	Element Length
T_i	Transformation Matrix
T_x	Torsional Force
t	Laminate thickness
u,v,w	Displacements
x,y,z	Coordinate Axes
Z_i	Distance From Midplane to *ith* Layer
α	Thermal Expansion
γ	Rotation About x-axis
γ_{12}	Shear Strain
γ°	Midplane Shear Strain
δ	Displacement
ε_j	Strain Vector
ε_x	Normal Strain
ε'	Strain in Rotated System
ε°	Midplane Normal Strain

List of Symbols (Continued)

ζ	Distance From Leading Edge to Shear Center
θ	Angle of Ply Rotation
κ	Curvature
ν	Poisson's Ratio
π	Pi (3.14159)
ρ	Radius of Curvature
σ_x	Normal Stress
σ_i	Stress Vector
σ'	Stress in Rotated System
Σ	Summation
τ_{12}	Shear Stress
ϕ	Rotation About y-axis
ψ	Rotation About z-axis
Ω	Rotational Velocity

Chapter One

Introduction

Aeroelastic tailoring is defined as "the incorporation of directional stiffness into an aircraft structural design to control aeroelastic deformation, static or dynamic, in such a fashion as to affect the aerodynamic and structural performance of that aircraft in a beneficial way" [1]. In recent years, numerous efforts have dealt with the effects of anisotropic design on the aeroelasticity or deformation coupling of fixed and swept wing aircraft, but very little has been done to research its effects on rotorcraft and specifically rotorsystems. Helicopter rotor blades operate in an aeroelastic environment consisting of inertial, aerodynamic and elastic loadings. This environment is ideal for anisotropic design and improvement and provides for the creative use of directional stiffness characteristics.

Composite material systems are now the primary materials for helicopter rotor system applications. Currently, attention is being focused on the use of composites for designing rotor blades in which the elastic coupling associated with unbalanced ply layup is employed to enhance the dynamic and aerodynamic characteristics. The type of rotor and its control determine largely the aeroelastic behavior of a helicopter. Of special interest nowadays are hingeless and bearingless rotor systems. The LHX helicopter project, with its bearingless rotor designs, is a prime example.

There are a number of aeroelastic phenomena associated with the design of helicopters. The dynamic stability and response characteristics of rotary-wing aircraft are

dependent on parameters which have to be defined in the preliminary design phase. In order to achieve maximum structural efficiency through aeroelastic tailoring, it is necessary to use composite laminates with different ply angles. As a result, composite beams will exhibit coupling among extensional stiffness, bending stiffness and torsional stiffness. For example, bending-torsional stiffness coupling is necessary for pitch-flap stability of rotor blades, and extensional-torsional stiffness coupling is desirable to change the linear twist distribution. Even isotropic beams with pretwist will exhibit coupling between extension and torsion [2].

Aeroelastic tailoring of a composite structure involves a design process in which the materials and dimensions are selected to yield specific torsional characteristics. Due to the directional nature of the composite materials, it is possible to construct blades with different ply orientations and laminae thicknesses. These laminations can be either symmetric or asymmetric, where "symmetric" means that a layer of material at some distance above a structural midsurface reference location has the identical ply thickness, angular orientation, and material properties as that of a lamina at an identical distance below the midsurface [1]. If the fibers are placed off-axis in the upper and lower portions of the blade, a twist should be induced when exerting a non-torsional force. This provides a potential for improving the performance of a lifting surface through aeroelastic tailoring of the primary load-bearing structure. The design of such advanced structures requires simple and reliable analytical tools which can take into consideration the directional nature of these materials.

The analysis of helicopter rotor blades has traditionally depended on classical beam or shell theory. This is inadequate for the dynamic characteristics of orthotropic and

anisotropically laminated shells which can be thought of as rudimentary rotor blade structures. While analyses based on beam-like representations are generally feasible methods of structural analyses for many composite rotor blade structures, the design of advanced rotor blades will often require a detailed shell-finite-element representation [3].

Finite element analysis has become an established and widely used tool in the design of rotorcraft airframes. Recently, however, research efforts have indicated a growing interest in applying these analysis techniques in composite rotor blade structural analysis.

Most of the previous work in this area involves the feasibility of modeling composite helicopter blades using finite element analysis and the treatment of the flexbeam or spar as the model base [2-5]. From this point investigators have attempted to determine the structural properties by theoretical and experimental methods. Although some work has been done on composite rotor design parameters that affect aeroelastic stability and response, it mainly centers around arbitrary cross-sectional warping and vibration response. It is uncertain if anyone has attempted to vary the lamination sequence and angular orientation to manipulate the classical beam equations.

In the present research, a composite rotor blade is modeled as a hollow beam with end caps. It can be shown that the composite rotor blade concept offers the chance to accomodate aeroelastic coupling effects which may improve or deteriorate the response behavior of the helicopter. Using the commercial package **PATRAN®**, a finite element model of the constructed blade is created and an evaluation of the blade sectional properties is conducted. Four individual loading conditions are applied to eight distinct blade laminations to achieve the desired reactions. The results of the analysis using **ANSYS®**

are applied to solve the classical beam equations.

Following a background chapter on the history of aeroelastic tailoring and a summary of the work already accomplished in this area, a concise but complete chapter on composite materials which includes lamination theory is provided. This has the advantage of building a firm basis for the later development of the model and the significance of the numerical results. The classical beam equations are then developed in Chapter 4 and their validity for use with composite material beams is demonstrated through laminate analysis theory. Chapter 5 involves the modeling process with the ensuing chapters reporting the results and conclusions. The readers may find the appendices useful for similar work involving **PATRAN®** and **ANSYS®**. The FORTRAN code for laminate analysis is also included as an appendix.

One aspect of this research which the author found both frustrating and enriching was the interfacing of the pre- and post-processors and the lessons learned when dealing with large commercial packages whose companies are clearly competitors.

Chapter Two

Background

M.H. Shirk, T.J. Hertz and T.A. Weisshaar describe the historical evolution of aeroelastic tailoring and cite significant examples of the early use of tailoring principles [6]. These consider primarily the well-known effects of the bending of a sweptback wing and the effective angles of attack which it induces. In his review paper, *"The First Fifty Years of Aeroelasticity"* [7], A. R. Collar mentions the application of this bending induced load relief principle to an unswept wing, where a downward bending would cause increased lift.

In a recent review article [8], H. Ashley and his co-authors note that, at the inception of manned powered flight, lifting surface flexibility was used to generate favorable aerodynamic loads. The biplane structural truss of the original Wright Flyer exhibited wing torsional flexibility which allowed a control cradle, operated by the prone pilot's hip movements, to provide differential twist to the biplane wings. The result was a rolling moment. While the use of structural deformability was quickly replaced by mechanical devices, the Wright Flyer provided what might be regarded as the world's first aeroservoelastic system.

Closer to home, Professor Max Munk, while at the Catholic University of America in Washington, D.C., used aeroelastic deformation to provide favorable propeller performance. This design, patented in 1949, was entitled *"Propeller Containing Diagonally*

Disposed Fibr ·us Material". The fibrous material was wood. The grain of the wood was oriented to provide spanwise anisotropy such that bending due to lift caused the propeller to twist nose-down in such a way that some lift, in this case propeller thrust, was decreased at high speeds. As a result, an automatic, passive, favorable pitch change in the propeller was achieved without the aid of a mechanical device. Wind tunnel tests verified predictions of increased propeller performance at high speed as a result of this tailored grain orientation [9].

Although ingenious, these first designs had minor repercussions in the aircraft industry. This was primarily due to a lack of elastic materials other than wood and a lack of understanding of the true need to incorporate this flexibility in the designs. However, this was a step toward its use for helicopter blade design and these problems would disappear with the introduction of composite materials.

In 1947, Cornell Aero Lab built what were probably the first composite rotor blades which used some fiberglass reinforced plastic (FRP) construction. These blades had wood spars with FRP skins. They flew on a Sikorsky R-5. In 1953, Glenview Metal Products built a GMP-2 Flyride helicopter with a main rotor blade of laminated spruce forward of the 30% chord and FRP skins on a balsa wood core aft of the 30% chord. In 1956, Prewitt Aircraft Company built three sets of research rotors for the Piasecki HUP-2 aircraft. One set was made of stainless steel, one of titanium, and one of FRP. The composite blade had a wood spar. The Gyrodine XRON-1 introduced in 1956 had all-fiberglass blades on some later versions. Parsons also built two different experimental blades for the H-21 from stainless steel and FRP in the same period. One of the composite blades failed in the whirl test stand and was never flight tested [10].

The early 1960's saw the introduction of several composite rotor blade designs. Among these were the Kaman H43-B blade of 1960 which had a wood core with FRP skins on the afterbodies. The Bolkow BO-103 helicopter which first flew in 1961 had a single main rotor blade made of FRP. The Boeing Vertol CH-47 blade of 1961 consisted of a steel D spar with aluminum ribs and FRP skins. In 1962, Kaman flew an all-FRP blade on the HH-43B helicopter [10].

It was the year 1968 that marked the beginning of the all-boron Advanced Geometry Blade program for the Boeing Vertol CH-47. An all-FRP version of this blade was designed and built in the same time period. Both of these blades were flight tested in the early 1970's. By this time, the future of helicopter rotor blades was clearly pointed in the direction of all-composite construction and would progress to the advanced graphite-epoxy blades of the 1980's [10].

By 1982, at least 50 different all-composite main rotor blades had been designed. A' out 25 of those had been flight tested and over 15 had progressed to limited or full production status. The US Army had approximately 25 different composite rotor blade programs underway at this time of which six had reached flight status. These six were [10]:

1) the CH-47 Advanced Geometry Blade (1972)
2) the AH-1 Multi Tubular Spar Blade (1975)
3) the CH-47D Composite Blade (1978)
4) the AH-1S Improved Main Rotor Blade (1980)
5) the AH-64 Prototype Blade (1981)
6) the BO-105 Bearingless Main Rotor (1981)

Helicopters are usually classified according to the mechanical arrangement of the hub in order to accommodate the blade flap and lead-lag motion and according to the blade and hub bending stiffness. The most widespread helicopter configuration uses a single main rotor and a small tail rotor. During the last two decades, the hingeless rotor concept and its successor, the bearingless rotor, have found continuosly growing interest among helicopter manufacturers and research organization.

With the evolution of advanced composites, the feasibility of designing rotor systems for high speed, demanding maneuver envelopes, and high aircraft gross weights had become a reality. The desire to tailor the elastic qualities of these blades was soon to follow.

Chapter Three

Composites

Advanced fiber-reinforced composite materials combine vastly superior specific stiffness and strength characteristics (i.e. stiffness/unit weight and strength/unit length) with reduced weight and increased fatigue life. These improved fatigue characteristics are very significant to helicopter design because fatigue is probably the primary cause of rotor blade failure. Composites make possible designs with fewer parts and improved maintainability. In terms of manufacturing, it is possible to achieve more general aerodynamic shapes such as flapwise variation in planform, section and thickness [11]. Composite materials are ideal for structural applications where high strength-to-weight and stiffness-to-weight ratios are required. The adjective "advanced" in advanced fiber-reinforced composite materials is used to distinguish composites with new ultrahigh strength and stiffness fibers such as boron and graphite from some of the more familiar fibers such as glass.

To understand fully the significance of composite materials, it is necessary to start with the very basic element or building block which is the lamina. A lamina is an assemblage of fibers oriented in the same direction in a supporting matrix. The fibers supply most of the strength and stiffness characteristics and the matrix holds these fibers in the desired position. Advanced composites are made by laminating individual laminae in specific directions in order to obtain the desired properties for the given structural com-

ponent. Therefore, the knowledge of the mechanical behavior of a lamina is essential to the understanding of laminated composites.

There are several assumptions which are made about a lamina and its components:

(a) The fibers are homogeneous, linearly elastic and isotropic. They are equally spaced and perfectly aligned.

(b) The matrix is homogeneous, linearly elastic and isotropic.

These assumptions then allow us to say that a lamina is macroscopically homogeneous, linearly elastic, macroscopically orthotropic or transversely isotropic and initially stress free.

The directional properties of the lamina are the key to the limitless uses of composite materials. In the fiber direction, the lamina is very stiff and strong while in the direction which is transverse to the fibers, the lamina is compliant and weak. The difference in the strength in these directions is usually at least one order of magnitude; it is not uncommon for the lamina to be 100 times stronger in the fiber direction. Figure 3.1 [12] helps to illustrate the directional properties of a lamina. The longitudinal direction is represented by $\theta = 0°$ and the transverse direction by $\theta = 90°$.

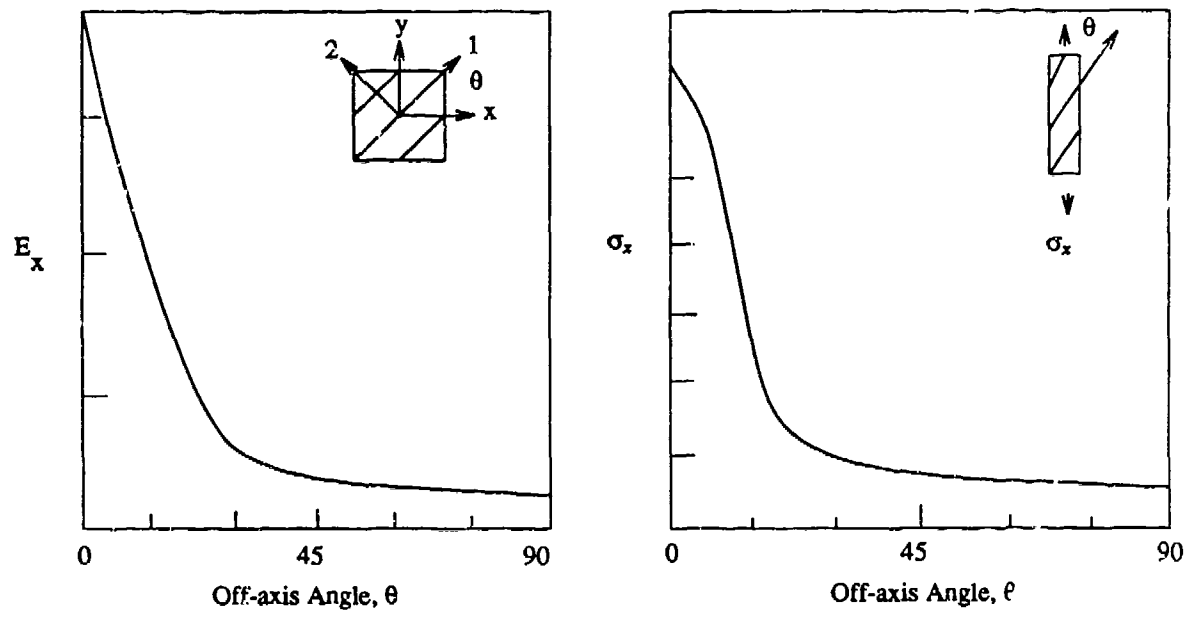

FIGURE 3.1. Directional Properties of Lamina

The description of the mechanical behavior of a composite lamina is based on stress-strain relations referred to as Hooke's Law. To model the stress-strain response of a lamina, we use the generalized version for an anisotropic body. These relations have two commonly accepted manners of expression; compliances and stiffnesses as coefficients of the stress-strain relations. Jones [12] provides a description of these relations. The generalized Hooke's law relating stresses to strains can be written in contracted notation as

$$\sigma_i = C_{ij}\varepsilon_j \qquad i,j = 1,...,6$$

where σ_i are the stress components, C_{ij} is the stiffness matrix, and ε_j are the strain components. The stiffness and compliance components are often referred to as elastic constants. Both sets of components can be represented by the engineering constants

E_i, ν_{ij}, G_{ij} which are Young's moduli, Poisson's ratio, and the shear moduli respectively. The engineering constants are particularly helpful in describing lamina behavior. These relations reduce to *21* independent constants and can be represented by Equation (3.1). These relations represent an *anisotropic* material since there are no planes of symmetry for the material properties. This is the case in which none of the axes of the lamina line up with the principal axes of material symmetry.

$$\begin{Bmatrix} \sigma_1 \\ \sigma_2 \\ \sigma_3 \\ \tau_{23} \\ \tau_{31} \\ \tau_{12} \end{Bmatrix} = \begin{bmatrix} C_{11} & C_{12} & C_{13} & C_{14} & C_{15} & C_{16} \\ C_{12} & C_{22} & C_{23} & C_{24} & C_{25} & C_{26} \\ C_{13} & C_{23} & C_{23} & C_{34} & C_{35} & C_{36} \\ C_{14} & C_{24} & C_{34} & C_{44} & C_{45} & C_{46} \\ C_{15} & C_{25} & C_{35} & C_{45} & C_{55} & C_{56} \\ C_{16} & C_{26} & C_{36} & C_{46} & C_{56} & C_{66} \end{bmatrix} \begin{Bmatrix} \varepsilon_1 \\ \varepsilon_2 \\ \varepsilon_3 \\ \gamma_{23} \\ \gamma_{31} \\ \gamma_{12} \end{Bmatrix} \tag{3.1}$$

If there is one plane of material property symmetry, the stress-strain relations reduce to Equation (3.2) which is termed *monoclinic*. This relationship represents a lamina in a coordinate system which is rotated in its plane.

$$\begin{Bmatrix} \sigma_1 \\ \sigma_2 \\ \sigma_3 \\ \tau_{23} \\ \tau_{31} \\ \tau_{12} \end{Bmatrix} = \begin{bmatrix} C_{11} & C_{12} & C_{13} & 0 & 0 & C_{16} \\ C_{12} & C_{22} & C_{23} & 0 & 0 & C_{26} \\ C_{13} & C_{23} & C_{33} & 0 & 0 & C_{36} \\ 0 & 0 & 0 & C_{44} & C_{45} & 0 \\ 0 & 0 & 0 & C_{45} & C_{55} & 0 \\ C_{16} & C_{26} & C_{36} & 0 & 0 & C_{66} \end{bmatrix} \begin{Bmatrix} \varepsilon_1 \\ \varepsilon_2 \\ \varepsilon_3 \\ \gamma_{23} \\ \gamma_{31} \\ \gamma_{12} \end{Bmatrix} \tag{3.2}$$

If there are two orthogonal planes of material property symmetry, the stress-strain relations are shown in Equation (3.3) and are said to define an *orthotropic* material. Note that there is no interaction between normal stresses σ_1, σ_2, σ_3 and shearing strains γ_{23}, γ_{31}, γ_{12} as in anisotropic materials.

$$\begin{Bmatrix} \sigma_1 \\ \sigma_2 \\ \sigma_3 \\ \tau_{23} \\ \tau_{31} \\ \tau_{12} \end{Bmatrix} = \begin{bmatrix} C_{11} & C_{12} & C_{13} & 0 & 0 & 0 \\ C_{12} & C_{22} & C_{23} & 0 & 0 & 0 \\ C_{13} & C_{23} & C_{33} & 0 & 0 & 0 \\ 0 & 0 & 0 & C_{44} & 0 & 0 \\ 0 & 0 & 0 & 0 & C_{55} & 0 \\ 0 & 0 & 0 & 0 & 0 & C_{66} \end{bmatrix} \begin{Bmatrix} \varepsilon_1 \\ \varepsilon_2 \\ \varepsilon_3 \\ \gamma_{23} \\ \gamma_{31} \\ \gamma_{12} \end{Bmatrix} \tag{3.3}$$

If at every point of a material, there is one plane in which the mechanical properties are equal in all directions, then the material is termed *transversely isotropic* and has the relations shown in Equation (3.4). This relationship expresses the response of a lamina in the principal material coordinate system (PMCS). The PMCS is the coordinate system in which the axes are aligned with respect to the structural material symmetry.

$$\begin{Bmatrix} \sigma_1 \\ \sigma_2 \\ \sigma_3 \\ \tau_{23} \\ \tau_{31} \\ \tau_{12} \end{Bmatrix} = \begin{bmatrix} C_{11} & C_{12} & C_{13} & 0 & 0 & 0 \\ C_{12} & C_{22} & C_{23} & 0 & 0 & 0 \\ C_{13} & C_{23} & C_{22} & 0 & 0 & 0 \\ 0 & 0 & 0 & 2(C_{22}-C_{23}) & 0 & 0 \\ 0 & 0 & 0 & 0 & C_{66} & 0 \\ 0 & 0 & 0 & 0 & 0 & C_{66} \end{bmatrix} \begin{Bmatrix} \varepsilon_1 \\ \varepsilon_2 \\ \varepsilon_3 \\ \gamma_{23} \\ \gamma_{31} \\ \gamma_{12} \end{Bmatrix} \tag{3.4}$$

If there are an infinite number of planes of material property symmetry, then the material is isotropic with only *two* independent constants and Equation (3.4) becomes:

$$\begin{Bmatrix} \sigma_1 \\ \sigma_2 \\ \sigma_3 \\ \tau_{23} \\ \tau_{31} \\ \tau_{12} \end{Bmatrix} = \begin{bmatrix} C_{11} & C_{12} & C_{13} & 0 & 0 & 0 \\ C_{12} & C_{22} & C_{23} & 0 & 0 & 0 \\ C_{13} & C_{23} & C_{33} & 0 & 0 & 0 \\ 0 & 0 & 0 & 2(C_{11}-C_{12}) & 0 & 0 \\ 0 & 0 & 0 & 0 & 2(C_{11}-C_{12}) & 0 \\ 0 & 0 & 0 & 0 & 0 & 2(C_{11}-C_{12}) \end{bmatrix} \begin{Bmatrix} \varepsilon_1 \\ \varepsilon_2 \\ \varepsilon_3 \\ \gamma_{23} \\ \gamma_{31} \\ \gamma_{12} \end{Bmatrix} \tag{3.5}$$

For plane stress in the plane of the lamina, Equation (3.4) can be rewritten in terms of the reduced stiffness matrix $[Q]$. Setting σ_3, τ_{23}, and τ_{31} equal to zero, which implies that ε_3, γ_{23}, and γ_{31} are zero also, leads to the following relationship between the inplane stress components and the inplane strain components:

$$\begin{Bmatrix} \sigma_1 \\ \sigma_2 \\ \tau_{12} \end{Bmatrix} = \begin{bmatrix} Q_{11} & Q_{12} & 0 \\ Q_{12} & Q_{22} & 0 \\ 0 & 0 & Q_{66} \end{bmatrix} \begin{Bmatrix} \varepsilon_1 \\ \varepsilon_2 \\ \gamma_{12} \end{Bmatrix} \tag{3.6}$$

Where the elements of the reduced stiffness matrix $[Q]$ are given in terms of the elements of the 3–D stiffness matrix $[C]$.

Equation 3.6 defines inplane stresses and strains in the principal material coordinate system of an orthotropic or transveresly isotropic material. However, the principal directions of orthotropy often do not coincide with coordinate directions that are geometrically natural to the structure elements. Therefore, a coordinate transformation is necessary in order to relate stresses and strains in a coordinate system not aligned with the PMCS. Suppose that a layer is rotated through an angle θ about the z axis as in Figure 3.2. We can express its constitutive equations in the rotated, that is x–y coordinate system by proceeding as follows.

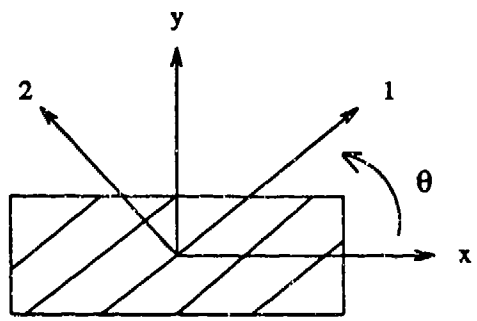

FIGURE 3.2. Rotation of Coordinate System

If we let

$$c = \cos\theta, \quad s = \sin\theta$$

then the inplane stress and strain components in the principal material coordinate system can be related to the inplane stress and strain components in the rotated coordinate system through the transformation matrices $[T_1]$ and $[T_2]$ defined below:

$$[T_1] = \begin{bmatrix} c^2 & s^2 & 2cs \\ s^2 & c^2 & -2cs \\ -cs & cs & c^2-s^2 \end{bmatrix} \tag{3.7}$$

and

$$[T_2] = \begin{bmatrix} c^2 & s^2 & cs \\ s^2 & c^2 & -cs \\ -2cs & 2cs & c^2-s^2 \end{bmatrix} \tag{3.8}$$

Using the above relations in Equation (3.6) allows us to relate the inplane stresses to the strains in the rotated coordinate system in the following fashion:

$$\underset{\sim}{\sigma}' = [\bar{Q}]\,\underset{\sim}{\varepsilon}' \quad or \quad \underset{\sim}{\varepsilon}' = [\bar{S}]\,\underset{\sim}{\sigma}' \tag{3.9}$$

where

$$[\bar{Q}] = [T_1]^{-1}\,[Q]\,[T_2] \tag{3.10}$$

and

$$[\bar{S}] = [T_2]^{-1}\,[S]\,[T_1] \tag{3.11}$$

With the other benefits of composite materials, comes the ability to design or prescribe laminate geometry. As mentioned previously, laminated composites consist of differently oriented layers or laminae that are bonded together.

It is important to understand the motivation for laminating the plies discussed above. Because each individual ply has very directional properties (Figure 3.1) we laminate to combine the best aspects of the constituent layers in order to achieve a more useful material. This is done by tailoring the directional dependence of strength and stiffness of a material to match the loading environment of the structural element. For example, a structure that has a dominant uniaxial loading in the fiber direction, such as the centrifugal force on a rotor blade, would need a predominantly unidirectional composite. For more general loa tuations, the principal material directions are oriented to

produce a structural element capable of resisting load in several directions. Figure 3.3 provides an example of layering with different ply orientations.

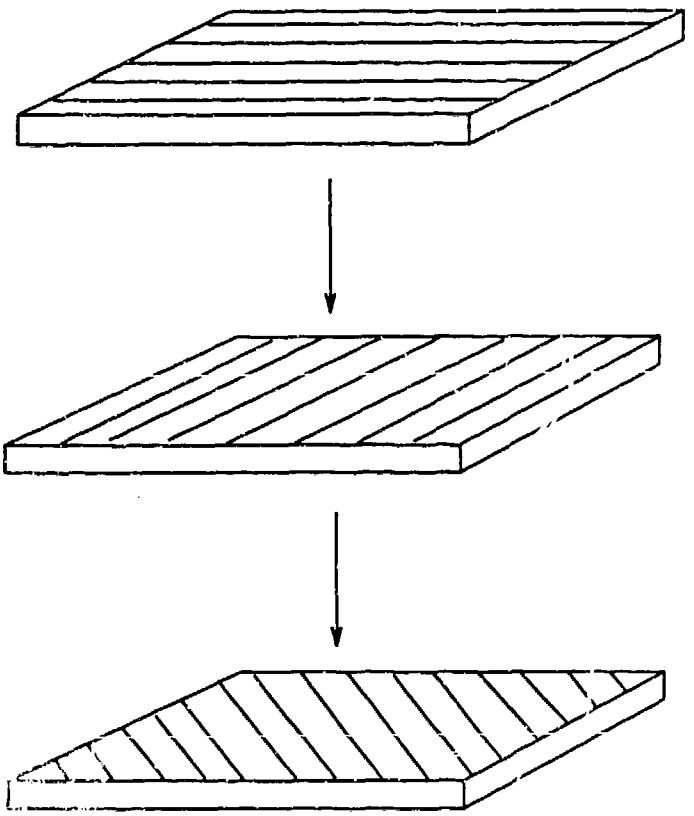

FIGURE 3.3. Laminate Construction

Laminated composites are generally strong and stiff in the plane of lamination and weak and flexible in the transverse direction. This stiffness is obtained from the proper-

ties of the constituent laminae. Laminated plates are one of the simplest and most widespread practical applications of composite laminates. They will be used in this work as they are uniquely suited to its objective. Therefore, a summary of lamination theory is provided.

Lamination theory allows us to predict the ensuing properties of a laminated plate or structure when the properties, dimensions and stacking sequence of individual plies are specified. Figure 3.4 [12] displays the geometry of a layered laminate.

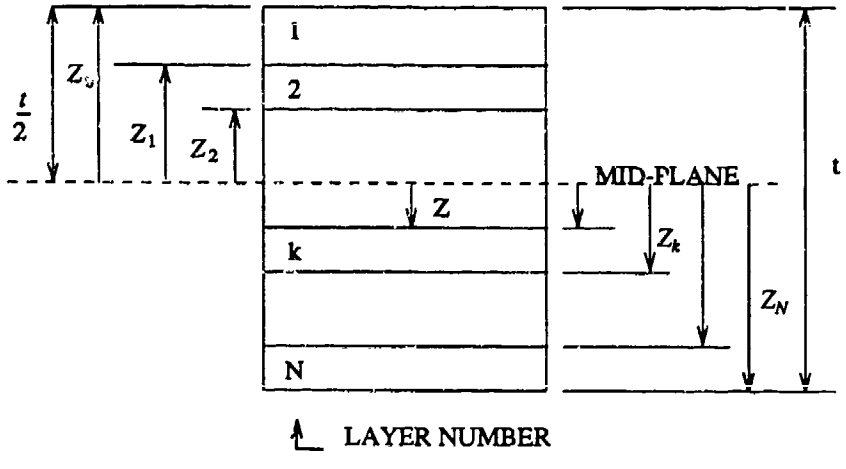

FIGURE 3.4. Geometry of an N-layered Laminate

There are two static parameters which are used to describe the response of a laminate. The first is in-plane force resultants defined as:

$$\begin{Bmatrix} N_x \\ N_y \\ N_{xy} \end{Bmatrix} = \int_{-H}^{H} \begin{Bmatrix} \sigma_x \\ \sigma_y \\ \tau_{xy} \end{Bmatrix} dz \tag{3.12}$$

The second is the in-plane moment resultants defined as:

$$\begin{Bmatrix} M_x \\ M_y \\ M_{xy} \end{Bmatrix} = \int_{-H}^{H} \begin{Bmatrix} \sigma_x \\ \sigma_y \\ \tau_{xy} \end{Bmatrix} z dz \tag{3.13}$$

The kinematic parameters which are used to describe the response of a laminate are based on the following assumptions:

(a) The laminate consists of perfectly bonded laminae, each of which are in a state of plane stress.

$$\begin{Bmatrix} \sigma_x \\ \sigma_y \\ \tau_{xy} \end{Bmatrix} = \begin{bmatrix} \bar{Q}_{11} & \bar{Q}_{12} & \bar{Q}_{16} \\ - & \bar{Q}_{22} & \bar{Q}_{26} \\ - & - & \bar{Q}_{66} \end{bmatrix} \begin{Bmatrix} \varepsilon_x \\ \varepsilon_y \\ \gamma_{xy} \end{Bmatrix} \tag{3.14}$$

(b) The normals to the midplane remain straight and normal to the deformed midplane.

(c) The normals do not change in length.

The last two assumptions are a consequence of the Kirchoff-Love hypothesis. This yields:

$$\frac{\partial u}{\partial z} = -\frac{\partial w}{\partial x} \tag{3.15}$$

and

$$\frac{\partial v}{\partial z} = -\frac{\partial w}{\partial y} \tag{3.16}$$

Also, by expressing the inplane displacement components in the following fashion:

$$u(x,y,z) = u^{\circ}(x,y) + zf(x,y) \tag{3.17}$$

and

$$v(x,y,z) = v^{\circ}(x,y) + zg(x,y) \tag{3.18}$$

which is consistent with the Kirchoff-Love hypothesis, it can be shown that the in-plane strains are a function of the in-plane strains of the midplane and the curvatures ($\underset{\sim}{\kappa}$) of the midplane:

$$\begin{Bmatrix} \varepsilon_x \\ \varepsilon_y \\ \gamma_{xy} \end{Bmatrix} = \begin{Bmatrix} \varepsilon^{\circ}_x \\ \varepsilon^{\circ}_y \\ \gamma^{\circ}_{xy} \end{Bmatrix} + z \begin{Bmatrix} \kappa_x \\ \kappa_y \\ \kappa_{xy} \end{Bmatrix} \tag{3.19}$$

where

$$\begin{Bmatrix} \kappa_x \\ \kappa_y \\ \kappa_{xy} \end{Bmatrix} = -\begin{Bmatrix} \dfrac{\partial^2 w}{\partial x^2} \\ \dfrac{\partial^2 w}{\partial y^2} \\ \dfrac{\partial^2 w}{\partial x \partial y} \end{Bmatrix} \tag{3.20}$$

Combining this equation with Equation (3.14) yields:

$$\underset{\sim}{\sigma}^{k}_{x-y} = \underline{\underline{\bar{Q}}}^{k}\, \underset{\sim}{\varepsilon}^{\circ} + z\underset{\sim}{\kappa} \tag{3.21}$$

By integrating the equation for in-plane forces with this equation, we arrive at the following result:

$$\underset{\sim}{N} = \underline{\underline{A}}\,\underset{\sim}{\varepsilon^{\circ}} + \underline{\underline{B}}\,\underset{\sim}{\kappa} \tag{3.22}$$

where $\underline{A}_{ij}$ is the extensional stiffness laminate matrix which is written as:

$$\underline{A}_{ij} = \sum_{k=1}^{N} \bar{Q}_{ij}^{k} (z_k - z_{k-1}) \tag{3.23}$$

and where $\underline{B}_{ij}$ is the extensional bending coupling matrix which is expressed as:

$$\underline{B}_{ij} = \frac{1}{2} \sum_{k=1}^{N} \bar{Q}_{ij}^{k} (z_k^2 - z_{k-1}^2) \tag{3.24}$$

This particular matrix will become zero when a symmetric laminate (see Chapter 1, page 2) is used. By integrating the equation for in-plane moments with equation (1.20) we get:

$$\underset{\sim}{M} = \underline{\underline{B}}\,\underset{\sim}{\varepsilon^{\circ}} + \underline{\underline{D}}\,\underset{\sim}{\kappa} \tag{3.25}$$

where $\underline{D}_{ij}$ is the bending stiffness matrix which is written as:

$$\underline{D}_{ij} = \frac{1}{3} \sum_{k=1}^{N} \bar{Q}_{ij}^{k} (z_k^3 - z_{k-1}^3) \tag{3.26}$$

The bending stiffness matrix is important to this research as it is the factor which causes the torsional motion of the blade. The D_{16} term is the key element of the matrix.

The final results of this procedure are the constitutive equations for laminate analysis theory. They are expressed for all composite material laminates as:

$$\begin{Bmatrix} \underset{\sim}{N} \\ \underset{\sim}{M} \end{Bmatrix} = \begin{bmatrix} \underline{\underline{A}} & \underline{\underline{B}} \\ \underline{\underline{B}} & \underline{\underline{D}} \end{bmatrix} \begin{Bmatrix} \underset{\sim}{\varepsilon^{\circ}} \\ \underset{\sim}{\kappa} \end{Bmatrix} \tag{3.27}$$

Laminates are not without their problems, however, as potentially adverse shearing and normal stresses are introduced between adjacent layers in the vicinity of the free edge. Such stresses may cause delamination. These stresses are out-of-plane or inter-laminar stresses which arise to satisfy equilibrium requirements at the free edge.

Chapter Four

Governing Equations

A thorough understanding of the mechanical behavior of a structure is essential for its effective design. This includes helicopter rotor blades. The use of physical properties of composite materials, as well as numerous theoretical laws and concepts, becomes the basis for this understanding. Mechanics of materials is a branch of applied mechanics that deals with the behavior of bodies subjected to various types of loading. The objective of this particular analysis will be the determination of the deflections and displacements of a simple blade model produced by these loadings. This data will then be applied to the Euler-Bernoulli beam equations to determine the off-diagonal term response to the loading of composite material lamination sequences.

This research will center around only one finite element model, however there will be eight individual blade cases examined. These eight cases are concerned with seven anisotropic composite material lay-ups and one isotropic lay-up. Each of these cases will be subjected to identical loading conditions consisting of four separate loads. They consist of two bending moments, a torsional force and an axial force, and will be described in detail at a later point.

There are certain properties of area which are needed for this beam theory, such as the location of the centroid, the first moment of the area and the second moment of the area or the moment of inertia with respect to each axis.

The *bending axis* of the beam under investigation is the longitudinal axis through which the transverse bending loads must pass in order that the bending of the beam shall not be accompanied by twisting (for isotropic materials). The *shear center* or *center of twist* for any transverse section of the beam is the point of intersection of the bending axis and the plane of the transverse section [13].

The bending axis and the shear center are of special importance in beams having cross sections composed of thin parts which offer large resistance to bending such as in airplane or rotor blade construction.

The bending axis for a beam whose cross section has two axes of symmetry is the longitudinal centroidal axis of the beam and hence the shear center for such a section is also the *centroid* of the section. When conducting experiments, for example, the axial force and constraints must act through this centroid of the cross-sectional area.

Calculation of the moments of inertia (second moments of the area) requires a substantial effort for complex geometry of this type. Using the equation

$$I_y = \iint_A z^2 dA \tag{4.1}$$

and the fact that the blade is symetric about the y axis, we obtain

$$I_y = 2\int \int_{A/2} z^2 dA \tag{4.2}$$

where $z = r\cos\beta$. See Figure 4.1. Substituting for z we obtain

$$I_y = \int\int_{A/2} r^2 \cos^2\beta dA \tag{4.3}$$

Since $dA = dst$ and $ds = rtd\beta$, then

$$I_y = 2\int_0^{\pi} tr^3 \cos^2\beta d\beta \tag{4.4}$$

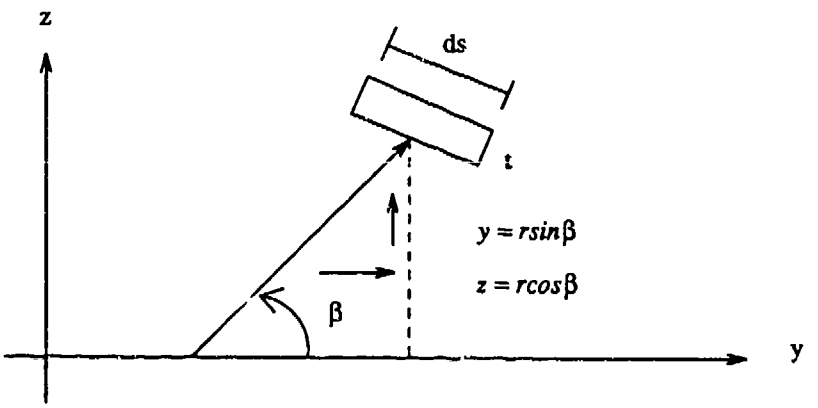

FIGURE 4.1. Blade Moment of Inertia

A similar derivation can be completed to determine the moment of inertia about the z axis. Since

$$I_z = \int_A y^2 dA \tag{4.5}$$

then

$$I_z = 2\int_0^{\pi} tr^3 \sin^2\beta d\beta \tag{4.6}$$

Since the radius r is an arbitrary function of β, a numerical solution to this equation is preferred. A short code was written to divide one half of the blade into 24 elements and to calculate the average radius for each element to the centroid. Then a simple summation for each moment of inertia was completed.

$$I_y = 2\sum_{i=1}^{24} t_i s_i m_i \tag{4.7}$$

and

$$I_z = 2\sum_{i=1}^{24} t_i s_i n_i \tag{4.8}$$

where s is the element length and where $m = r\cos\beta$ and $n = r\sin\beta$.

The four loading conditions will now be examined. In this problem, a rotor blade represented by a hollow shell beam of length L with end caps as shown in Figure 4.2, will be used. The beam is considered symmetrical about the y or transverse axis and the x axis runs along the length of the blade.

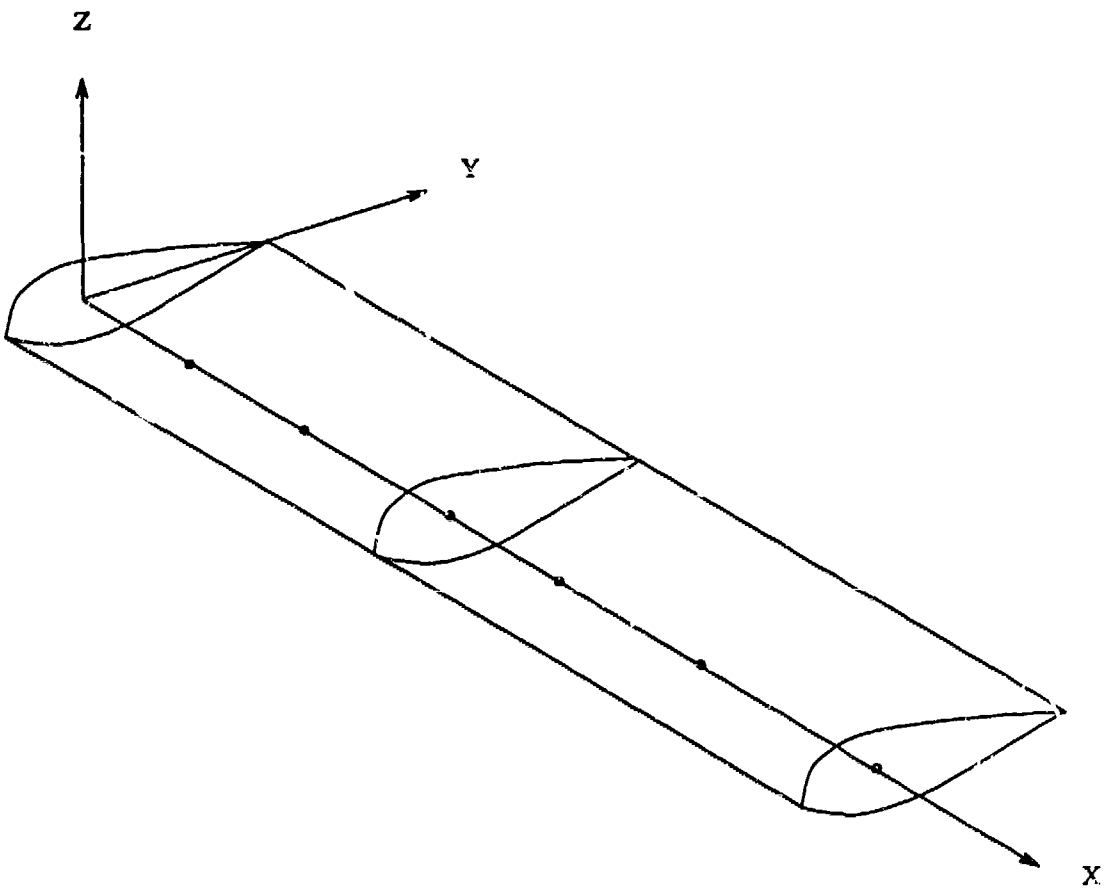

FIGURE 4.2. Rotor Blade Model

The blade is loaded in tension by an axial force P and constrained at the other end. See Figure 4.3 [14].

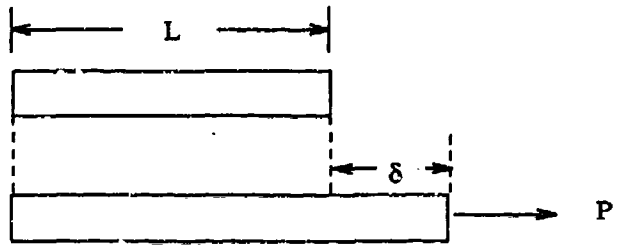

FIGURE 4.3. Axially Loaded Beam

If the force P acts at the centroid of the cross section, the stress in the beam at sections away from the ends is given by:

$$\sigma = \frac{P}{A} \tag{4.9}$$

where A is the cross-sectional area. Additionally, the strain can be expressed as

$$\varepsilon = \frac{\delta}{L} \tag{4.10}$$

where δ is the displacement produced by the axial force. Utilizing Hooke's law ($\sigma = E\varepsilon$), the equation for beam displacement is given as:

$$\delta = \frac{PL}{EA} \tag{4.11}$$

Since the axial force varies along the axis of the beam, an expression for displacement along the entire length of the beam is obtained. Also, we will denote the displacement of

the beam in the x direction by u.

$$u = \int_0^L \frac{P(x)}{EA_x} dx \tag{4.12}$$

The second force to be examined is that of torsion. Torsion refers to the twisting of a structural member when loaded by couples that produce rotation about its longitudinal axis. In this case, the x-axis is the longitudinal axis. This type of loading is pictured in Figure 4.4 which shows the same beam now constrained at one end and loaded at the other end with a moment about the x axis.

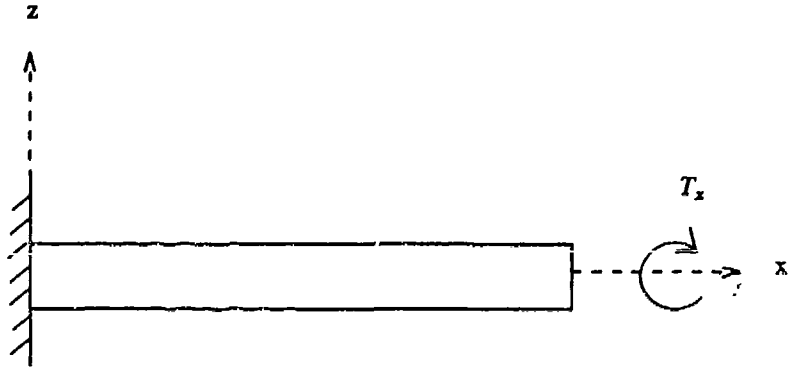

FIGURE 4.4. Torsional Loading

During twisting, there will be a rotation about the x-axis of one end of the blade with respect to the other. The free end will rotate through a small angle β with respect to

the fixed end. The angle β is referred to as the *angle of twist.*

This angle of twist can be expressed in the form:

$$\beta = \frac{TL}{GI_p} \tag{4.13}$$

where T is the torque and GI_p is the *torsional rigidity*. A combination of the *polar moment of inertia*, I_p, the *shear modulus*, G, and the length yields the *torsional flexibility* or $\frac{L}{GI_p}$. This expression is analagous to the *axial flexibility*, $\frac{L}{EA}$, given in Equation (4.11) [14]. The shear modulus relates to the modulus of elasticity by the equation

$$G = \frac{E}{2(1+\nu)} \tag{4.14}$$

The term I_p, or the polar moment of inertia, is not an ideal term for this model. It is best suited for solid circular beams. Thin walled beam theory describes a similar term, J, or *torsion constant*, which will be used where:

$$J = \frac{4A_m^2}{\int_0^{L_m} \frac{ds}{t}} \tag{4.15}$$

For constant thickness t, this equation becomes:

$$J = \frac{4tA_m^2}{L_m} \tag{4.16}$$

where L_m is a *median line* (see Figure 4.5) and A_m is the area enclosed by the median line.

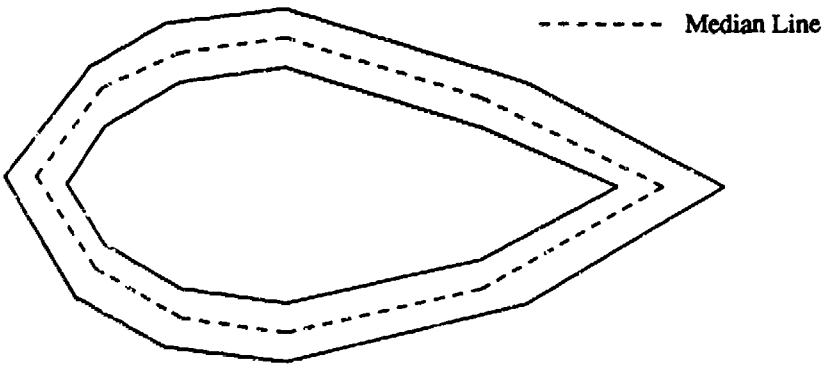

FIGURE 4.5. Median Line of Cross Section

The next loading condition will be acting transversely to the longitudinal axis. The created load is that of a bending moment. These lateral loads cause the beam to bend or flex, thereby deforming the axis of the beam into a curved line. An illustration is given in Figure 4.6 which shows the same beam which is subjected to a bending moment about the transverse or *y* axis.

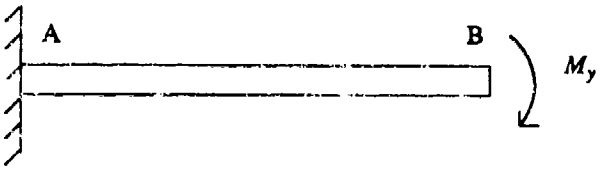

FIGURE 4.6. Cantilever Beam Under Bending Moment

After loading, the axis is bent into a curve that is known as the *deflection curve* of the beam. Now consider two points m_1 and m_2 on the deflection curve (Figure 4.7) [14], where point m_1 is at distance x from the z axis and point m_2 is situated a small distance ds further along the curve.

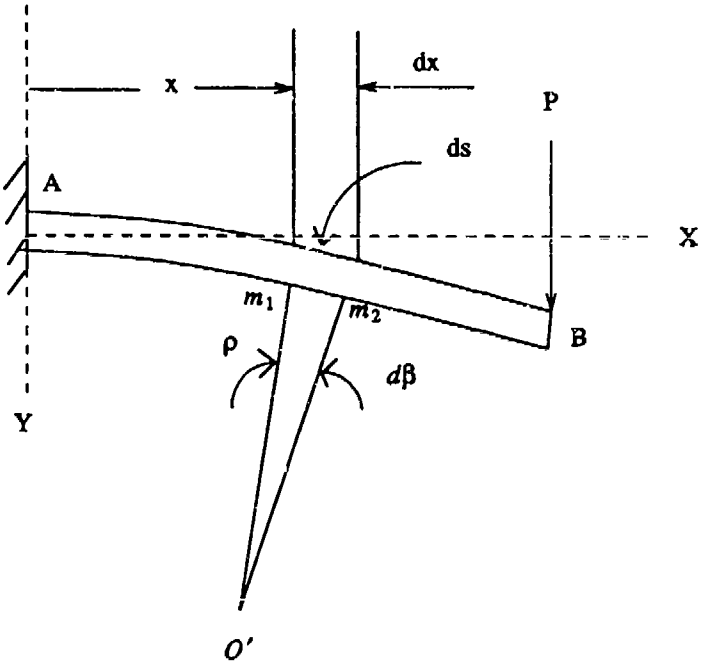

FIGURE 4.7. Curvature of a Bent Beam

At each point, if we draw a line normal to the tangent to the deflection curve, a *center of curvature* will occur at point O'. The length of this normal is called the *radius of curvature* and is defined as ρ. As defined in calculus and analytic geometry, the *cur-*

vature κ, is the reciprocal of the radius of curvature:

$$\kappa = \frac{1}{\rho} \tag{4.17}$$

Also, from the geometry of the figure, we obtain

$$\rho d\phi = ds \tag{4.18}$$

where $d\phi$ is the small angle between the normals and ds is the distance along the curve between the normals. If the deflections of the beam are small, which is the case in this research, then the deflection curve is very flat and the distance ds along the curve may be set equal to its horizontal projection dx and we obtain

$$\kappa = \frac{1}{\rho} = \frac{d\phi}{dx} \tag{4.19}$$

Using the fact that the integral of all elemental moments over the entire cross-sectional area must result in the total applied moment

$$M_o = -\int \sigma_x y dA \tag{4.20}$$

and Hooke's law for uniaxial stress

$$\sigma_x = -E\kappa y \tag{4.21}$$

we obtain

$$M = -\kappa EI \tag{4.22}$$

Rearranging and combining with equation (4.17) we arrive at [14]

$$\kappa = \frac{1}{\rho} = -\frac{M}{EI} \tag{4.23}$$

and consequently

$$\frac{\partial \phi}{\partial x} = -\frac{M_y}{EI} \tag{4.24}$$

A similar bending moment about the vertical or z axis yields an analagous equation:

$$\frac{\partial \psi}{\partial x} = -\frac{M_z}{EI} \tag{4.25}$$

The result of each of these loadings and the equations which will be used to analyze the data can be expressed in matrix form as follows:

$$\begin{Bmatrix} \frac{\partial \beta}{\partial x} \\ \frac{\partial \phi}{\partial x} \\ \frac{\partial \psi}{\partial x} \\ \frac{\partial u}{\partial x} \end{Bmatrix} = \begin{bmatrix} \frac{1}{GJ} & 0 & 0 & 0 \\ 0 & \frac{1}{E_x I_y} & 0 & 0 \\ 0 & 0 & \frac{1}{E_x I_z} & 0 \\ 0 & 0 & 0 & \frac{1}{E_x A} \end{bmatrix} \begin{Bmatrix} T_x \\ M_y \\ M_z \\ P \end{Bmatrix} \tag{4.26}$$

The off-diagonal terms of Equation (4.26) in general will not be zero for anisotropic materials. This is due to coupling. The response of these terms for different laminations sequences will be the focus of the present research. As anisotropic composite materials are loaded, these terms should take on a non-zero identity and should have varied reactions to different lay-ups.

It is important to note at this point that one can use the displacement information for this model which is taken at a sufficient distance from the ends as a result of St. Venant's

principle. We can say that the effects of surface tractions over a part of the boundary that are felt relatively far into the interior of an elastic solid are dependent only on the rigid-body resultant of the applied tractions over this part of the boundary. By this principle we can replace the complex supporting force distribution exerted by the constraints on the beam by a single force and couple. Although we shall not present them here, it is pointed out that mathematical justifications have been advanced for St. Venant's principle (Goodier, 1937; Hoff, 1945; Fung, 1965) [13].

Before moving on to another area, some mention of the relationship of equation (4.26) to composite materials must be made. Since beam type specimens under loading conditions are utilized in composite material characterization, a theory for laminated, anisotropic beams is also desirable.

Beam bending is often based on homogeneous isotropic beam theory. For laminated materials such as the composite blade model in this research, the classical beam formulas must be modified to account for the stacking sequence of individual plies. Whitney provides the best description of this modification [15].

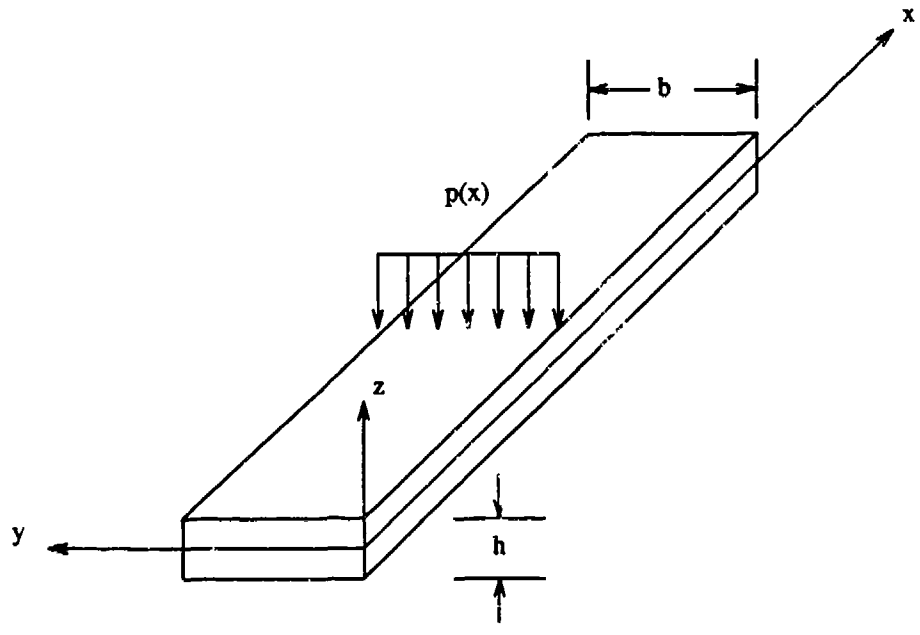

FIGURE 4.8. Laminated Beam

Consider the laminated beam shown in Figure 4.8. It has been shown by Hoff and Pagano that layered beams of this type in which the plies are oriented symmetrically about the midplane and the orthotropic axes of material symmetry in each ply are parallel to the beam edges can be analyzed by the classical beam theory previously explained if the bending stiffness EI is replaced by the equivalent stiffness $E_x^b I$ defined in the following manner:

$$E_x^b I = \sum_{k=1}^{N} E_l^k I^k \tag{4.27}$$

where E_x^b is the effective bending modulus of the beam, E_l^k is the modulus of the kth

layer relative to the beam axis and N is the number of layers in the laminate.

Equations which are applicable to a general class of symmetric laminates can be derived by considering a beam as a special case of a laminated plate with a length much larger than the width, i.e., $L \gg b$.

For bending of symmetric laminates, the constitutive relations (Chapter 3) reduce to the form:

$$\begin{Bmatrix} M_x \\ M_y \\ M_{xy} \end{Bmatrix} = \begin{bmatrix} D_{11} & D_{12} & D_{16} \\ D_{12} & D_{22} & D_{26} \\ D_{16} & D_{26} & D_{66} \end{bmatrix} \begin{Bmatrix} \kappa_x \\ \kappa_y \\ \kappa_{xy} \end{Bmatrix} \tag{4.28}$$

where

$$\kappa_x = -\frac{\partial^2 w}{\partial x^2}\,,\ \kappa_y = -\frac{\partial^2 w}{\partial y^2}\,,\ \kappa_{xy} = -2\frac{\partial^2 w}{\partial x \partial y} \tag{4.29}$$

For this derivation, it is useful to consider Equation (4.28) in the inverted form

$$\begin{Bmatrix} \kappa_x \\ \kappa_y \\ \kappa_{xy} \end{Bmatrix} = \begin{bmatrix} D_{11}^* & D_{12}^* & D_{16}^* \\ D_{12}^* & D_{22}^* & D_{26}^* \\ D_{16}^* & D_{26}^* & D_{66}^* \end{bmatrix} \begin{Bmatrix} M_x \\ M_y \\ M_{xy} \end{Bmatrix} \tag{4.30}$$

where D_{ij}^* are elements of the inverse matrix of D_{ij}.

In order to derive a beam theory the following assumptions are made:

$$M_y = M_{xy} = 0 \tag{4.31}$$

Using Equations (4.29) and (4.30) in conjuction with Equation (4.31), we find

$$\kappa_x = -\frac{\partial^2 w}{\partial x^2} = D_{11}^* M_x \tag{4.32}$$

Since this beam is assumed to have a high length-to-width ratio, we can state that

$$w = w(x) \tag{4.33}$$

Combining Equations (4.32) and (4.33), we obtain the following result:

$$\frac{d^2 w}{dx^2} = -\frac{M}{E_x^b I} \tag{4.34}$$

where

$$E_x^b = \frac{12}{h^3 D_{11}^*},\ M = bM_x,\ I = \frac{bh^3}{12} \tag{4.35}$$

and b is the width of the beam. Equation (4.34) is in the same form as classical beam theory with the homogeneous, isotropic modulus E replaced by the effective bending modulus of the laminated beam, E_x^b [15]. This composite beam analysis allows an elastically-coupled composite structure to be described in terms of its equivalent engineering properties (EA, EI, GJ).

Chapter Five

The Model

5.1. Finite Element Modeling

The first step toward the complete analysis of an aeroelastic problem is the development of an accurate geometric and structural model. This chapter summarizes that development process. A theoretical rotor blade model based upon composite construction is used in this research. Certain structural elements, such as spars and helicopter rotor blades, can be approximated as beams. Rotor blades almost always involve complicated cross-sectional geometries, and combined axial, bending and torsional loadings. A major obstacle in applying this model toward understanding the effects of composite materials on aeroelastic tailoring is that analytical tools for such a purpose are limited.

The finite element method was chosen for this work as it provides a basis of modern structural analysis. It is a powerful method to treat nonuniformities and complex geometries such as a twisting helicopter blade. Finite element analysis has been used previously (Hong, 1985) to examine the aeroelastic stability of helicopter blades in both hovering and forward flight [16].

As stated earlier, finite element analysis has become an established and widely used tool in the design of rotorcraft and more recently in composite rotor blade analysis. In addition to multi-purpose finite element codes which have composite material capability,

composite plate and shell finite elements have been formulated. Numerous research efforts have resulted in the development of shell elements with anisotropic laminate capabilities. The result of these efforts are found in numerous large commercially available packages such as **PATRAN®** which can be used for comprehensive analytical representations using detailed shell finite element models.

The specific advantages of a finite element solution procedure are as follows [4]:

(a) The formal derivation of the complex nonlinear equations of motion of the problem is not required.

(b) Each of the nonlinear terms is dealt with in a rational fashion while bypassing the need for an ordering scheme.

(c) The complex structural behavior of the blade is accurately modeled.

(d) Both the undeformed and deformed geometry of the blade are taken into account in a natural fashion and are available for graphics viewing.

For the analysis of a slender rotor blade, a beam element seems most appropriate since only a small number of degrees of freedom are required. However, the accuracy of a simple Euler-Bernoulli beam model for this research has been questioned in Chapter 3. This problem therefore requires a two-dimensional laminated shell element to model elastic couplings of anisotropic composite materials.

In the present work, the composite static blade is treated as a hollow semi-cantilevered laminated shell beam with end caps as shown in Figure 5.1.1. The model is representative of the size of a main rotor blade in order to assess the importance of ply angle orientation. The beam section is assumed to be a single airfoil shaped cell consisting of six sections which represent laminates; two on top, two on bottom and two as end caps. Figures 5.1.2 and 5.2 provide a cross-sectional view of the end cap and laminate

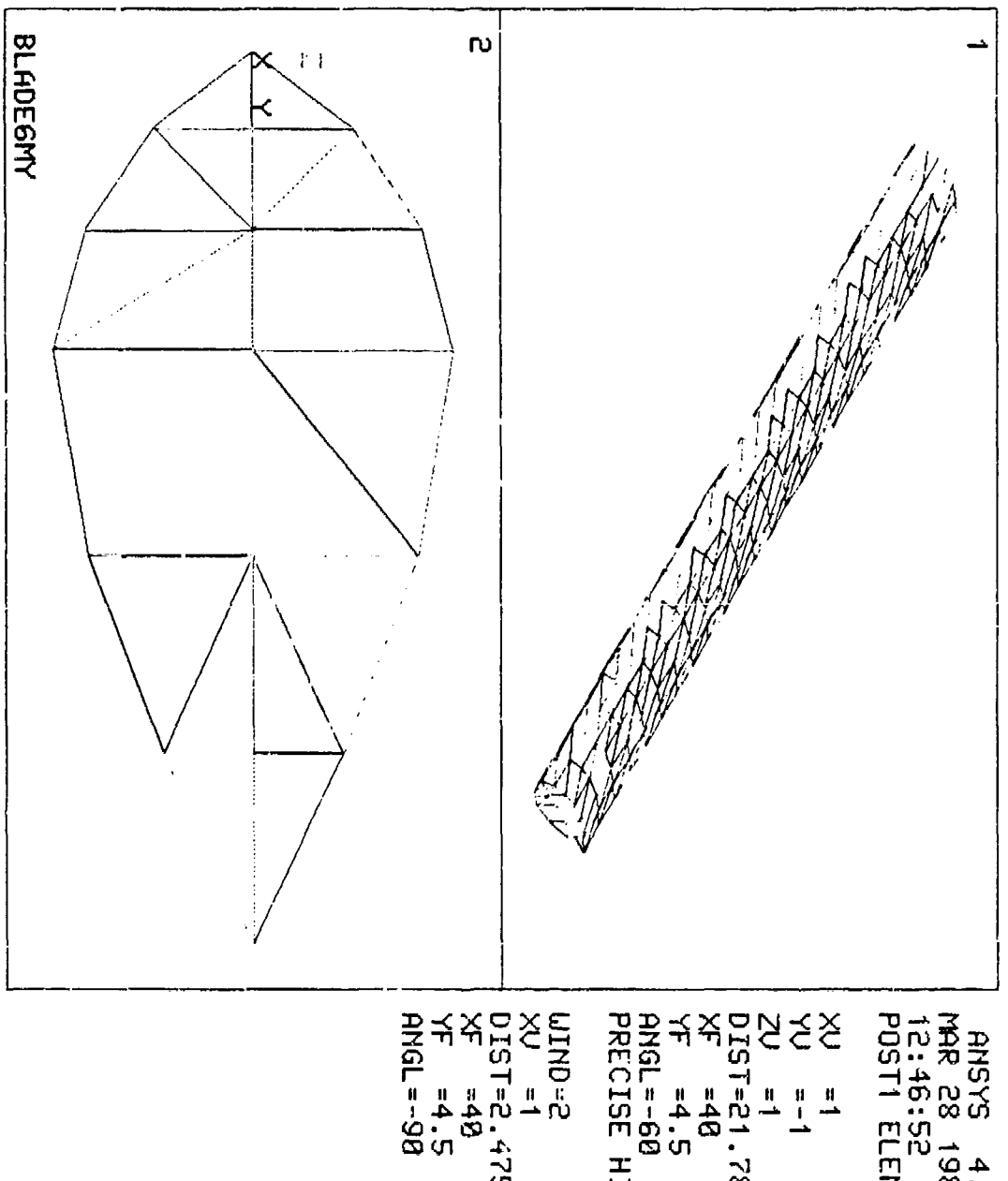

FIGURE 5.1

Finite Element Beam Model and End Cap

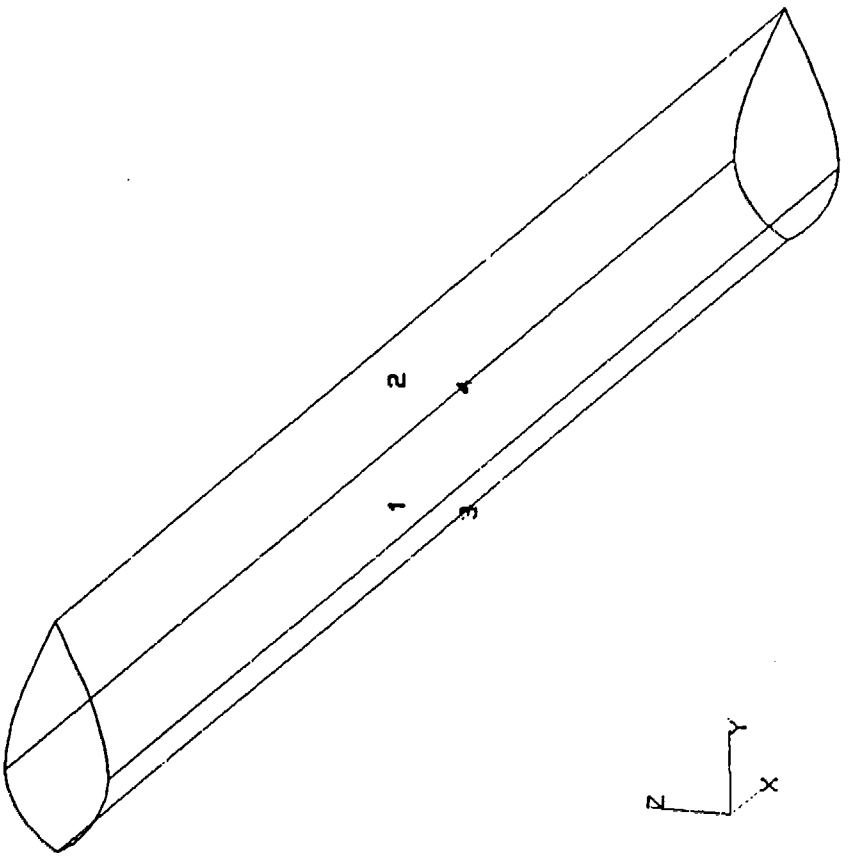

FIGURE 5.2

PATRAN 4-Patch Construction

section view respectively.

The solid modeling is done on **PATRAN®** by using a series of grids, lines and patches. **PATRAN®** is an interactive engineering program with the ability to construct, view, verify, analyze, manipulate, and demonstrate [17]. The four surface laminates and two end caps were constructed as six individual patches. Each patch was assigned a material property identification. This property was based on the construction of a number of composite layers with specified angle orientations and thicknesses. The material property option of **LAM** or **LAMS** in **PATRAN®** was used to specify the number of plies, their individual thicknesses and their orientations. A description of all of the commands for model generation is given as a session file in Appendix B.

The constitutive relations of an orthotropic graphite fiber *(T50 Fiber)* and isotropic matrix *(Fiberite 934 Epoxy Resin)* were used. The volume mix of fiber to matrix used for the composite was *60% to 40%* respectively. The properties can be found in Table 5.1 below.

MATERIAL PROPERTIES			
Property	(Units)	T50 Fiber	Epoxy Matrix
E_L	(Psi)	56.3	0.674
E_T	(Psi)	1.10	0.674
ν_{LT}	---	0.41	0.363
ν_{TT}	---	0.45	0.363
G_{LT}	(Psi)	2.20	0.247
G_{TT}	(Psi)	0.50	0.247
α_L	$(\mu in/in\ F)$	0.50	25.0
α_T	$(\mu in/in\ F)$	6.50	25.0

TABLE 5.1

The resultant graphite/epoxy composite properties are shown in Table 5.2.

Graphite/Epoxy		
Property	(Units)	Gr/Ep
E_1	(Psi)	19.2×10^6
E_2	(Psi)	1.56×10^6
E_3	(Psi)	1.56×10^6
ν_{12}	---	1.95×10^{-2}
ν_{23}	---	.21
ν_{13}	---	$.801 \times 10^{-2}$
G_{12}	(Psi)	8.2×10^5

TABLE 5.2

The analysis code used was ANSYS® by Swanson Analysis Systems Inc. The ANSYS® program is a large-scale, general purpose computer program for the solution of several classes of engineering analyses. It uses the wave-front direct solution method for the system of simultaneous linear equations developed by the matrix displacement method. The program has the capability of solving large structures with no limit on the number of elements used in an analysis [18]. There is no "band width" limitation in the analysis definition; however, there is a "wave-front" restriction of *2000* degrees of freedom. There are some peculiarities in ANSYS® associated with the elements used for this laminated shell model. The element is an elastic flat triangular element with both bending and membrane capabilities (See Figure 5.3) [18]. Up to *15* different layers of material are permitted per element and both in-plane and normal loads may be applied. The element has six degrees of freedom at each node. There is no significant stiffness associated with rotation about the element *z* axis. A nominal value of stiffness may be

present to prevent free rotation at the node. The triangular *2-D* elements are less accurate than equivalent-sized quadrilateral elements but must be used for laminated shell analysis. When using triangular elements in a rectangular array of nodal points, the best results are obtained from an element pattern having alternating diagonal directions. Also, since the element coordinate system is relative to the I-J line, the stress results are most easily interpreted if the I-J lines of the elements are all parallel.

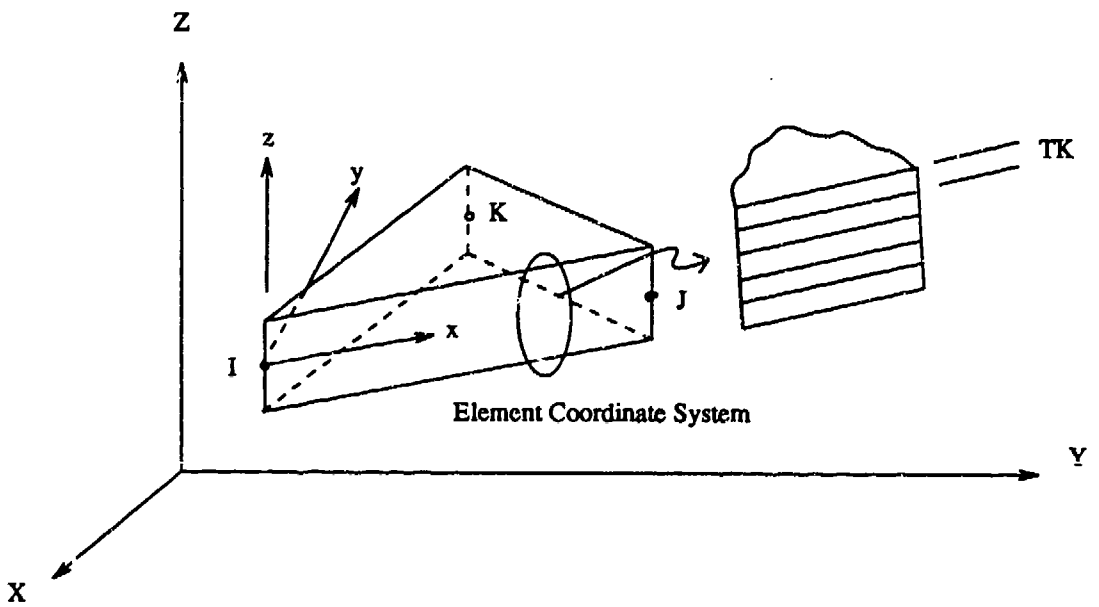

FIGURE 5.3. Laminated Shell Element (STIF53) Geometry

The model was set up for finite element analysis using flat two-dimensional triangular elements constructed over three nodes, *TRI/3/53*, where *53* is the stiffness coefficient corresponding to the laminated shell configuration of ANSYS®. A nine node element,

TRI/9, was preferred but was impossible under the ANSYS® restriction of three nodes per element when using laminated shells. The result was *760* elements and *310* nodes constructed over the entire blade region. In addition, the end caps were assumed rigid and were therefore modeled with much thicker and stiffer elements. Once these finite elements were defined using the connectivity sub-program of PATRAN®, the model was subjected to automated geometric equivalencing over each of the elements. This is simply the process of selecting a single ID for all node points which coexist at a given point (and as a result have different ID numbers) and propagating that change through any existing connectivity definitions. The next step was the optimization of the model by selection of the maximum wavefront criterion for both the *Cuthill-Mckee* and *Gibbs-Poole-Stockmeyer* methods. The result is element compaction based on the assignment of sequential ID numbers to remove any "holes" or spaces in the original numbering sequence.

Forces, displacements, pressures and constraints are initiated at this point. It required several attempts to determine the best way to constrain this model. The accuracy of the displacement results was very much dependent on the constraints chosen. An example of a poorly constrained model can be seen in Figure 5.4. This particular model was constrained (six degrees of freedom) at one node on the leading edge of the center of the blade. An axial force was applied at each end in opposite directions. The result should have looked something like Figure 5.5.

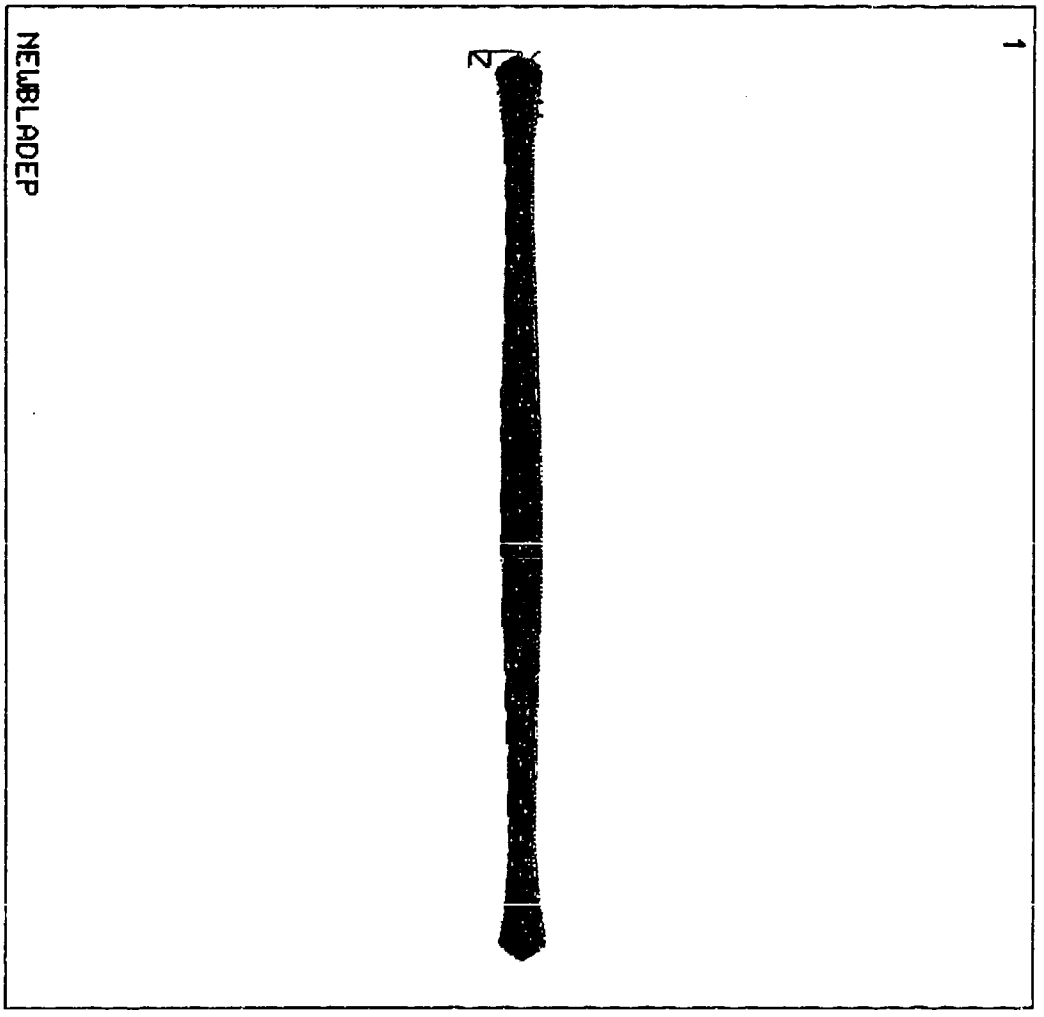

FIGURE 5.4

Improperly Constrained Model

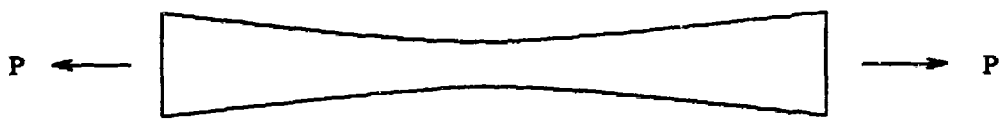

FIGURE 5.5. Beam Response to Axial Load

Finally, for simplicity in arriving at a solution, one end of the blade model was constrained. This constraint occurred at each node on the end cap in each of its six degrees of freedom (three translational and three rotational). This was used to simulate the hub attachment for the blade.

The other end underwent forces in varying amounts and directions. Each of the eight ply configurations were subjected to identical loadings. Three of the four loading conditions were applied at a node on the end cap which represented the centroid (See Chapter 4) of the blade and consisted of an individually applied torsional load T_x, and moments about the y and z axes, M_y and M_z. The fourth load was an axial force P and was applied at the neutral axis of the blade. Since there was not a node located on the neutral axis, the force was distributed over the nodes of the element in which the neutral axis was located.

All of this information is pre-processed by **PATRAN®** and compiled in a neutral file in preparation for analysis by **ANSYS®**. Following the analysis, the information would normally go through a reverse translator and be post-processed by **PATRAN®**.

However, we were unable to post-process in PATRAN® due to the two commercial programs being incompatible on the University of Virginia's current version of PRIMOS (Version 21.0.2). Instead the post-processing was done using POST1 in ANSYS43.A®. The results are displayed graphically for deformed and undeformed geometries, fringe, carpet and contour plots, or stress and displacement plots. The graphics capability of this new version are much improved over the older version of ANSYS43®.

5.2. Coordinate System

The rotor blade is treated as a nonrotating ($\Omega = 0$) elastic beam. Therefore, a rectangular coordinate system, x, y, z, is used and attached to the undeformed blade. The longitudinal direction of the blade aligns with the x axis and the y axis corresponds to the transverse direction. The z axis correlates to a right-handed coordinate system. The angles of rotation about each of the axes, (β, ϕ and ψ for x,y,z respectively) are shown in Figure 5.6.

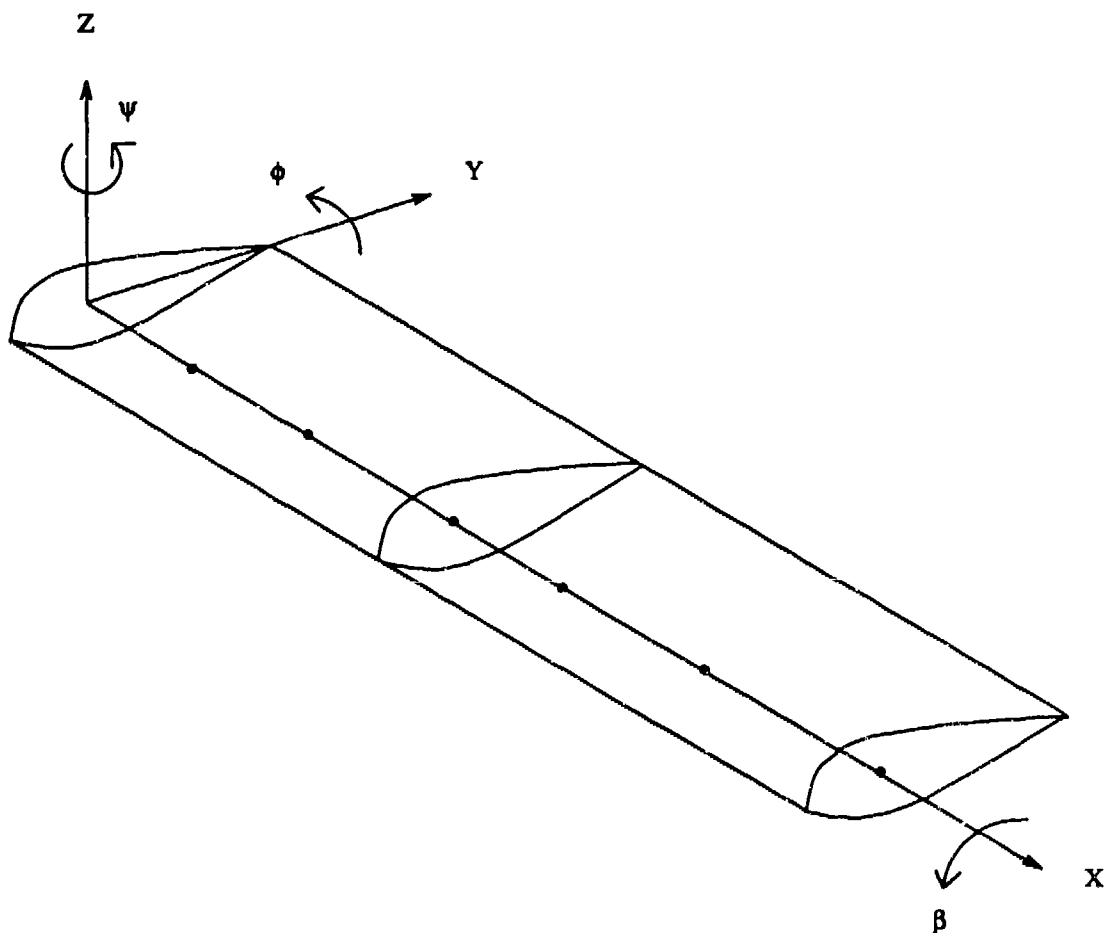

FIGURE 5.6. Coordinate System With Rotations

It is assumed that the end caps provide the required blade structural stiffnesses in each direction. Each laminate consists of a number of laminae with ply orientations which are different than the beam axis orientation. A point p on the undeformed axis, undergoes displacements u, v, w in the x, y, z directions respectively and occupies point p' on the newly deformed axis.

5.3. Ply Configuration

Two criteria were used in the selection of ply lay-ups and orientations for each configuration. The first required that the blade did not exhibit static instability and the second was that the result would have coupling characteristics which were large enough to have identifiable effects. The blades are eight-ply graphite-epoxy laminate beams which have strong bending-twisting coupling. Favorable and unfavorable angle-of-attack changes can be obtained depending on the bending-twisting coupling (D_{16}) terms. There are eight different lay-ups used in this research. Seven are anisotropic configurations with the angle orientation of two layers changing systematically to determine its result as a parameter of the off diagonal terms in the beam equations. The eighth lay-up is an isotropic configuration and is used to verify the accuracy of the blade model. These ply configurations can be seen in Table 5.3.

SYMMETRIC LAMINATION CONFIGURATIONS								
PLY	BLADE 1	BLADE 2	BLADE 3	BLADE 4	BLADE 5	BLADE 6	BLADE 7	BLADE 8
1	0°	0°	0°	0°	0°	0°	0°	0°
2	30°	30°	30°	30°	30°	30°	30°	45°
3	0°	15°	30°	45°	60°	75°	90°	135°
4	90°	90°	90°	90°	90°	90°	90°	90°
MIDPLANE								
5	90°	90°	90°	90°	90°	90°	90°	90°
6	0°	15°	30°	45°	60°	75°	90°	135°
7	30°	30°	30°	30°	30°	30°	30°	45°
8	0°	0°	0°	0°	0°	0°	0°	0°

TABLE 5.3

Table 5.4 shows the laminate properties for each blade. They were calculated using the

laminate analysis program in Appendix A.

LAMINATE PROPERTIES								
---	BLADE 1	BLADE 2	BLADE3	BLADE4	BLADE5	BLADE6	BLADE7	BLADE8
$\bar{E}_x$	11.63×10^6	9.19×10^6	7.63×10^6	7.23×10^6	7.29×10^6	7.33×10^6	7.24×10^6	7.58×10^6
$\bar{E}_y$	6.11×10^6	6.11×10^6	6.13×10^6	6.44×10^6	7.29×10^6	8.96×10^6	10.51×10^6	7.58×10^6
$\bar{G}_{xy}$	1.43×10^6	1.38×10^6	1.63×10^6	1.85×10^6	1.71×10^6	1.44×10^6	1.36×10^6	2.92×10^6
ν_{xy}	.117	.105	.123	.106	.057	.023	.068	.298
ν_{yx}	.062	.070	.099	.094	.057	.028	.099	.298

TABLE 5.4

5.4. Blades I-VII (Anisotropic)

The first seven blades were designed to exhibit bending-coupling characteristics. Using the **LAMS** option for laminated materials, an eight layer composite was built. Each layer had the same thickness of *0.015 inches*. The four layers on the top were symmetric with the bottom four plies. The angles of orientation can be seen in Table 5.3 above. The *60/40* mix of *T50 Fiber (Graphite)* and *Fiberite 934 Epoxy Resin* was used. The angle of ply orientation, θ, was changed systematically for the third and sixth layers. The first blade has $\theta = 0°$ and blade seven has $\theta = 90°$ with a 15° increment for blades two through six. Four forces, M_x, M_y, M_z and P, were applied individually to each blade.

5.5. Blade VIII (Isotropic)

This blade model was designed to exhibit isotropic characteristics. It was built using the **LAMS** option of **PATRAN®**. There are eight layers of equal thickness *(0.015*

inches). The angles of ply orientation are shown in Table 5.3 and should produce isotropic behavior when the forces are applied. Once again, four forces, M_x, M_y, M_z and P, were applied individually.

Chapter Six

Results

Numerical calculations are carried out through finite element analysis for a composite material rotor blade. The blade is discretized into *616* elements and the data is collected at twelve nodes; six along the leading edge and six along the trailing edge. The behavior at two blade sections is evaluated. One section (Section 1) is located at the center of the blade length and the other section (Section 2) is located in the last quarter of the blade but at a sufficient distance from the end cap. The model is analyzed for eight blade laminations (seven anisotropic and one isotropic) which undergo four seperate loading conditions.

The output from ANSYS® (See Appendix E), consists of displacements in the three principal directions; UX, UY, and UZ for each node. The selected nodal displacements are entered into a data file for further evaluation by the FORTRAN code in Appendix C. This program calculates the rotations about each axis (β, ϕ, ψ for x,y,z respectively) and the displacements along the longitudinal axis. The data is also manipulated to produce the first derivative of each of these values with respect to the blade span. The stiffness matrix, $[C]$, is formed for both sections of each blade. A modified finite differencing method is used to calculate the rotations from the given displacements and is explained below.

The beam equation matrix which is represented by Equation (4.26) can be expressed again as:

$$\begin{Bmatrix} \frac{\partial \beta}{\partial x} \\ \frac{\partial \phi}{\partial x} \\ \frac{\partial \psi}{\partial x} \\ \frac{\partial u}{\partial x} \end{Bmatrix} = \begin{bmatrix} a_{11} & a_{12} & a_{13} & a_{14} \\ a_{21} & a_{22} & a_{23} & a_{24} \\ a_{31} & a_{32} & a_{33} & a_{34} \\ a_{41} & a_{42} & a_{43} & a_{44} \end{bmatrix} \begin{Bmatrix} T_x \\ M_y \\ M_z \\ P \end{Bmatrix} \tag{6.1}$$

Since the forces are known, one must calculate $\frac{\partial \beta}{\partial x}$, $\frac{\partial \phi}{\partial x}$, $\frac{\partial \psi}{\partial x}$ and $\frac{\partial u}{\partial x}$ in order to solve for the stiffness terms in the matrix above. The use of

$$\frac{\partial \beta}{\partial x} = \frac{\beta_{i+1} - \beta_{i-1}}{2l} \tag{6.2}$$

where

$$\beta_{i+1} = \frac{-\left[UZ^L_{i+1} - UZ^T_{i+1}\right]}{b} \tag{6.3}$$

and similarly

$$\beta_{i-1} = \frac{-\left[UZ^L_{i-1} - UZ^T_{i-1}\right]}{b} \tag{6.4}$$

and where $i-1$, i, and $i+1$ are consecutive increments of length (l) along the blade length allows for the computation of β and its first derivative and leads to the solution of the first column of the stiffness matrix.

If

$$\phi_{i,i+1} = \frac{UZ^o_{i+1} - UZ^o_i}{l} \tag{6.5}$$

where

$$UZ^o_i = UZ^L_i \left[1 - \zeta\right] + UZ^T_i \zeta \tag{6.6}$$

and

$$UZ^o_{i+1} = UZ^L_{i+1} \left[1 - \zeta\right] + UZ^T_{i+1} \zeta \tag{6.7}$$

then

$$\frac{\partial \phi}{\partial x} = \frac{UZ^o_{i+1} - 2UZ^o_i - UZ^o_{i-1}}{l^2} \tag{6.8}$$

And similarly,

$$\frac{\partial \psi}{\partial x} = \frac{UY^o_{i+1} - 2UY^o_i - UY^o_{i-1}}{l^2} \tag{6.9}$$

Finally, the derivative of u is defined as:

$$\frac{\partial u}{\partial x} = \frac{UX^o_{i+1} - UX^o_{i-1}}{2l} \tag{6.10}$$

Equations 6.8, 6.9 and 6.10 are used to solve for the second, third and fourth columns of the stiffness matrix respectively. The matrices are then assembled for each blade. They are shown below.

MATRIX FOR SECTION: 1, BLADE: 1

.582198E-07 -.648599E-08 .110397E-09 -.372616E-08
-.646000E-08 .259820E-07 -.590831E-09 -.966120E-08
.202181E-09 -.594695E-09 .579233E-08 .210487E-09
-.357498E-08 -.969197E-08 .195244E-09 .501077E-07

MATRIX FOR SECTION: 2, BLADE: 1

.576136E-07 -.677641E-08 .129622E-09 -.360332E-08
-.636547E-08 .258174E-07 -.682216E-09 -.968831E-08
-.138691E-09 -.536155E-09 .565750E-08 .274261E-10
-.412470E-08 -.972916E-08 -.237509E-09 .495678E-07

MATRIX FOR SECTION: 1, BLADE: 2

.597071E-07 -.998768E-08 .828957E-10 -.101376E-07
-.996914E-08 .287017E-07 -.391494E-09 -.691174E-08
.210321E-09 -.396723E-09 .669389E-08 .795812E-10
-.993147E-08 -.693385E-08 .685059E-10 .555784E-07

MATRIX FOR SECTION: 2, BLADE: 2

.592261E-07 -.104780E-07 .649079E-10 -.100703E-07
-.981416E-08 .283538E-07 -.585838E-09 -.694357E-08
-.130799E-09 -.419017E-09 .641803E-08 -.478981E-10
-.104133E-07 -.722706E-08 -.769398E-09 .550485E-07

MATRIX FOR SECTION: 1, BLADE: 3

.500480E-07 -.111859E-07 .221594E-10 -.971455E-08
-.111937E-07 .308369E-07 -.194795E-09 -.400552E-08
.138787E-09 -.190835E-09 .737674E-08 .145800E-11
-.952498E-08 -.399955E-08 .483645E-11 .604304E-07

MATRIX FOR SECTION: 2, BLADE: 3

.497724E-07 -.118054E-07 -.164852E-10 -.969432E-08
-.110411E-07 .305075E-07 -.370755E-09 -.405130E-08
-.306253E-09 -.238398E-09 .703087E-08 -.109083E-09
-.100369E-07 -.433010E-08 -.902971E-09 .598740E-07

MATRIX FOR SECTION: 1, BLADE: 4

.438927E-07 -.114499E-07 -.295917E-11 -.422881E-08
-.114735E-07 .307596E-07 -.104341E-09 -.212956E-08
.902146E-10 -.995612E-10 .742222E-08 -.171720E-10
-.408496E-08 -.212293E-08 -.112840E-10 .604906E-07

MATRIX FOR SECTION: 2, BLADE: 4

.437602E-07 -.121026E-07 .872368E-11 -.419622E-08
-.113331E-07 .304896E-07 -.217743E-09 -.216331E-08
-.404176E-09 -.585793E-10 .704398E-08 -.153504E-09
-.465988E-08 -.225900E-08 -.887374E-09 .599169E-07

MATRIX FOR SECTION: 1, BLADE: 5

.473131E-07 -.118224E-07 -.357026E-10 -.135087E-10
-.118509E-07 .290284E-07 -.993379E-12 .184891E-11
.404266E-10 -.140037E-12 .701748E-08 -.167640E-10
.927771E-10 -.132395E-11 -.189042E-10 .565798E-07

MATRIX FOR SECTION: 2, BLADE: 5

.472095E-07 -.124535E-07 .223954E-10 .139275E-10
-.116972E-07 .287571E-07 -.564925E-10 -.283551E-10
-.369083E-09 .118199E-09 .662338E-08 -.184275E-09
-.466199E-09 .330131E-10 -.905433E-09 .560019E-07

MATRIX FOR SECTION: 1, BLADE: 6

.566060E-07 -.112748E-07 -.112823E-09 -.139777E-08
-.112952E-07 .264781E-07 .201259E-09 .315211E-08
-.452902E-10 .200743E-09 .633755E-08 .155130E-10
-.129999E-08 .314820E-08 .374775E-11 .510225E-07

MATRIX FOR SECTION: 2, BLADE: 6

.119927E-05 -.117927E-07 -.825691E-10 -.145466E-08
.410326E-05 .261994E-07 .182398E-09 .309478E-08
-.257063E-09 .250628E-09 .600472E-08 -.165144E-09
-.170257E-08 .312056E-08 -.807286E-09 .504383E-07

MATRIX FOR SECTION: 1, BLADE: 7

.607422E-07 -.802202E-08 -.136835E-09 -.840365E-08
-.803070E-08 .247008E-07 .377322E-09 .546028E-08
-.693500E-10 .377721E-09 .578679E-08 .743851E-10
-.827150E-08 .546064E-08 .605670E-10 .476835E-07

MATRIX FOR SECTION: 2, BLADE: 7

.603513E-07 -.834859E-08 -.168020E-09 -.855583E-08
-.784810E-08 .245449E-07 .337192E-09 .538241E-08
-.123595E-09 .262184E-09 .564403E-08 -.122913E-09
-.848671E-08 .517938E-08 -.345758E-09 .470697E-07

MATRIX FOR SECTION: 1, BLADE: 8

.287997E-07	-.150000E-11	.563859E-11	-.935840E-11
-.259201E-11	.259144E-07	-.178833E-11	-.248651E-12
.184126E-10	-.232749E-12	.619388E-08	-.486900E-10
.453763E-10	.968932E-12	-.228322E-10	.543169E-07

MATRIX FOR SECTION: 2, BLADE: 8

.285857E-07	.166050E-09	.185933E-10	-.479692E-11
.275293E-09	.259307E-07	.158014E-10	-.262454E-11
-.276093E-09	.804174E-12	.632200E-08	-.187553E-09
-.347824E-09	.253299E-10	.373140E-09	.538126E-07

To examine the accuracy of the resultant matrices, it is important to begin with the isotropic blade. Examination of Blade 8 reveals that the diagonal terms are all positive and representative of the correct responses. Theoretically, the off-diagonal terms of this matrix should be zero. Since the finite element method was used for analysis and numerical methods are not exact, these terms will never quite be zero. The values of these terms range from two to five orders of magnitude smaller than the diagonal terms and can be considered zero. The only term which is marginally acceptable is the a_{43} term (Equation 6.1). The value is only one or two orders of magnitude smaller than the diagonal term in that column and may represent some unwanted coupling in the isotropic model. This term represents an extensional-bending coupling caused by a moment about the z-axis. This is probably due to the fact that the bending moment is applied about the usymmetric axis of the model and that the point of application is in error. Because of this discrepancy in the isotropic case, the a_{43} term in each of the other blades must be considered to be slightly inaccurate. There are distinct coupling terms present in each of the anisotropic blades. The value of a coupling term, say a_{13}, of one lamination can be compared to the same term of another anisotropic lamination to determine the impact that the ply orientation angle has on the coupling effect. This information could be stored in a

file which contained similar data for numerous blades and laminations and might be useful for an aeroelastician who is attempting to construct a composite blade which exhibits elastic coupling responses desirable for given flight conditions. It might even be possible with enough research and data collection to construct a catalog of composite blades which exhibit unique aeroelastic properties.

After all of the calculations are completed, the response of β', ϕ', ϕ' and u' are plotted with respect to the ply angle θ. The results are shown in Figures 6.1 through 6.8.

In the plot of β' versus the ply angle, (Figure 6.1), the results are as expected. The rate of twist of the blade (for a fixed torque) should be inversely proportional to the in-plane shear modulus, $\overline{G}_{xy}$, of the laminate. The value of the laminate in-plane shear modulus increases from $\theta = 0°$ to $\theta = 45°$ where it reaches a maximum. As the ply angle continues to increase to $\theta = 90°$, the in-plane shear modulus decreases. If the values of $\overline{G}_{xy}$ for this model (See Table 5.4) are plotted with respect to the ply angle, the inverse of Figure 6.1 is the result. Both of these plots are offset to the right so that the minimum angle of twist and the maximum in-plane shear stress are located near 49°. This is due to the geometry of the blade which employs a curved laminate and therefore the effect of $\overline{G}_{xy}$ is altered.

Figures 6.2, 6.3 and 6.4 demonstrate the effect of the ply angle on the curvature, rotation and rate of displacement of the blade. These plots should follow the functional dependence of the laminate E_x and E_y on the ply angle. The results correlate closely with the moduli from $\theta = 0°$ to $\theta = 45°$. However, one would expect the curvature and rotation to continue to increase as the the ply angle increases up to $\theta = 90°$. This is the expected behavior since the strength in the longitudinal direction is about 17 times

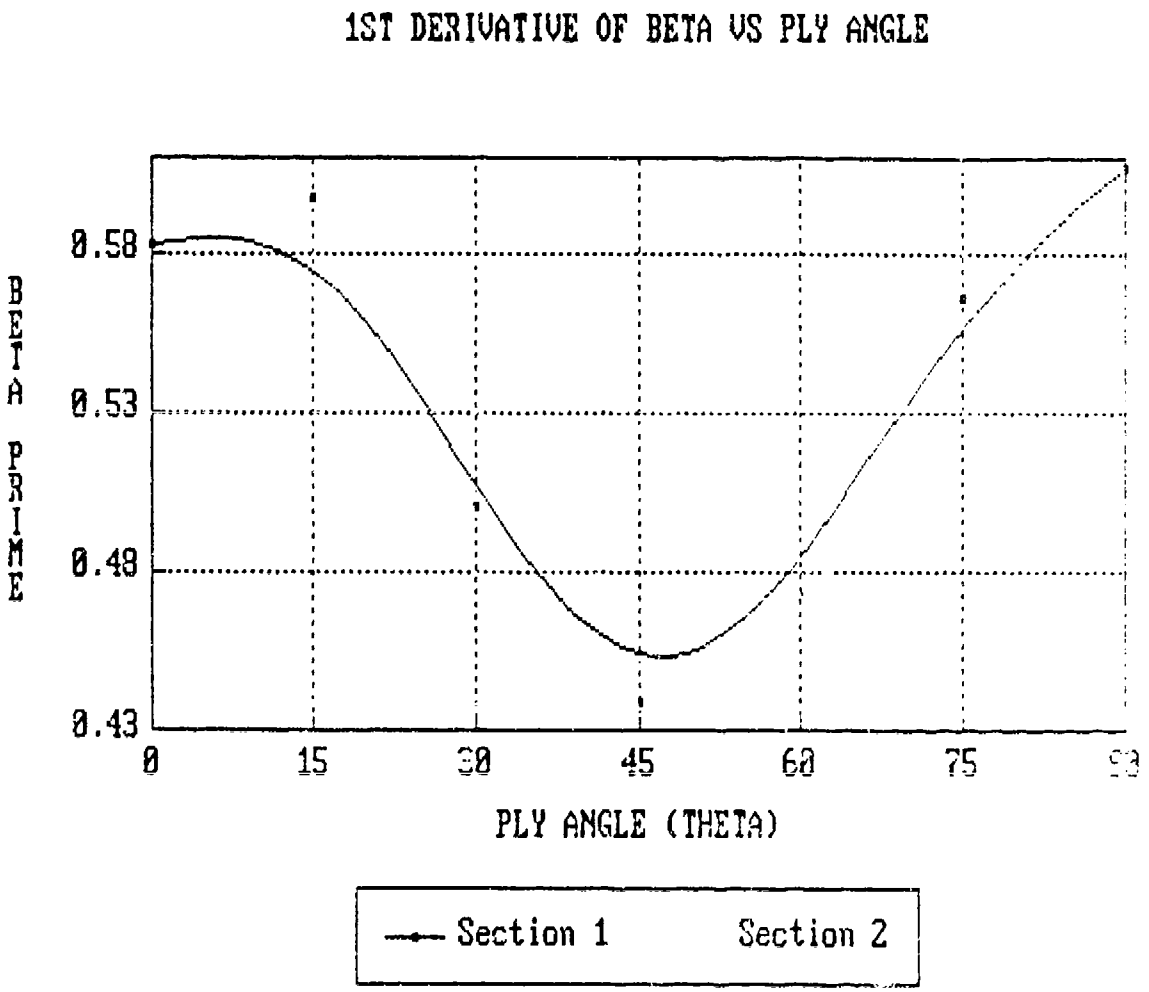
1ST DERIVATIVE OF BETA VS PLY ANGLE
BETA PRIME
0.58
0.53
0.48
0.43
0
15
30
45
60
75
90
PLY ANGLE (THETA)
Section 1
Section 2

FIGURE 6.1

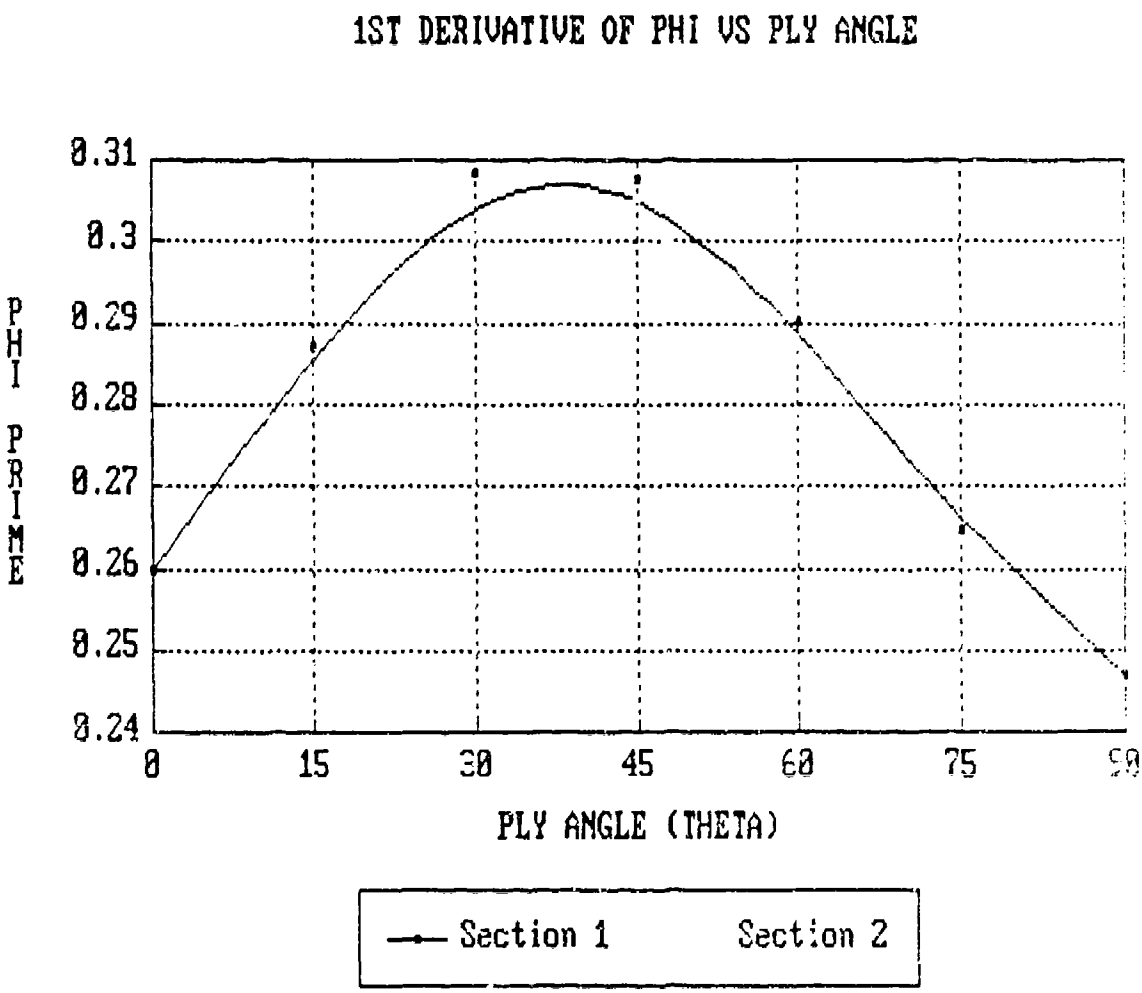
1ST DERIVATIVE OF PHI VS PLY ANGLE
PHI PRIME
0.31
0.3
0.29
0.28
0.27
0.26
0.25
0.24
0
15
30
45
60
75
90
PLY ANGLE (THETA)
Section 1
Section 2

FIGURE 6.2

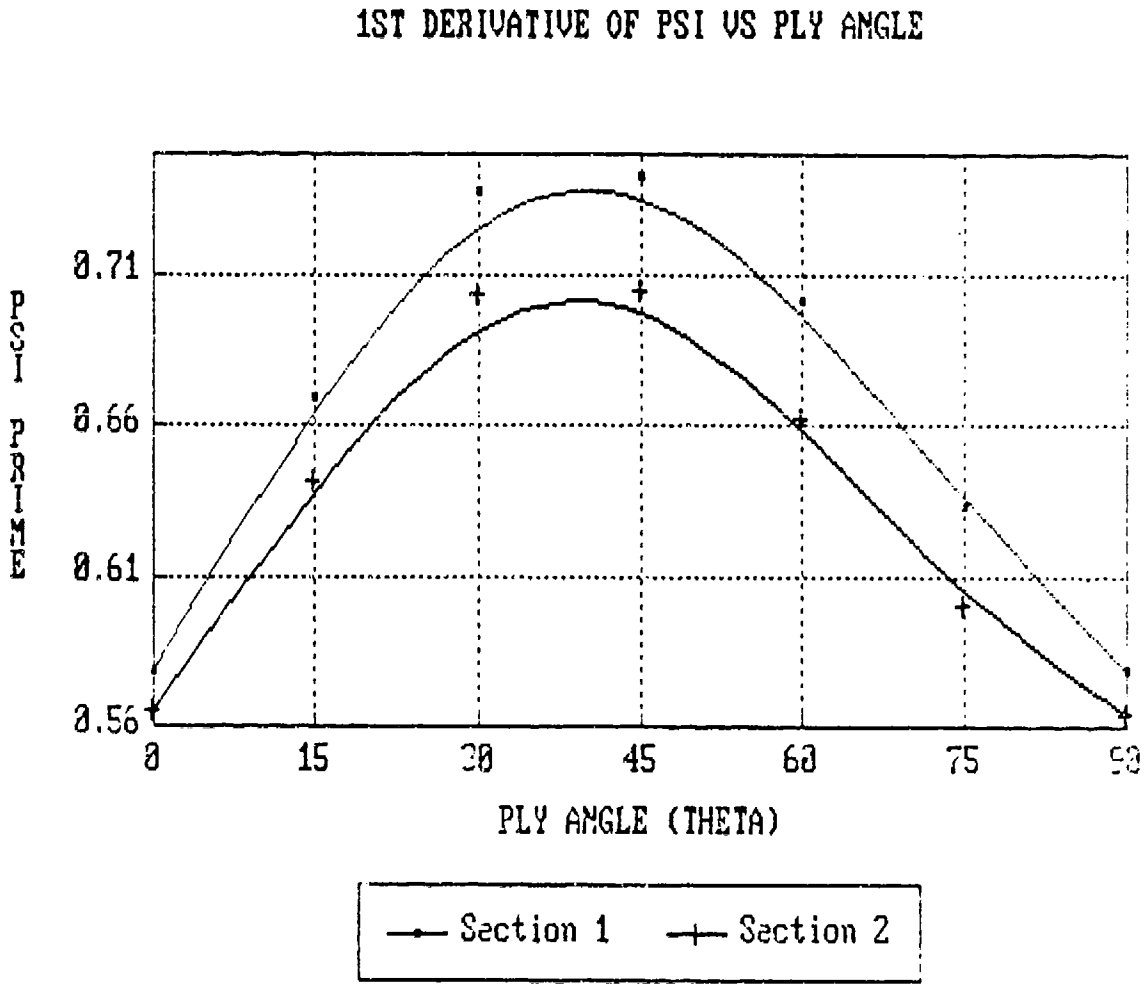
1ST DERIVATIVE OF PSI VS PLY ANGLE
PSI PRIME
0.71
0.66
0.61
0.56
0
15
30
45
60
75
90
PLY ANGLE (THETA)
Section 1
Section 2

FIGURE 6.3

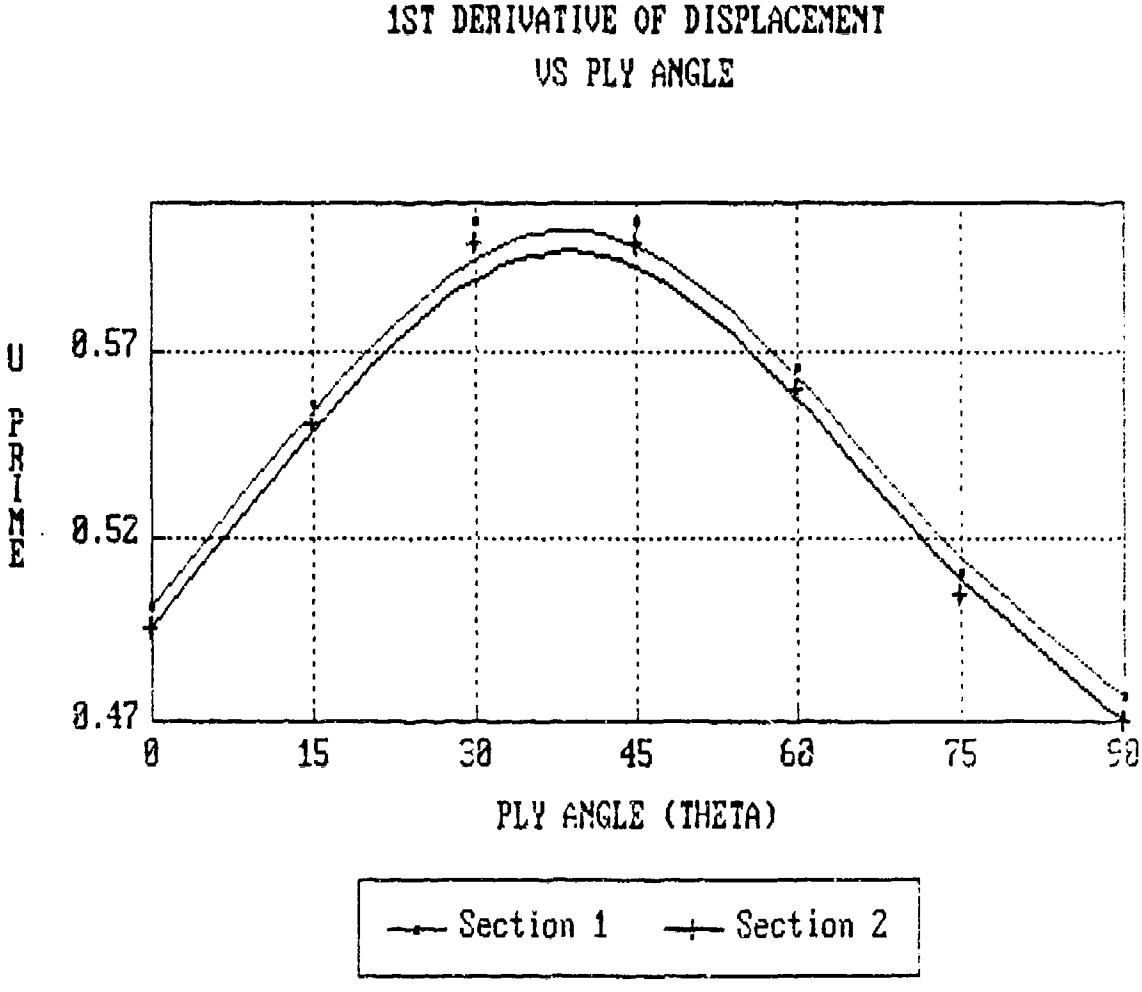
1ST DERIVATIVE OF DISPLACEMENT
VS PLY ANGLE
U PRIME
0.57
0.52
0.47
0
15
30
45
60
75
90
PLY ANGLE (THETA)
Section 1
Section 2

FIGURE 6.4

greater than the strength in the transverse direction. The UZ and UY displacements were examined for each blade and were determined to be correct. The laminate properties (Table 5.4) do not behave as expected but have been verified by three laminate analysis programs. It is also assumed that the geometry of the blade, modeled as a hollow unsymmetric laminated beam, causes the deviation from the plot of E_x and E_y which actually correspond to a flat laminated plate.

The responses of β, ϕ, ψ and u are plotted along the blade length and are shown by Figures 6.5 through 6.8. The results are as expected.

In Figure 6.5, which is the plot of the angle of twist along the blade length, it is expected that the twist of Blade 4 (See Chapter 6 for blade designation and description) would exhibit the minimum values for the anisotropic cases. It is also expected that Blade 1 and Blade 7 would be similar to each other and reach the highest values for twist. This was the case in Figure 6.5. The isotropic blade (Blade 8) results are plotted on this graph as a reference or base line case and are depicted by a straight line which reflects a minimum value linear twist. Figures 6.5 through 6.8 also accurately reflect the increase in twist, curvature, rotation and displacement along the blade span as the distance from the constrained end increases. There do not appear to be any negative end effects and one can assume that the data was taken at a sufficient distance from the end of the beam.

The nodal displacements and blade deformations provide valuable information in determining the elastic coupling responses of the anisotropic blade models. They also provide an acceptable vehicle for comparing the effects of ply orientation as a design parameter. In reference to the blade displacements, two points need to be made. First, the end caps were designed to be extremely stiff. To verify the accuracy of the force

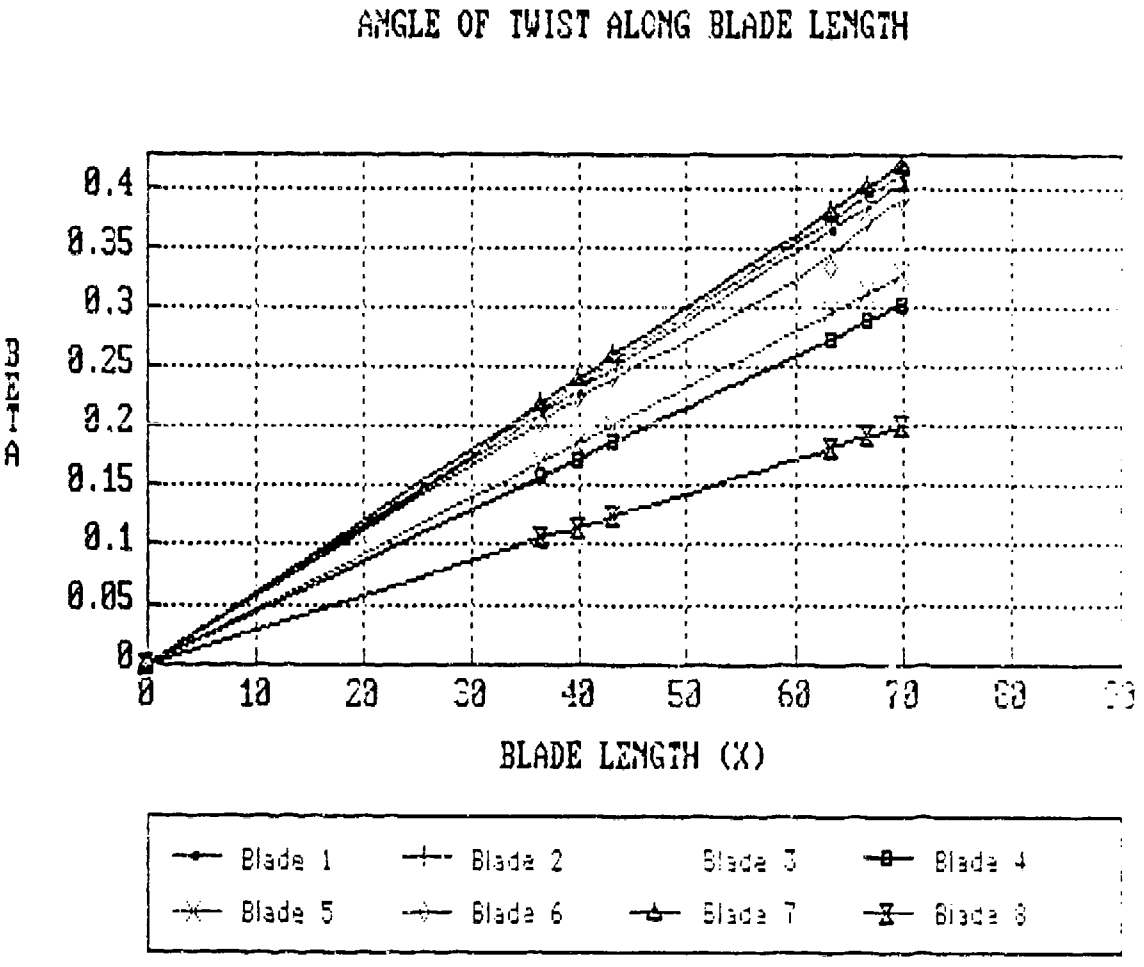
ANGLE OF TWIST ALONG BLADE LENGTH
BETA
0.4
0.35
0.3
0.25
0.2
0.15
0.1
0.05
0
0
10
20
30
40
50
60
70
80
BLADE LENGTH (X)
Blade 1
Blade 2
Blade 3
Blade 4
Blade 5
Blade 6
Blade 7
Blade 8

FIGURE 6.5

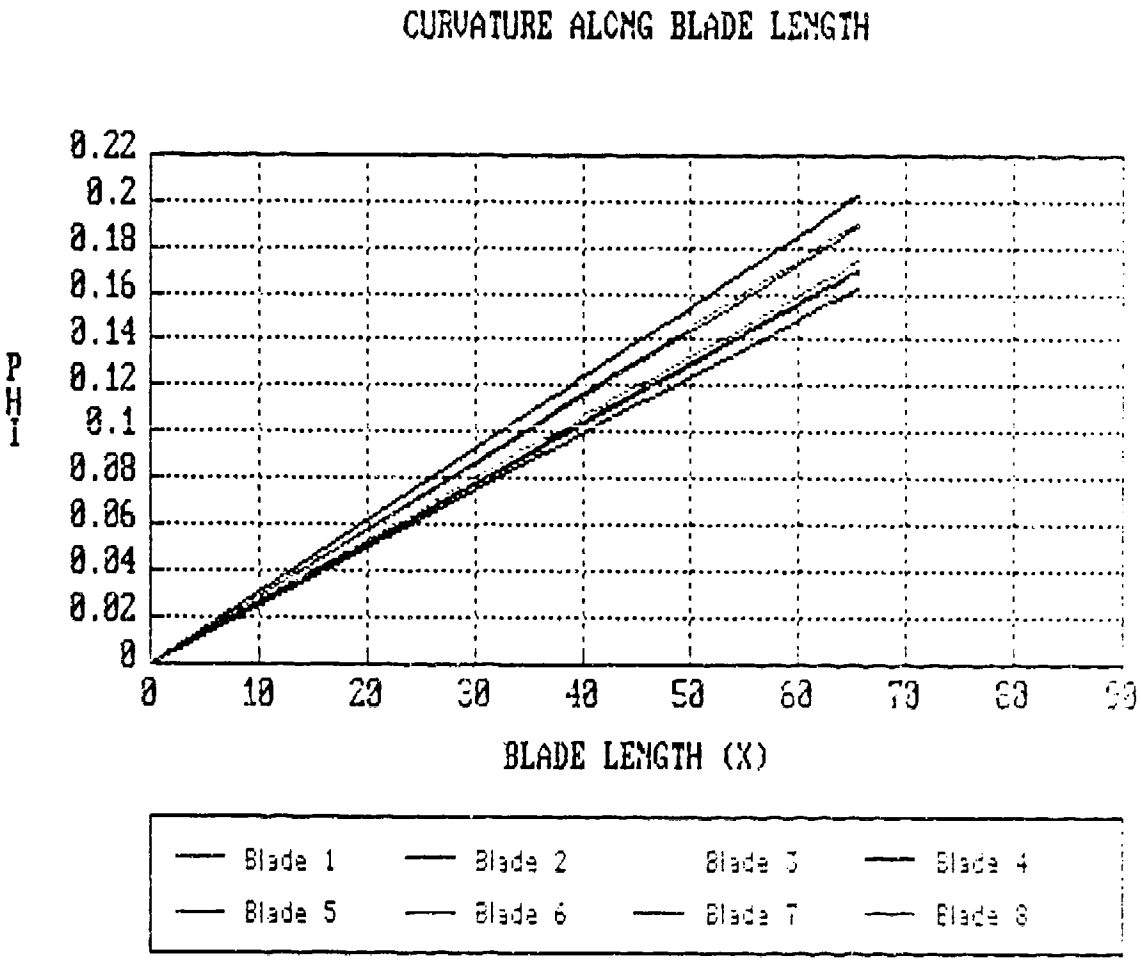
CURVATURE ALONG BLADE LENGTH
PHI
0.22
0.2
0.18
0.16
0.14
0.12
0.1
0.08
0.06
0.04
0.02
0
0
10
20
30
40
50
60
70
80
90
BLADE LENGTH (X)
Blade 1
Blade 2
Blade 3
Blade 4
Blade 5
Blade 6
Blade 7
Blade 8

FIGURE 6.6

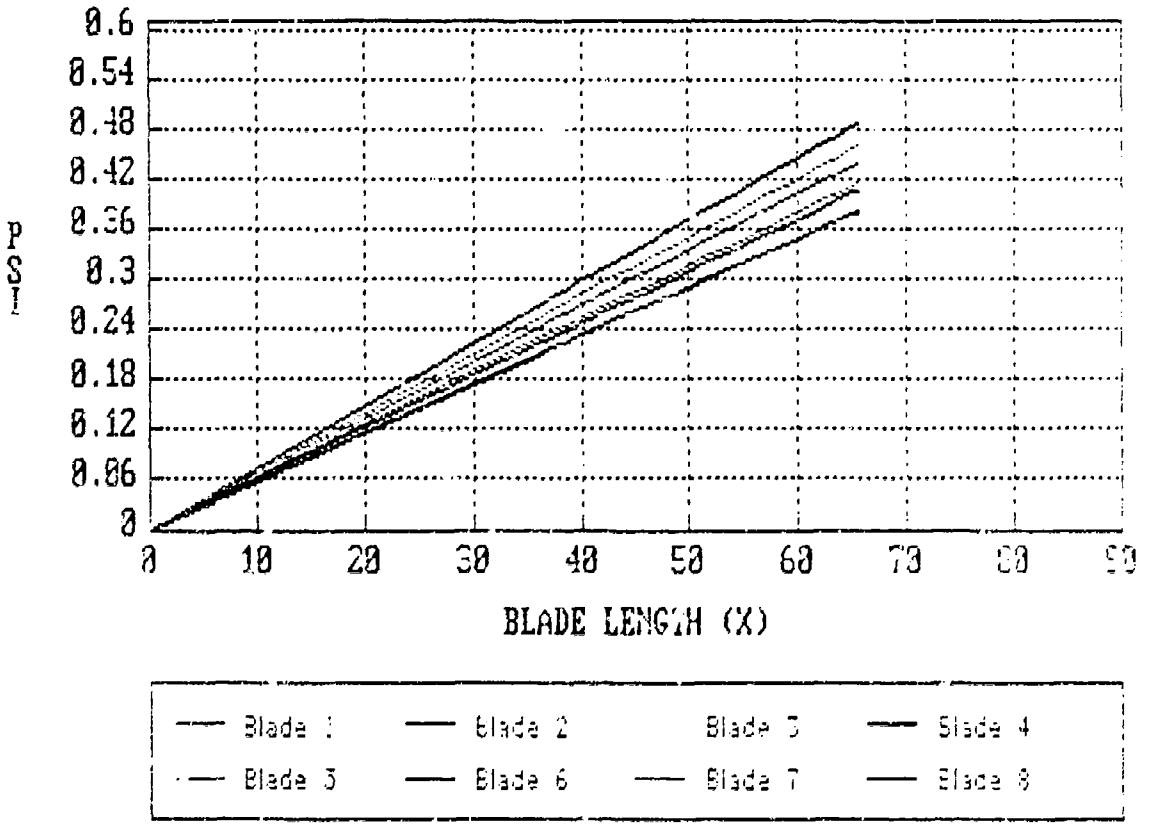
ROTATION ALONG BLADE LENGTH
0.6
0.54
0.48
0.42
0.36
0.3
0.24
0.18
0.12
0.06
0
PSI
0
10
20
30
40
50
60
70
80
90
BLADE LENGTH (X)
Blade 1
Blade 2
Blade 3
Blade 4
Blade 5
Blade 6
Blade 7
Blade 8

FIGURE 6.7

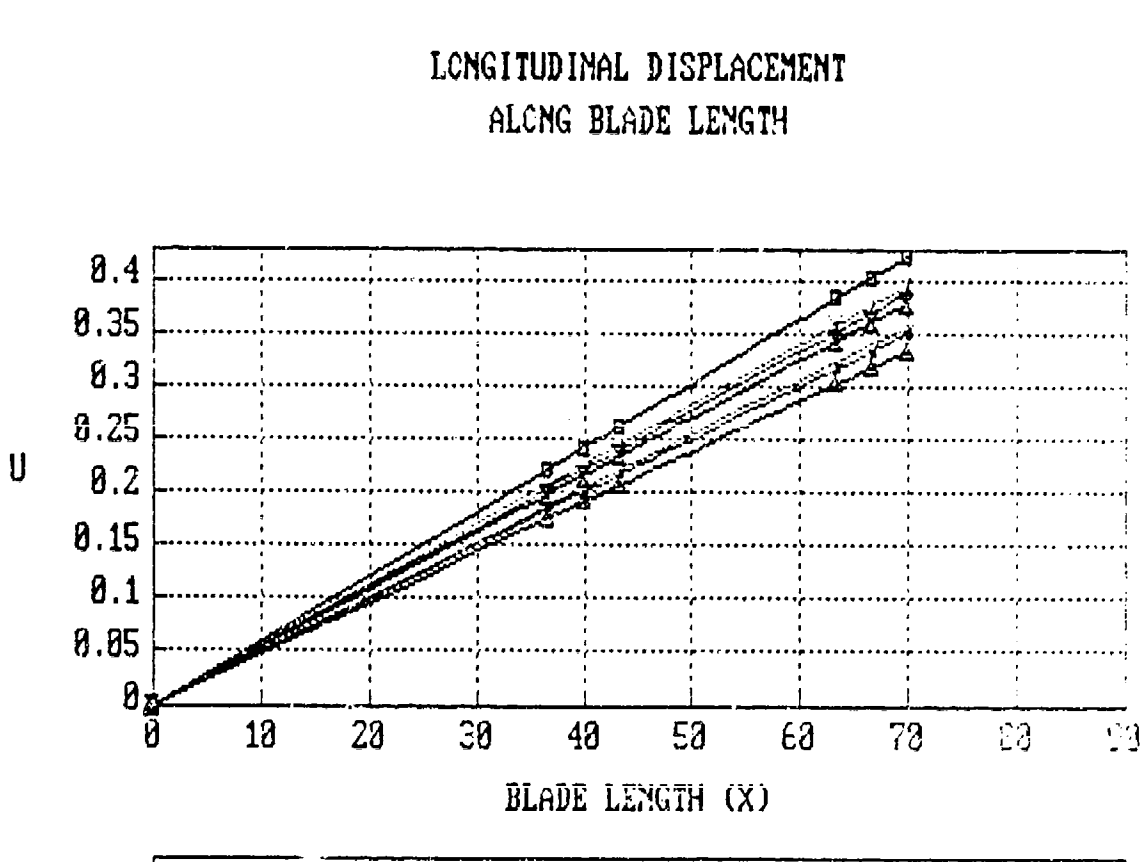
LONGITUDINAL DISPLACEMENT
ALONG BLADE LENGTH
U
0.4
0.35
0.3
0.25
0.2
0.15
0.1
0.05
0
0
10
20
30
40
50
60
70
80
90
BLADE LENGTH (X)
Blade 1
Blade 2
Blade 3
Blade 4
Blade 5
Blade 6
Blade 7
Blade 8

FIGURE 6.8

application on the end cap, two procedures were attempted. A bending moment of *1000* units was applied at one node on the end cap and the displacements were recorded. The bending moment was then distributed about each node on the outside edge of the endcap and the displacements were again recorded. The displacements were identical in both cases and verified that the end cap was not deforming undesirably and that the moment application was correct. The second point of interest is that the outside surface of the blade had a tendency to deform unfavorably under stress and as a result the displacement data was only taken at the leading and trailing edges. To correct for this, the model needs to be reinforced with ribs along the entire length of the blade. These ribs could be constructed in a similar fashion as the end caps.

Figure 6.9 represents a theoretical view of what might happen when a single force is applied to an anisotropic blade. The actual displacements can be seen in Figures 6.10 through 6.41 which are located at the end of this chapter. As a point of reference, the isotropic blade (Blade 8) needs to be examined. Figures 6.38 through 6.41 present a visual representation of the blade response of an isotropic lamination sequence under torsion, bending and extension. Figure 6.38 reveals that as a constant torque is applied at the shear center, the entire blade twists around that point. When comparing that with an anisotropic lay-up, Figure 6.18 for example, one can see that the blade twists about a different axis which is located toward the trailing edge and that there is some flapping or bending about the *y*-axis. This is the coupling which is a result of the anisotropic lamination and which is predicted in the bending-stiffness matrix, [D], of lamination theory. A similar investigation of the application of an axial force along the neutral axis, (Figure 6.41), reveals that as the isotropic blade is pulled, the result is extension in the *x* direction and nothing else. When this is compared to the response of an anisotropic blade under

identical loading conditions, Figure 6.21 for example, one can see that in addition to

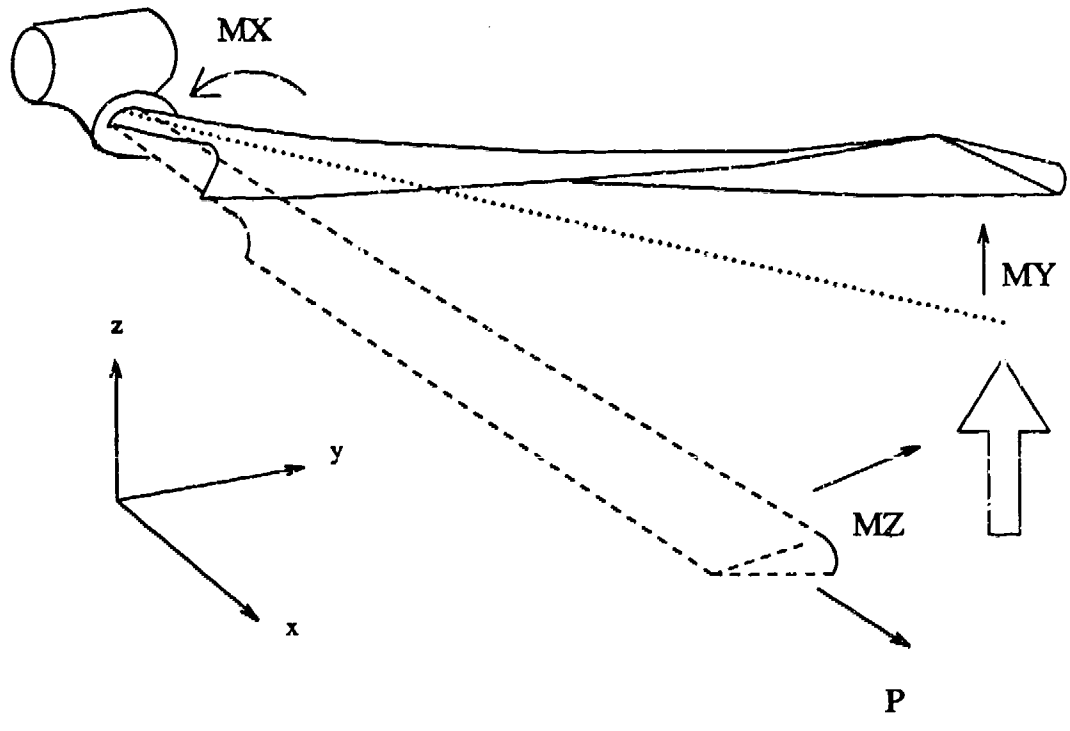

FIGURE 6.9. Elastic Bending-Torsion Coupling of Rotor Blade

extension, the blade underwent bending about the y and z axes and twisting about the x-axis. This can be predicted by the extensional-stiffness matrix, [A], and the bending-stiffness matrix [D]. Since the laminates used in this research were symmetric (See page 2), the extensional-bending coupling matrix, [B], is zero and would not normally have any effect on the response of the model. However, since the model is not symmetric with respect to the $x-z$ plane, there are some minor effects from this type of coupling. These

can be seen in Figures 6.19 and 6.20. All of the blade deformations are depicted in Figures 6.10 through 6.41 and can be used to examine the varying effects of lamination sequence on displacement and coupling.

The results provided by each of these media allow us to examine the effects of ply orientation and to compute the coupling terms of the accompanying stiffness matrices. This work should lead to a much improved capability for evaluating blade properties for use in rotorsystems.

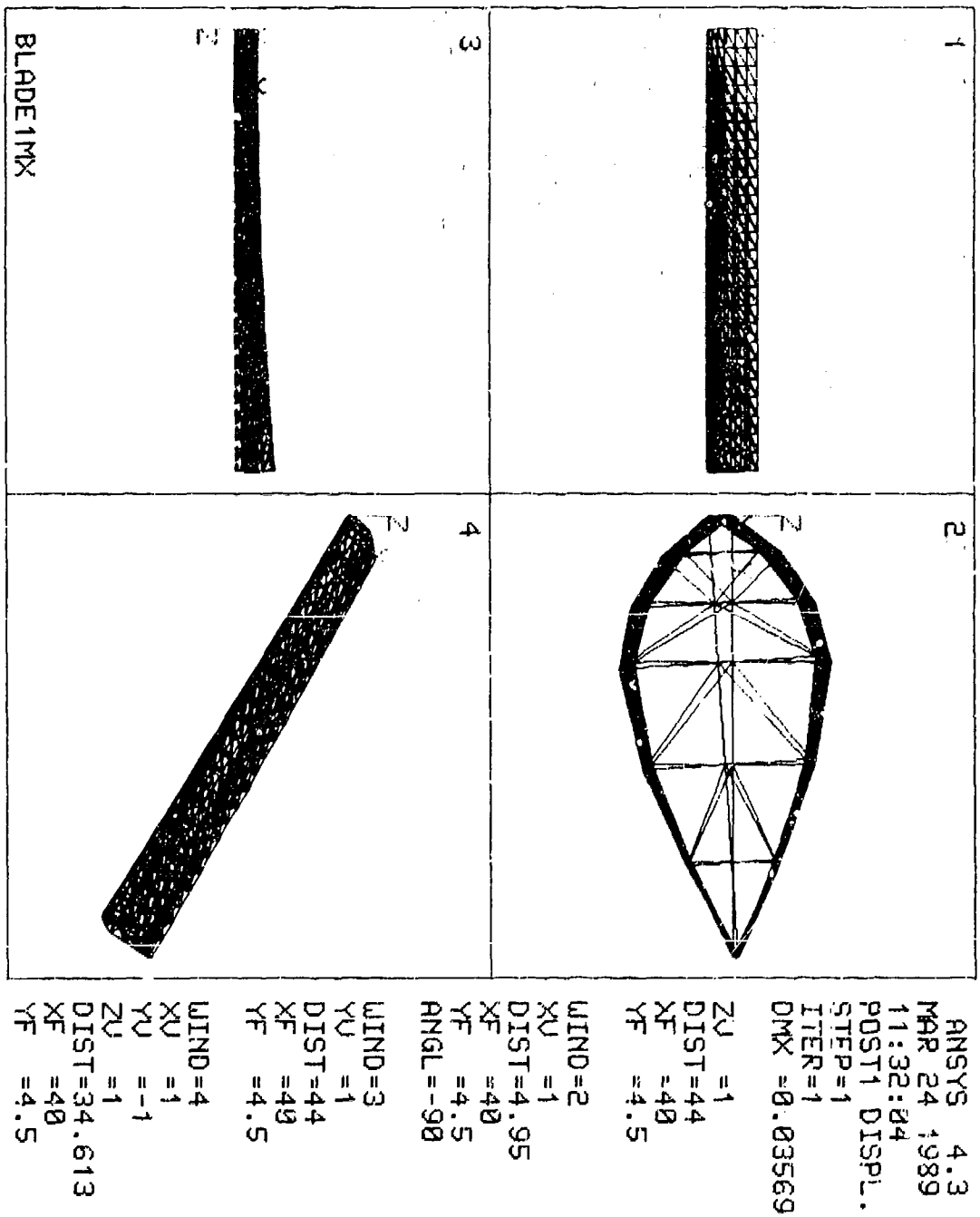

FIGURE 6.10

Blade One (Anisotropic) Under Torsional Load

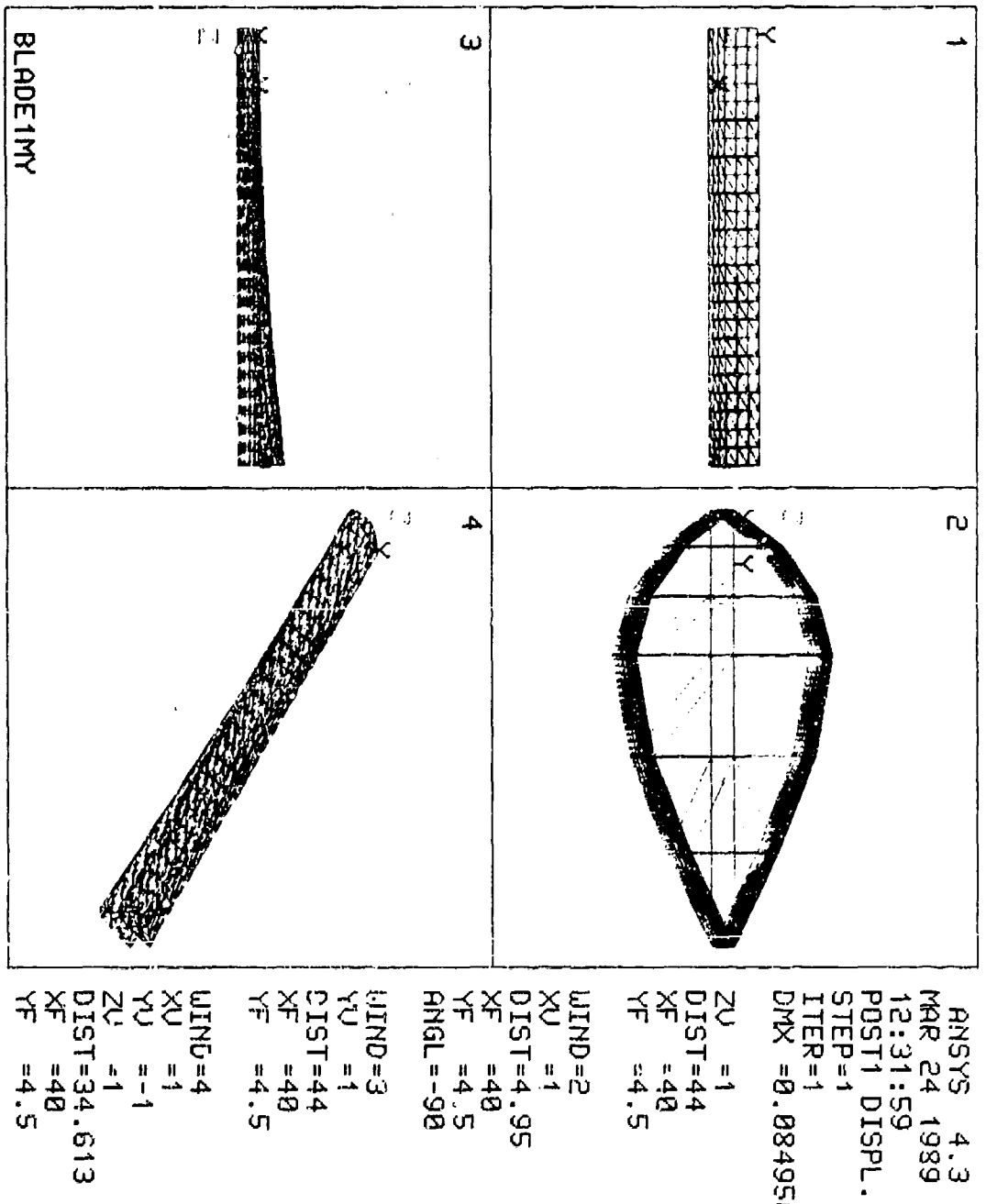

FIGURE 6.11

Blade One (Anisotropic) Under Bending Moment (Y)

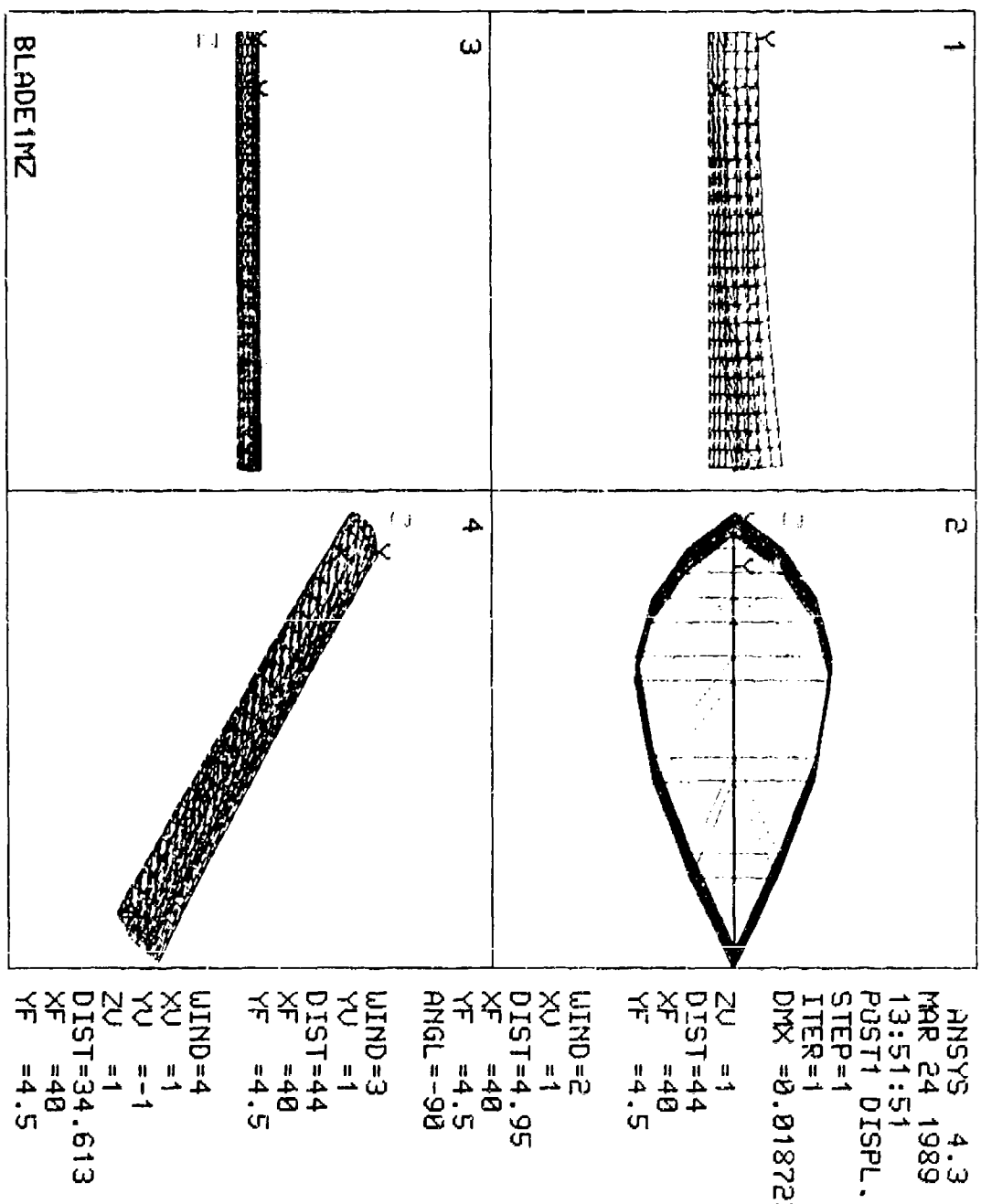

FIGURE 6.12

Blade One (Anisotropic) Under Bending Moment (Z)

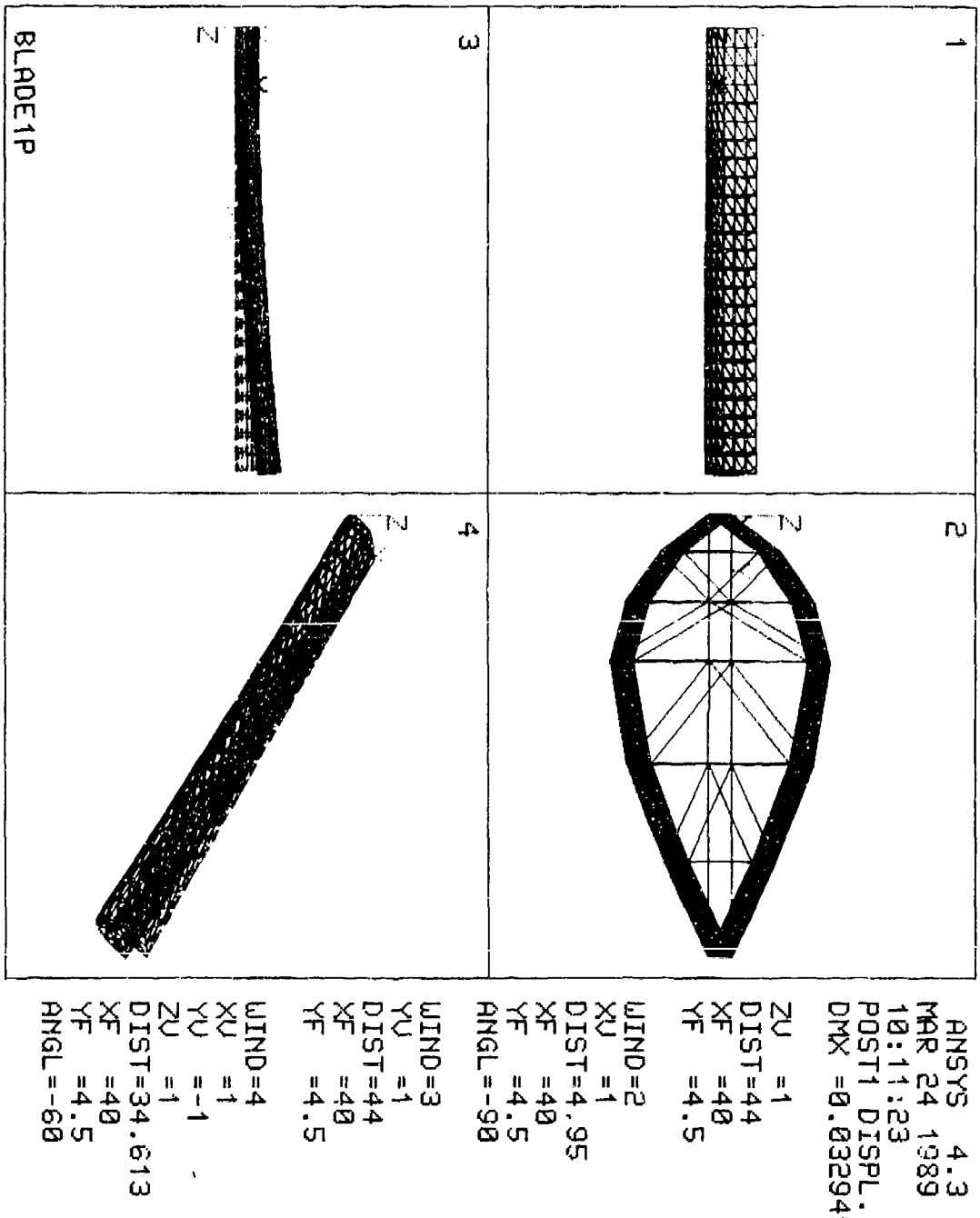

FIGURE 6.13

Blade One (Anisotropic) Under Axial Load

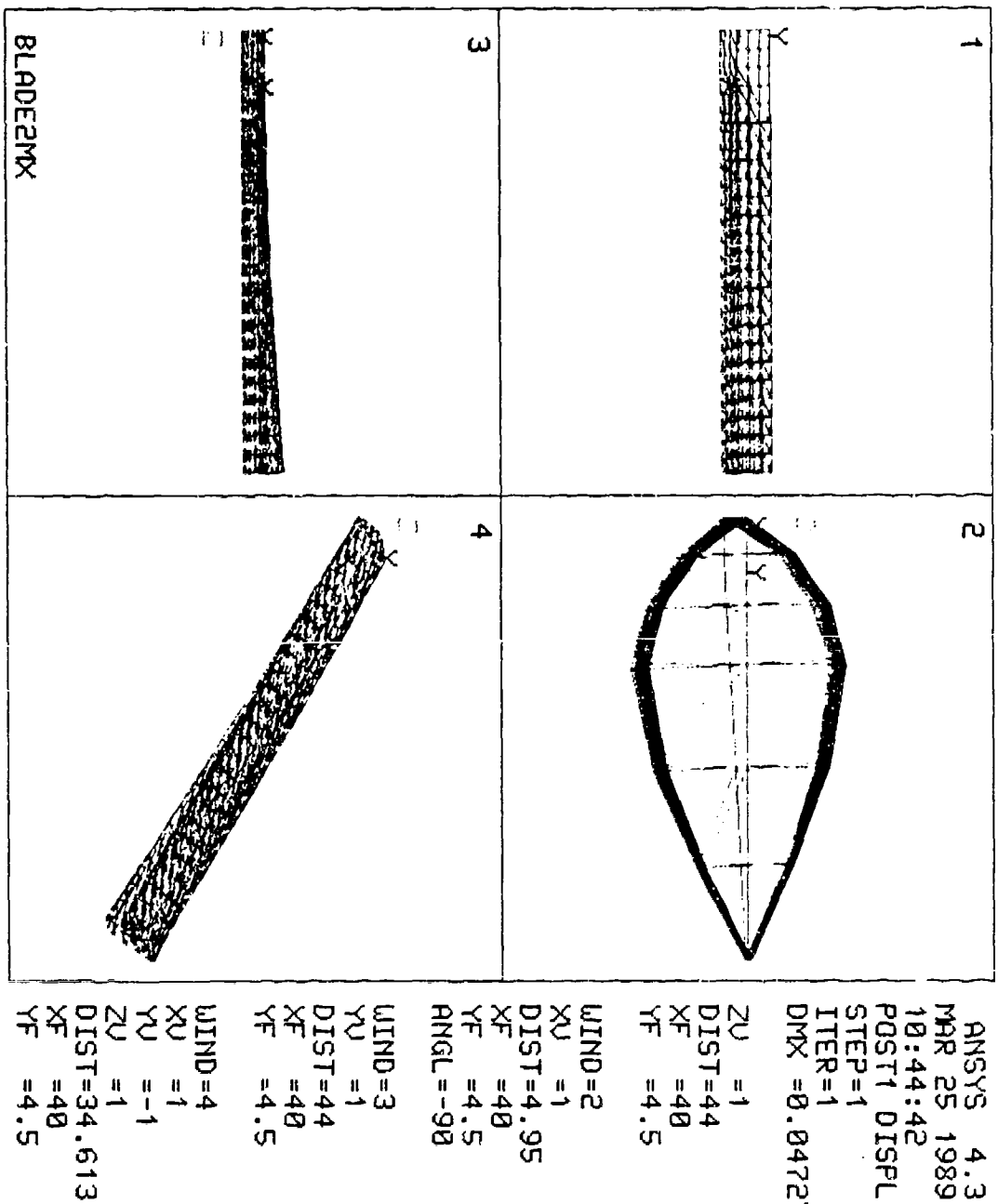

FIGURE 6.14

Blade Two (Anisotropic) Under Torsional Load

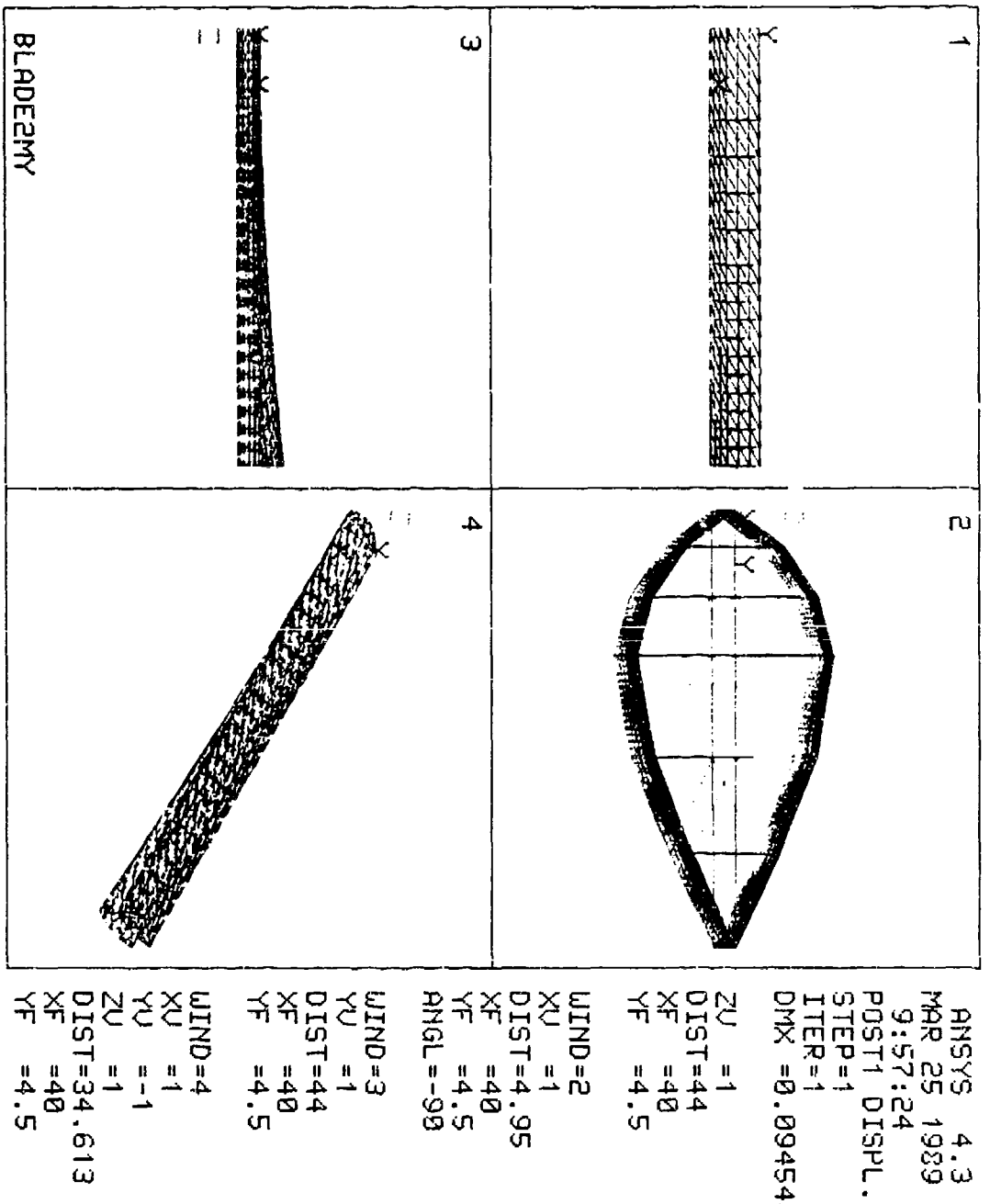

FIGURE 6.15

Blade Two (Anisotropic) Under Bending Moment (Y)

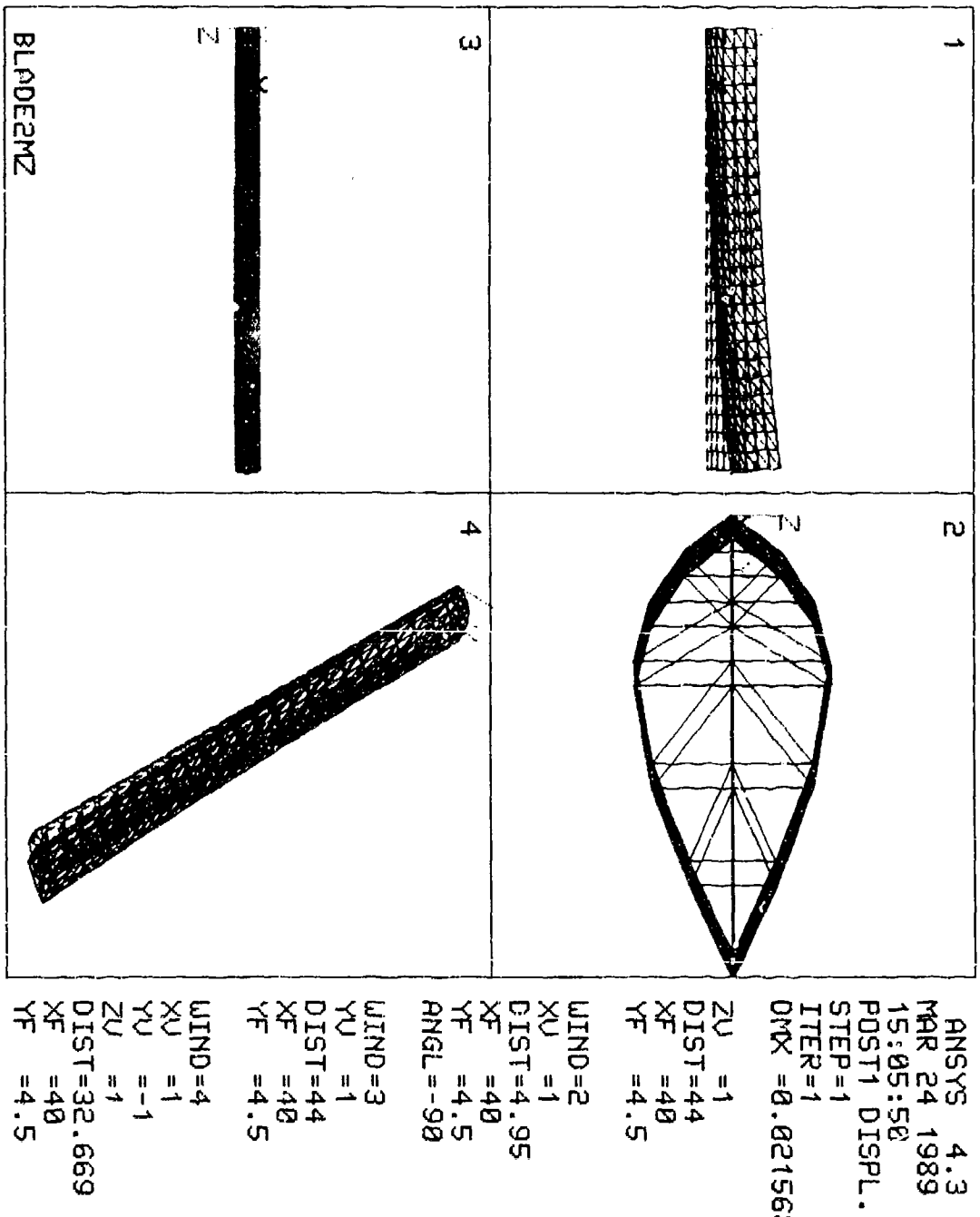

FIGURE 6.16

Blade Two (Anisotropic) Under Bending Moment (Z)

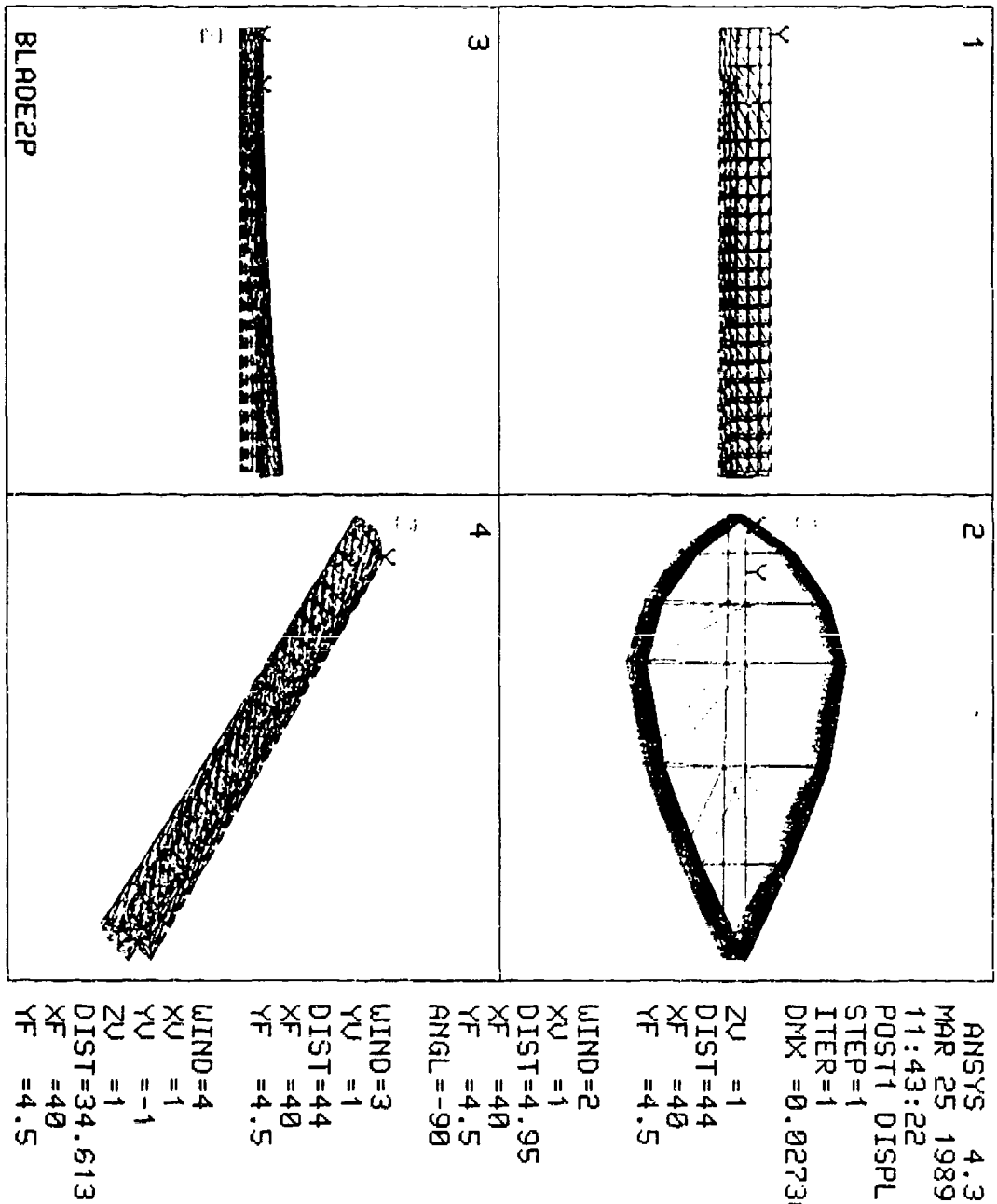

FIGURE 6.17

Blade Two (Anisotropic) Under Axial Load

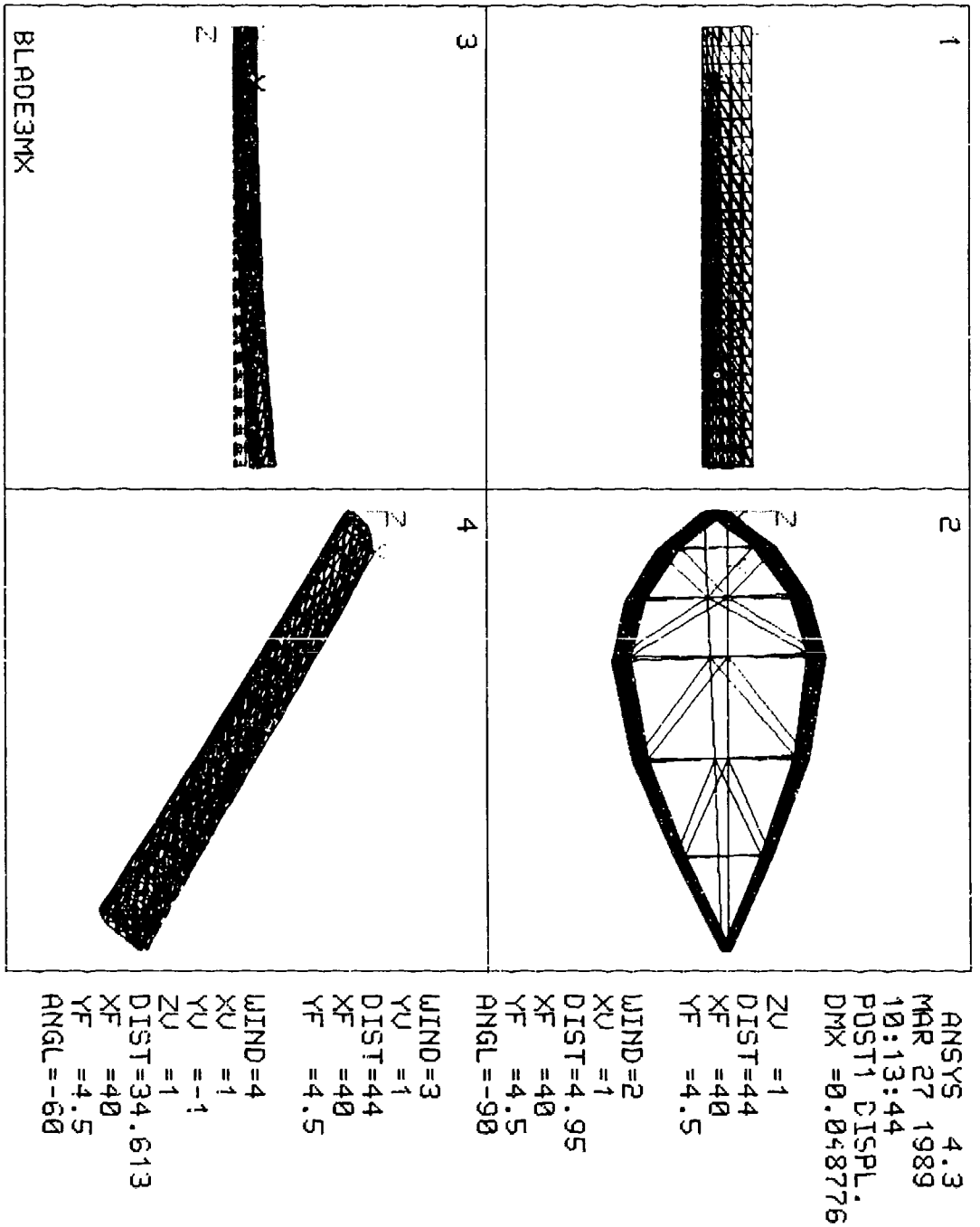

FIGURE 6.18

Blade Three (Anisotropic) Under Torsional Load

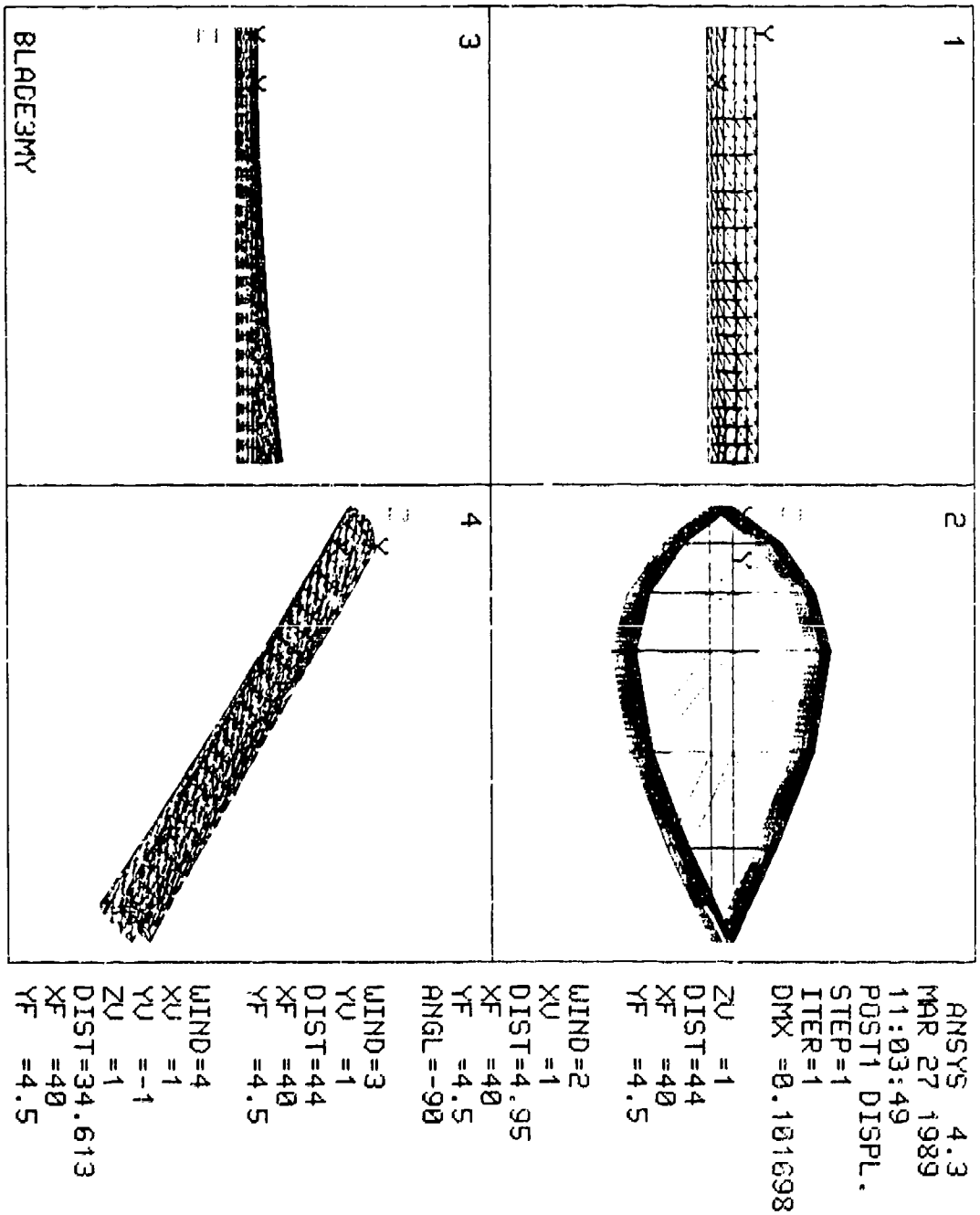

FIGURE 6.19

Blade Three (Anisotropic) Under Bending Moment (Y)

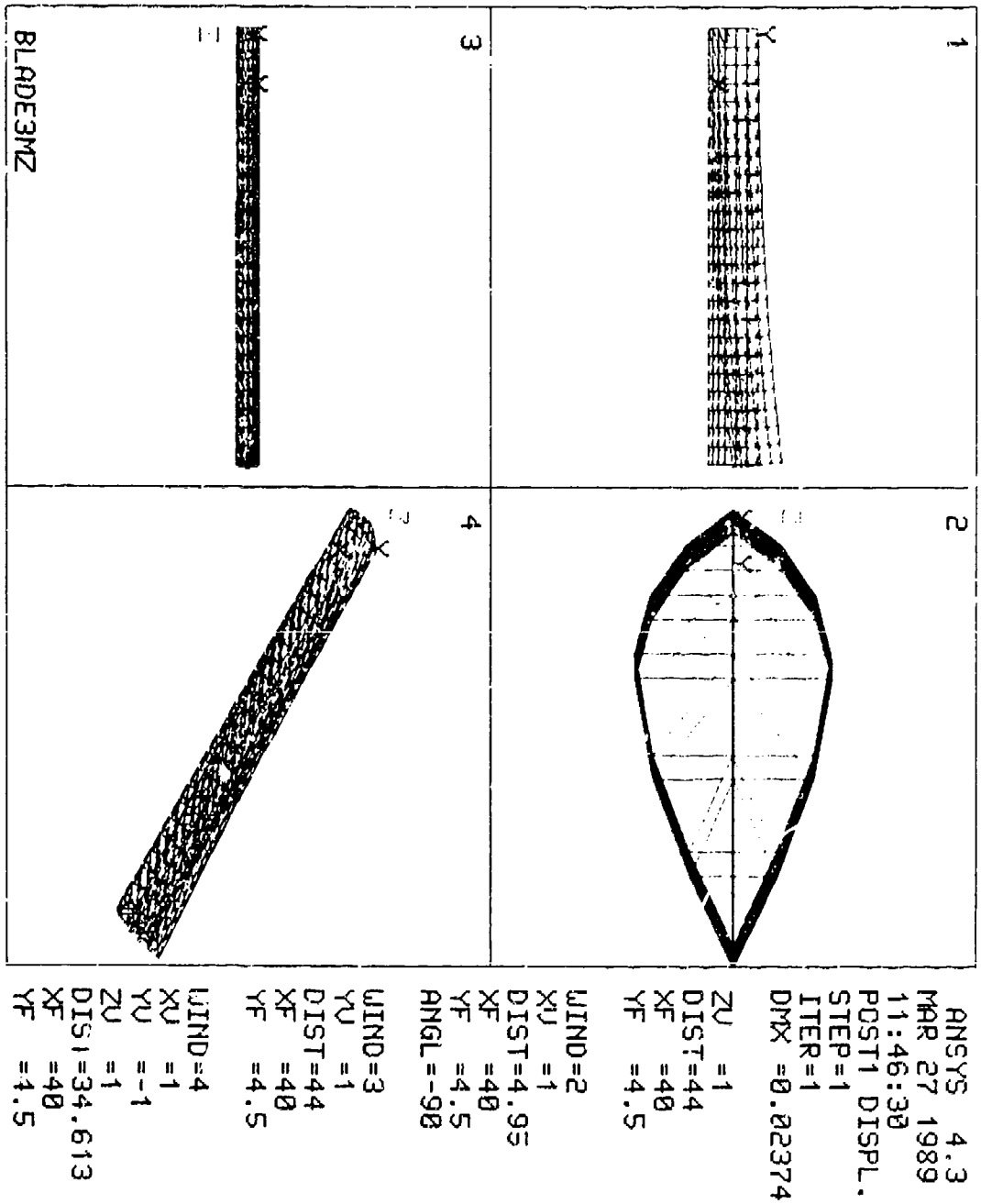

FIGURE 6.20

Blade Three (Anisotropic) Under Bending Moment (Z)

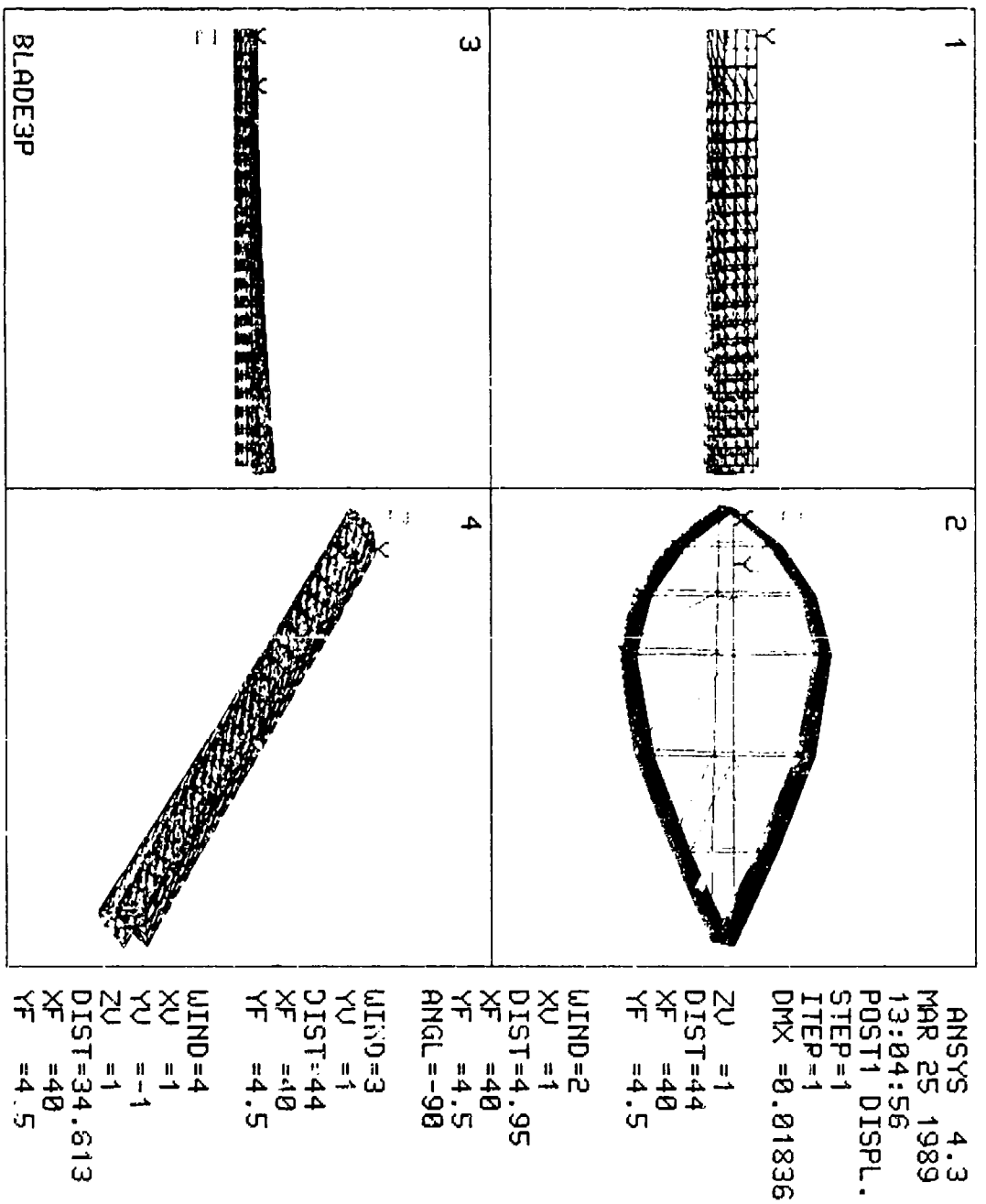

FIGURE 6.21

Blade Three (Anisotropic) Under Axial Load

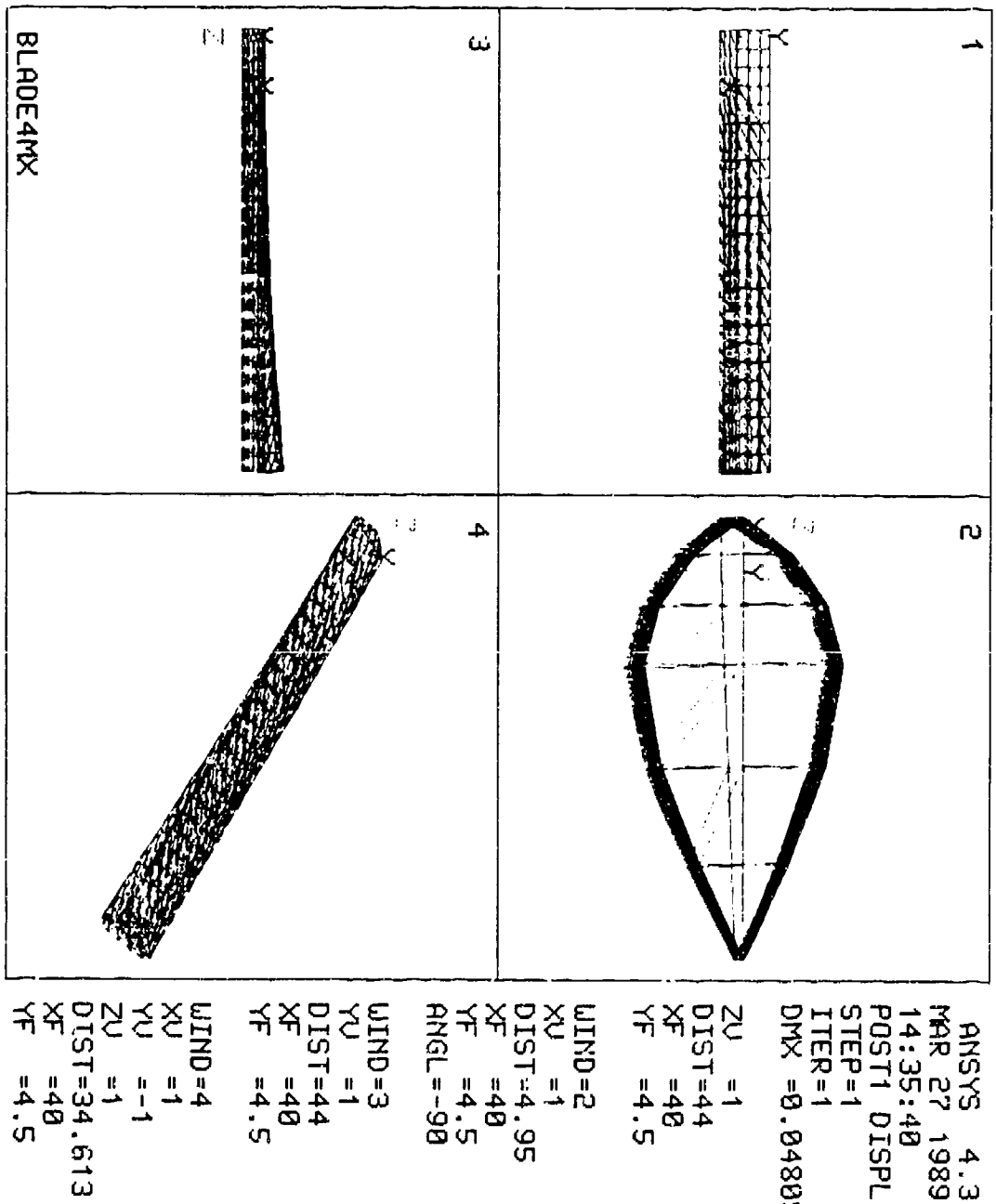

FIGURE 6.22

Blade Four (Anisotropic) Under Torsional Load

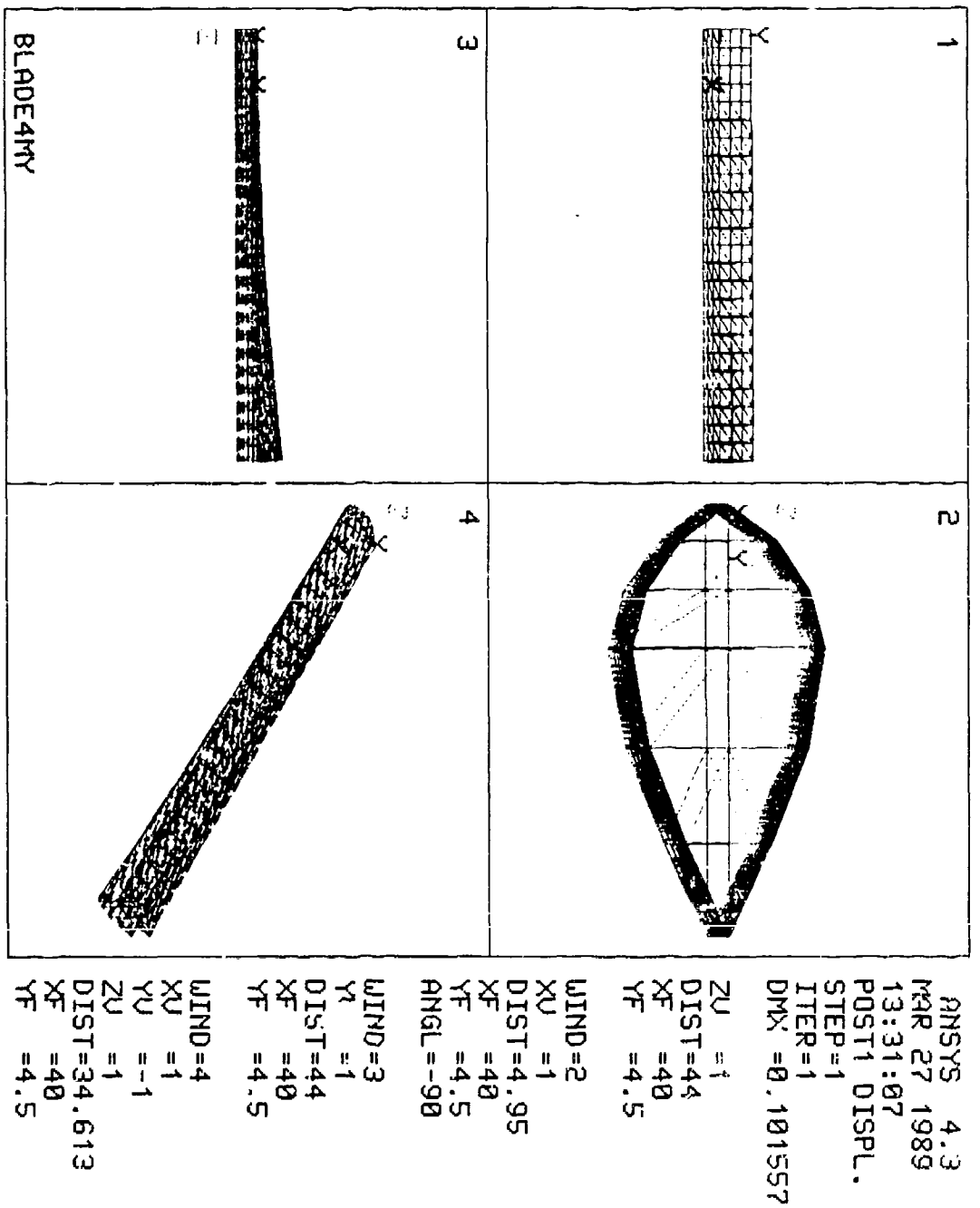

FIGURE 6.23

Blade Four (Anisotropic) Under Bending Moment (Y)

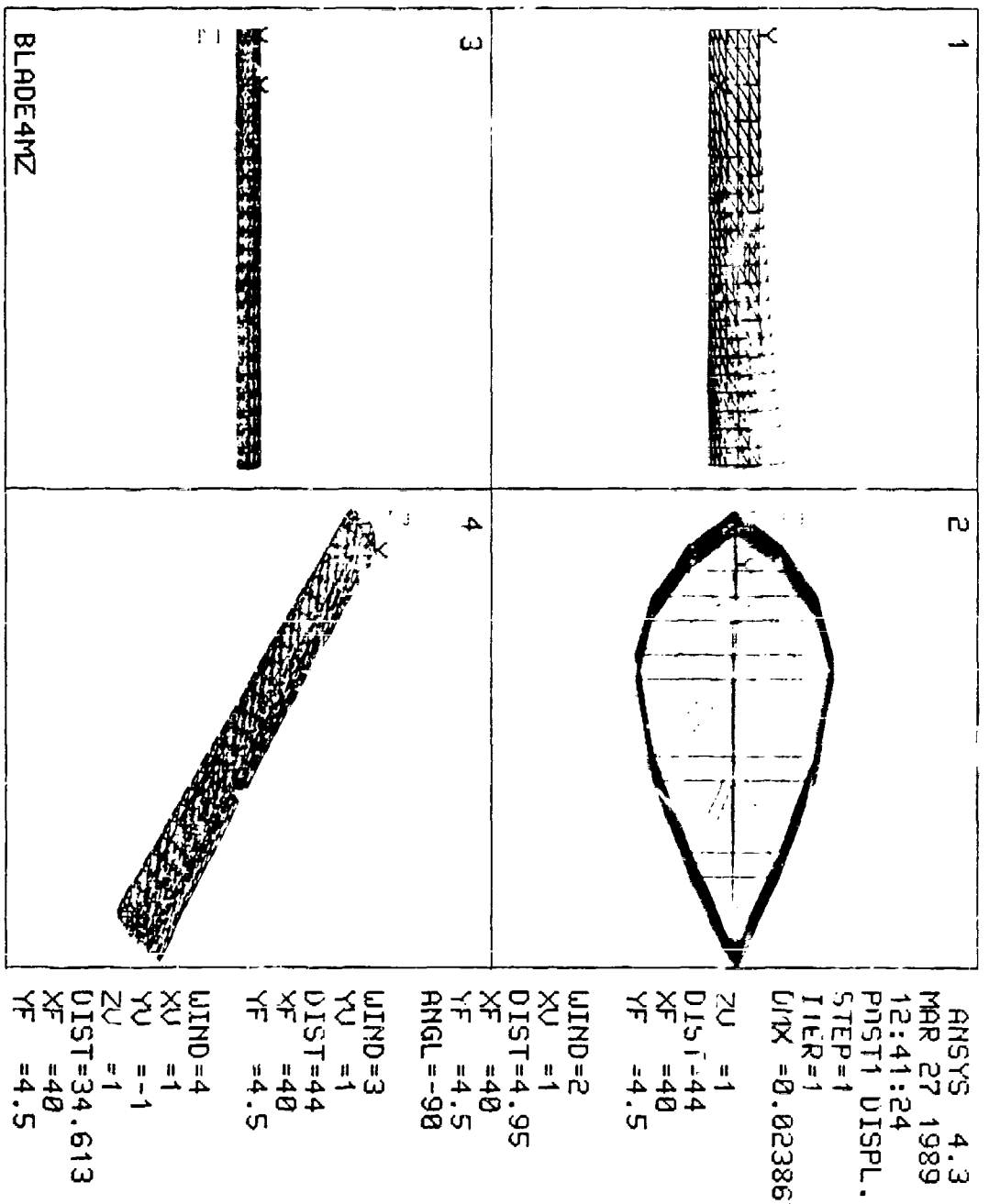

FIGURE 6.24

Blade Four (Anisotropic) Under Bending Moment (Z)

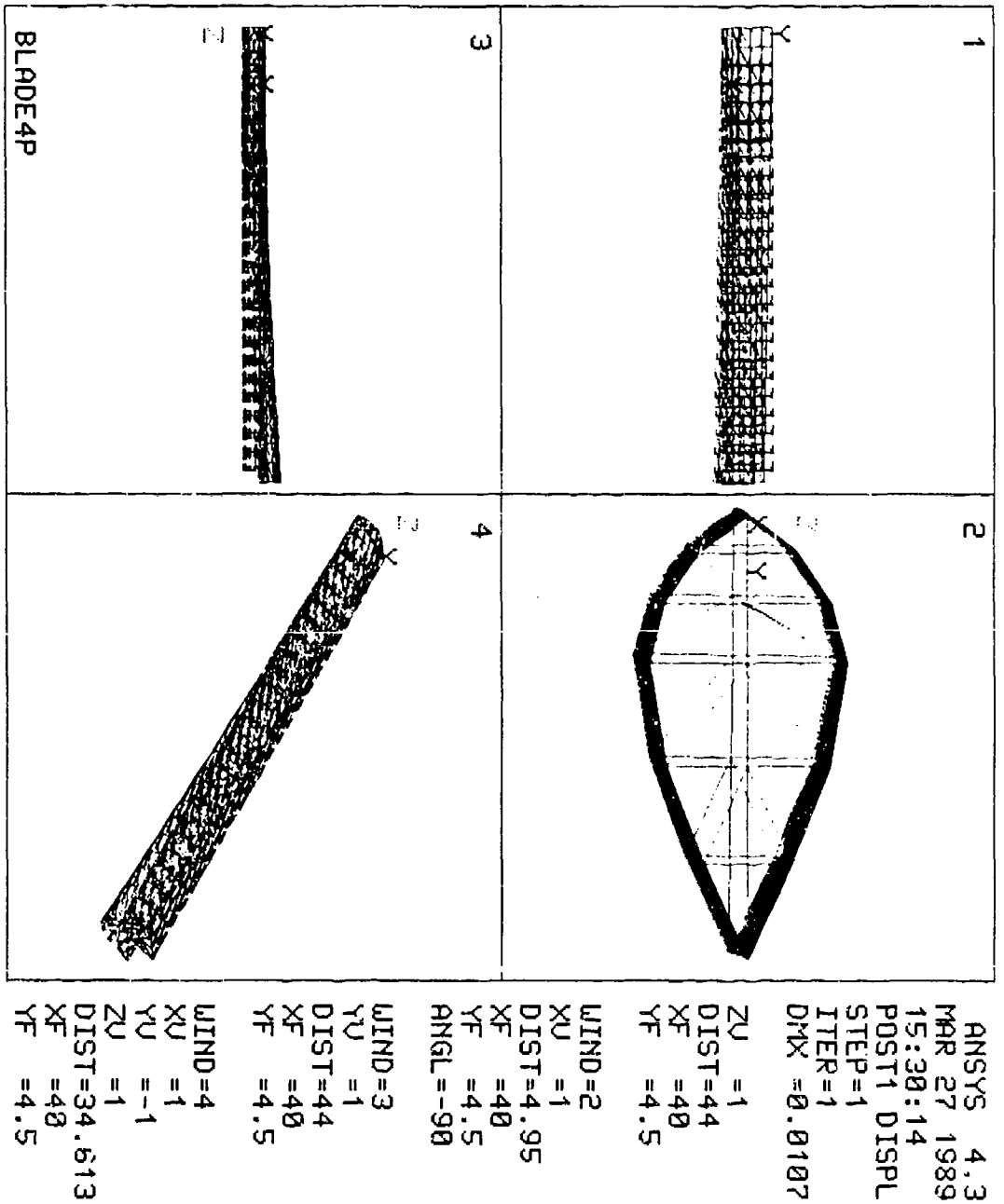

FIGURE 6.25

Blade Four (Anisotropic) Under Axial Load

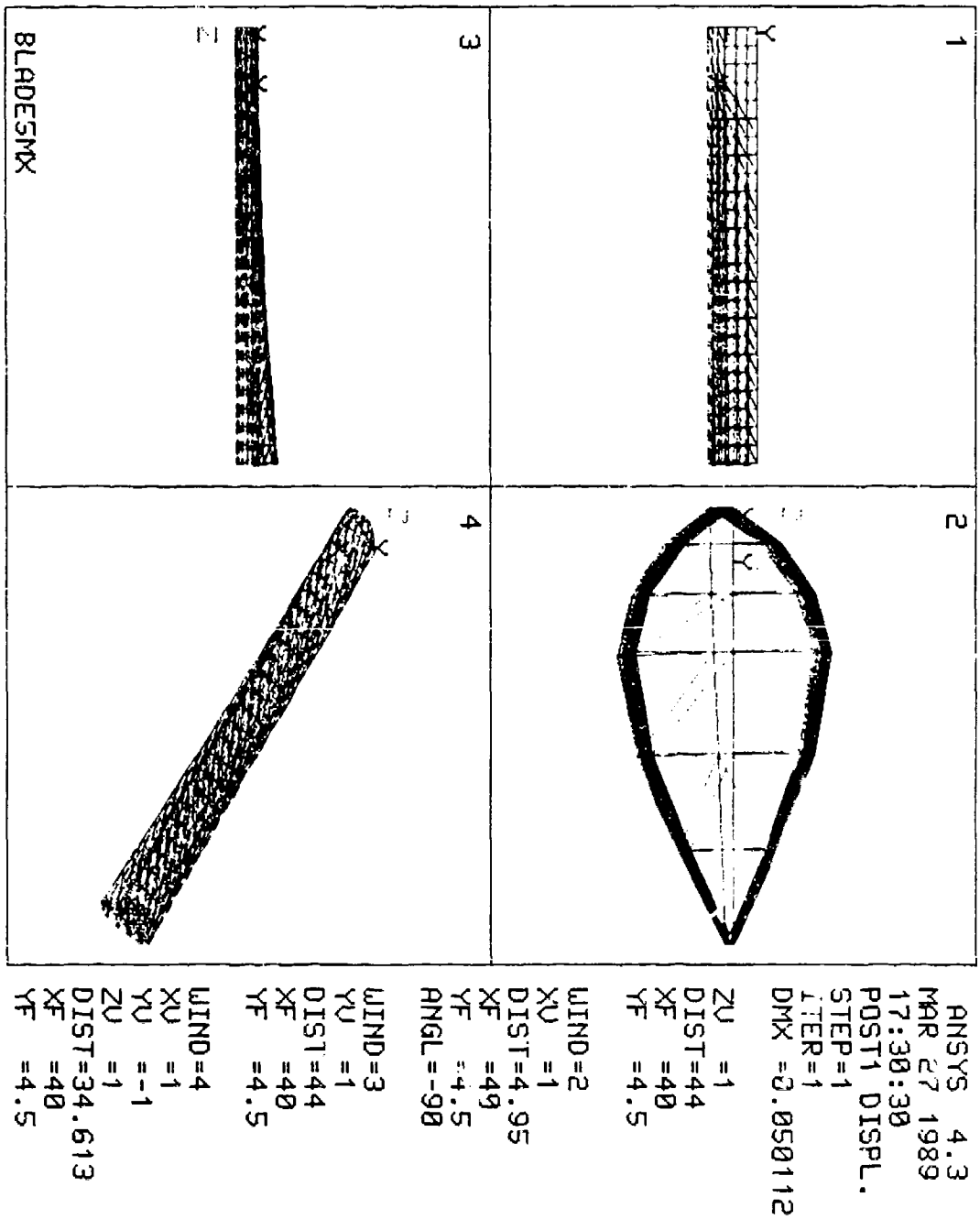

FIGURE 6.26

Blade Five (Anisotropic) Under Torsional Load

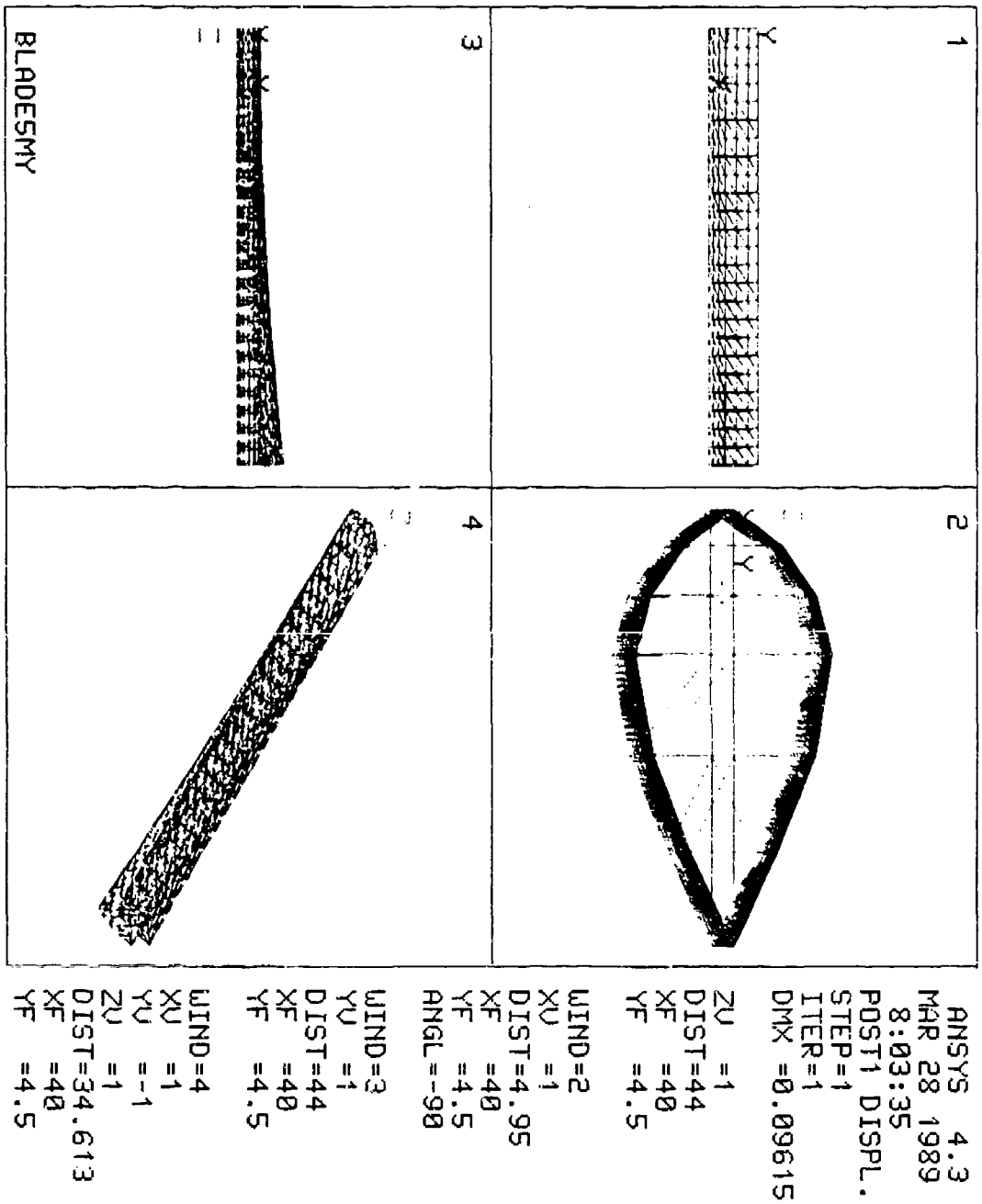

FIGURE 6.27

Blade Five (Anisotropic) Under Bending Moment (Y)

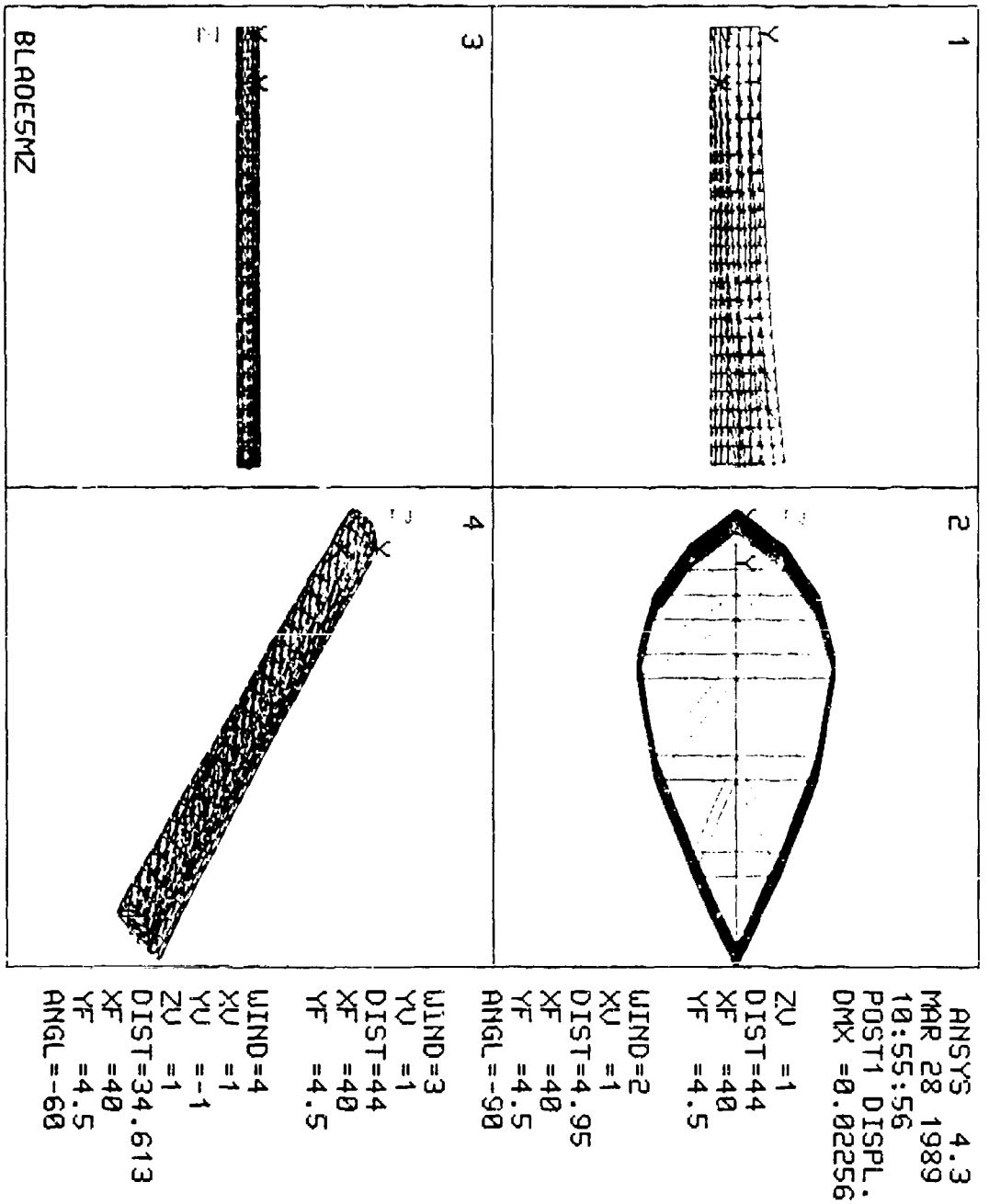

FIGURE 6.28

Blade Five (Anisotropic) Under Bending Moment (Z)

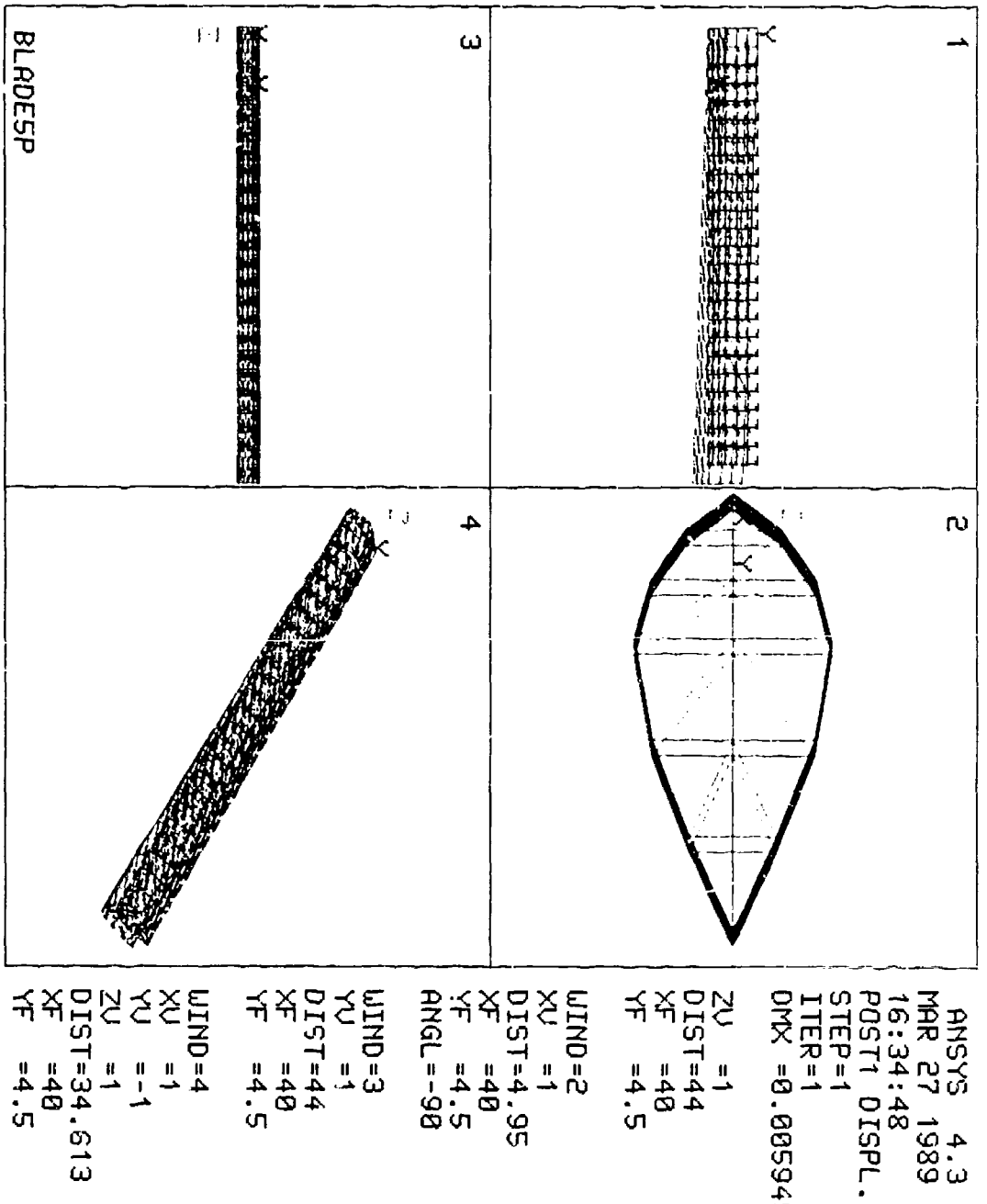

FIGURE 6.29

Blade Five (Anisotropic) Under Axial Load

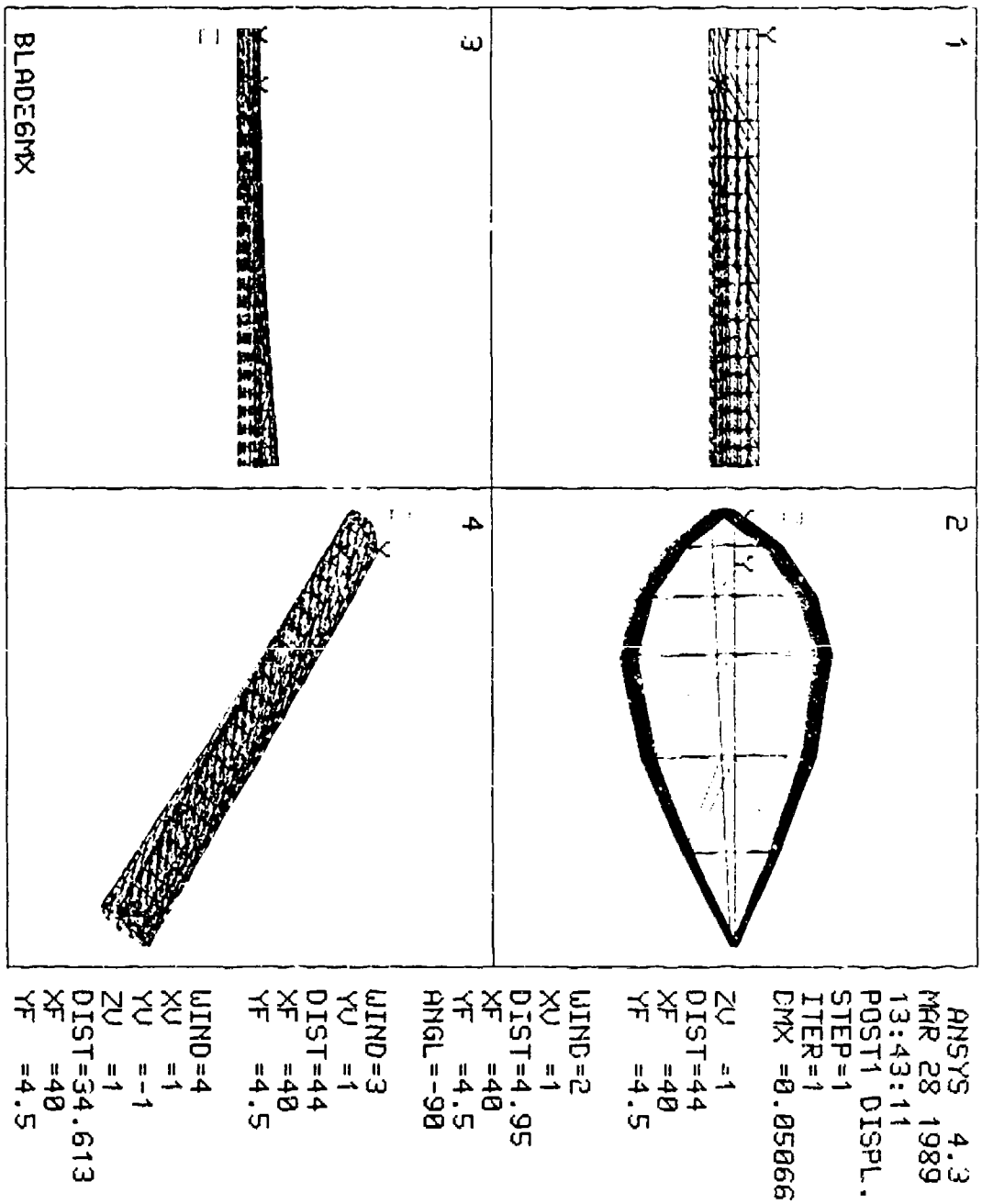

FIGURE 6.30

Blade Six (Anisotropic) Under Torsional Load

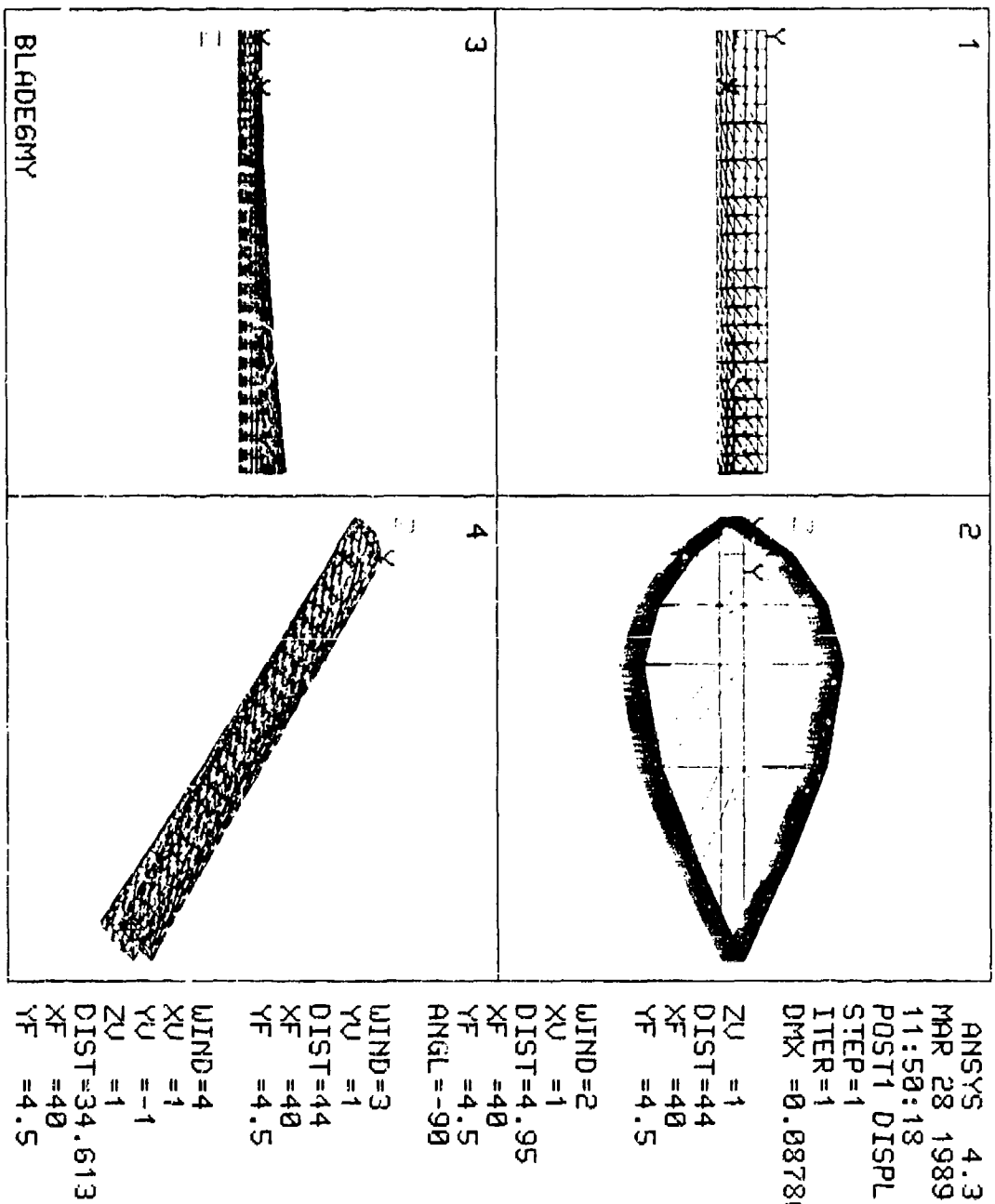

FIGURE 6.2'

Blade Six (Anisotropic) Under Bending Moment (Y)

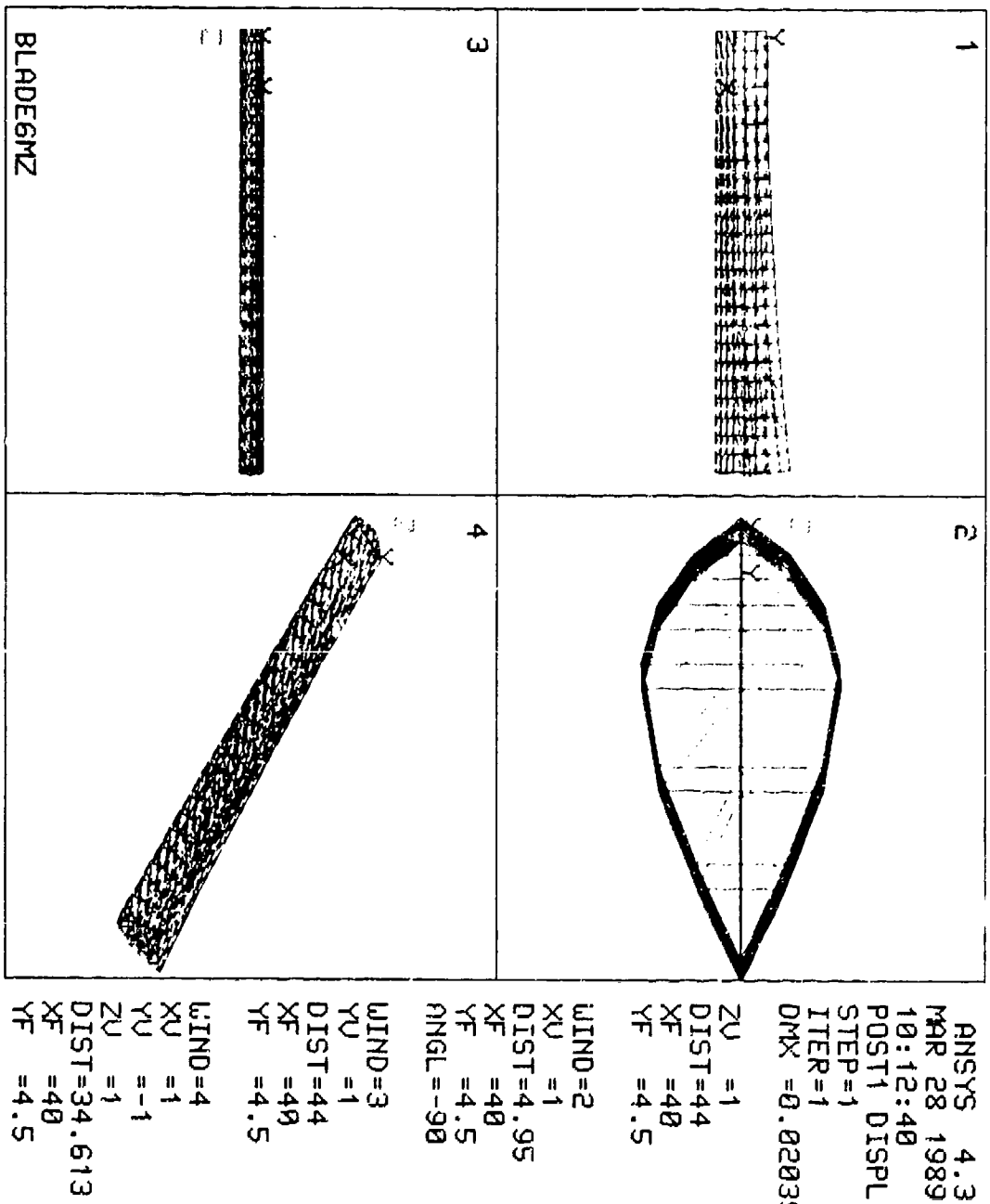

FIGURE 6.32

Blade Six (Anisotropic) Under Bending Moment (Z)

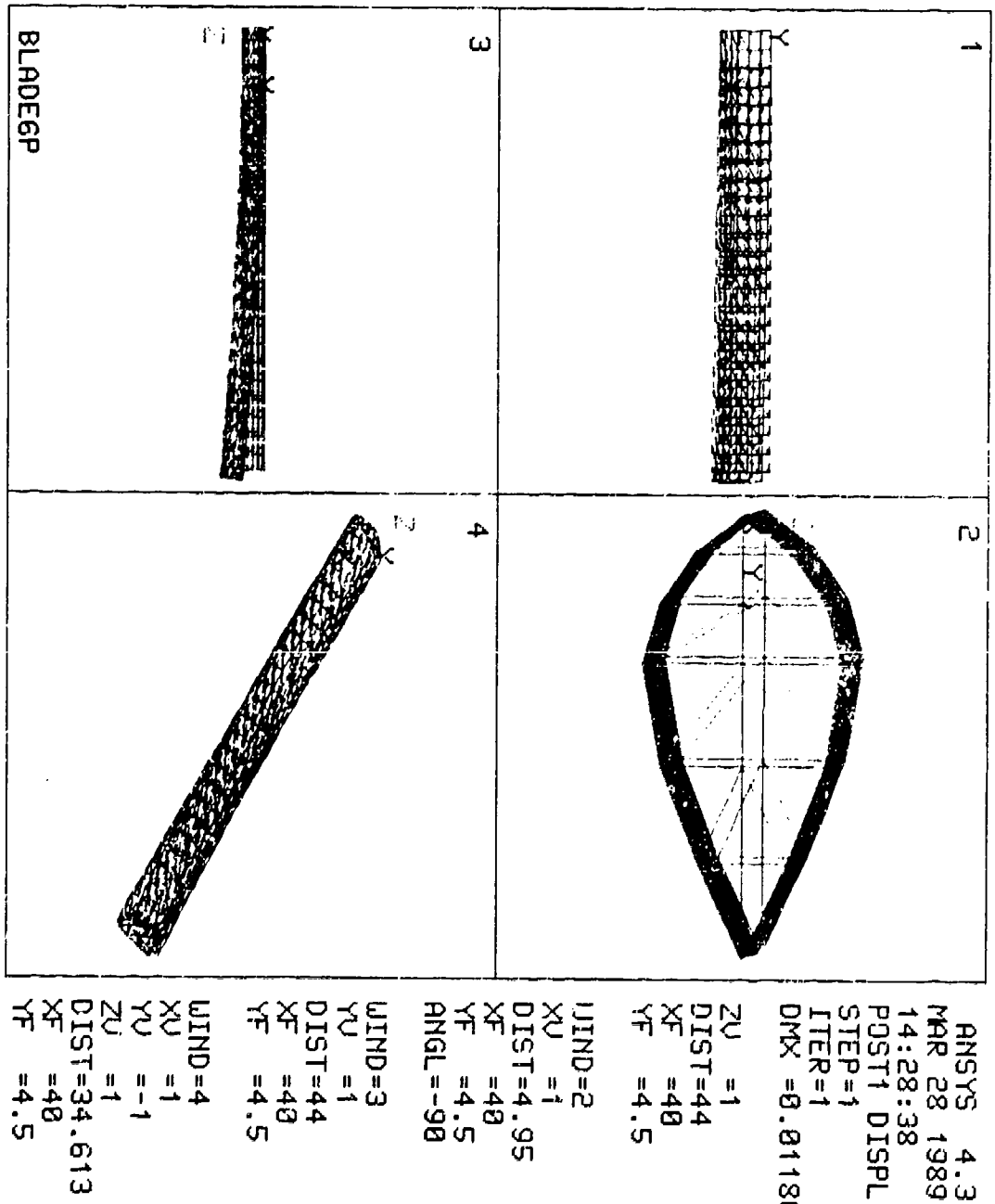

FIGURE 6.33

Blade Six (Anisotropic) Under Axial Load

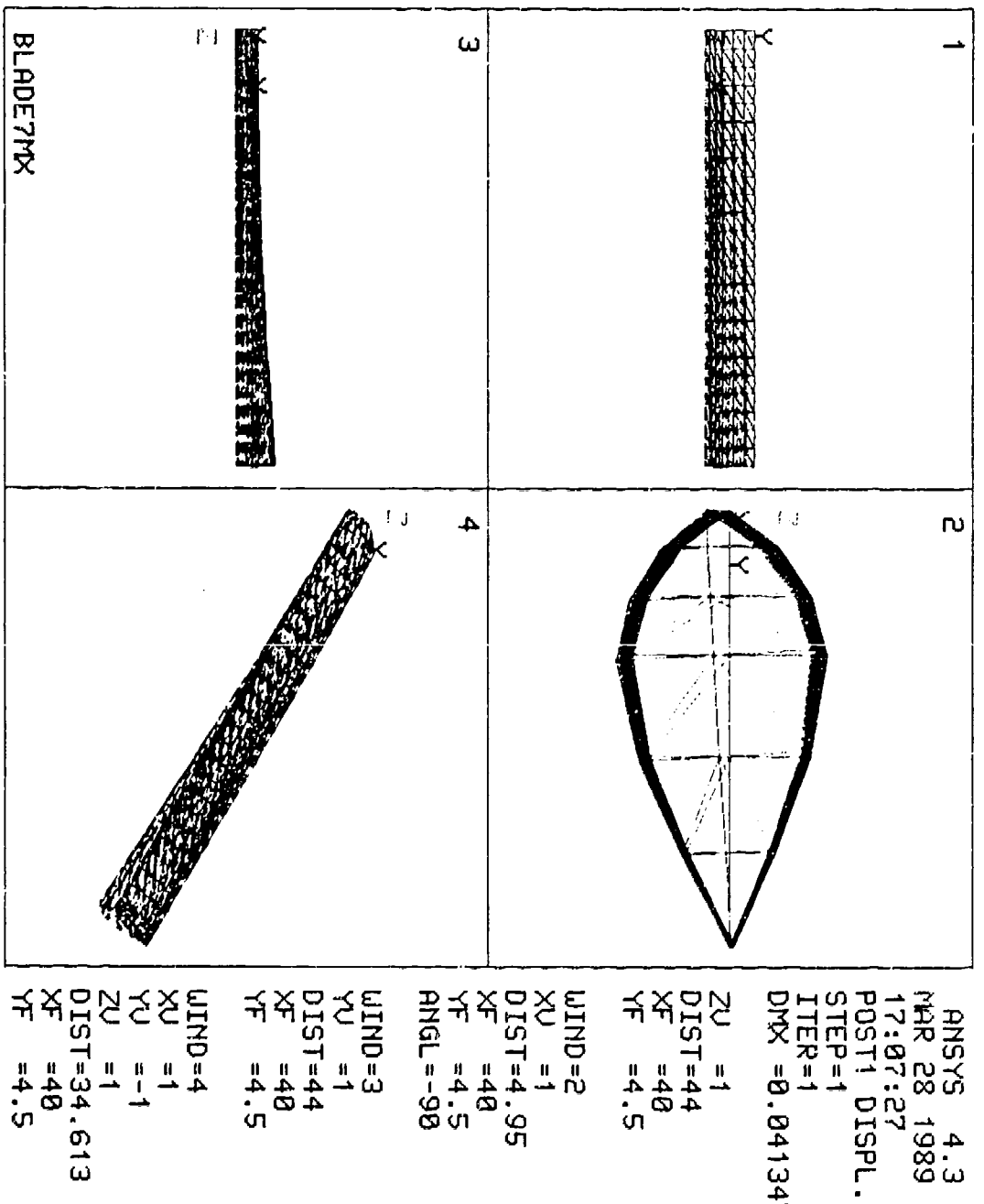

FIGURE 6.34

Blade Seven (Anisotropic) Under Torsional Load

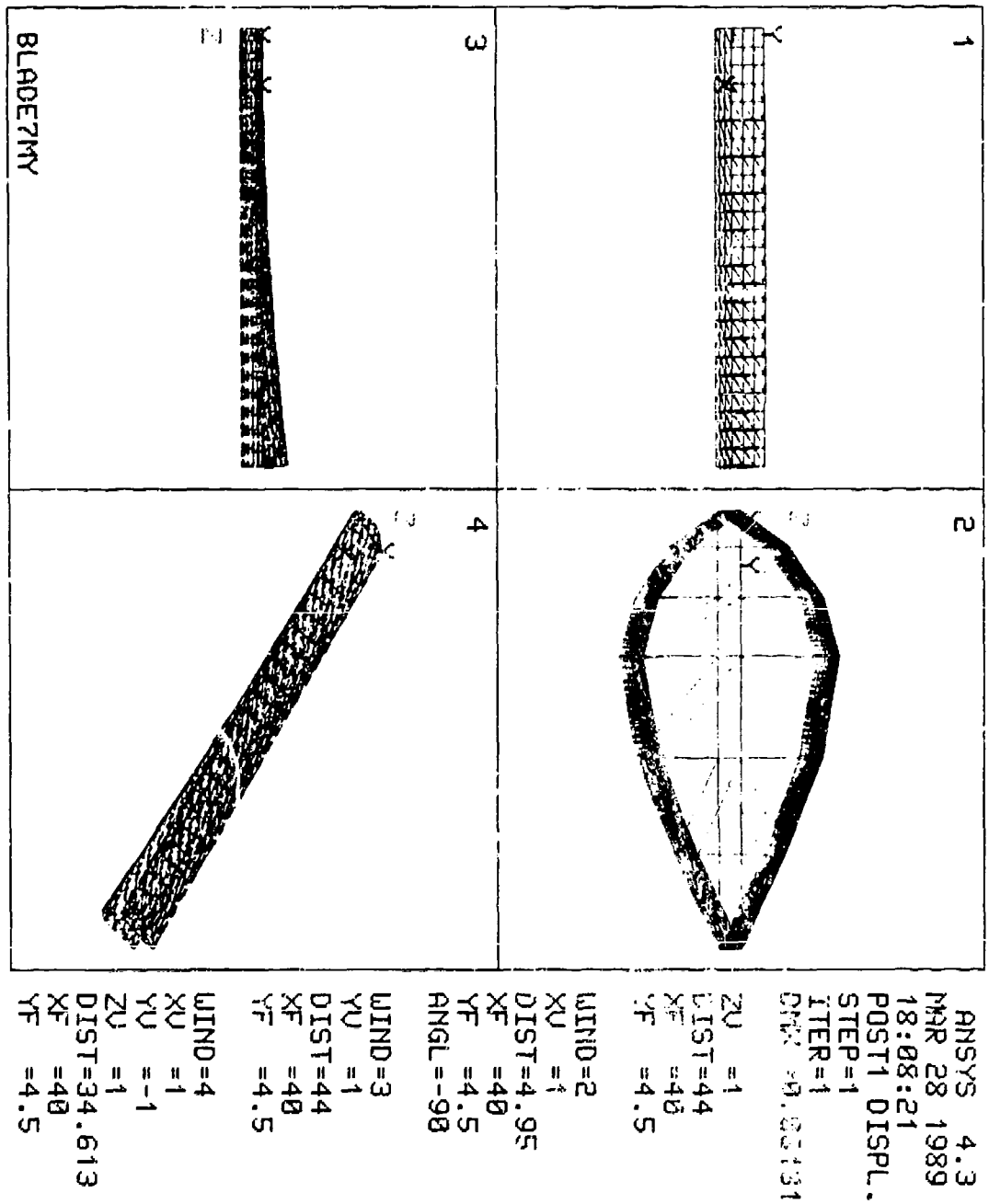

FIGURE 6.35

Biade Seven (Anisotropic) Under Bending Moment (Y)

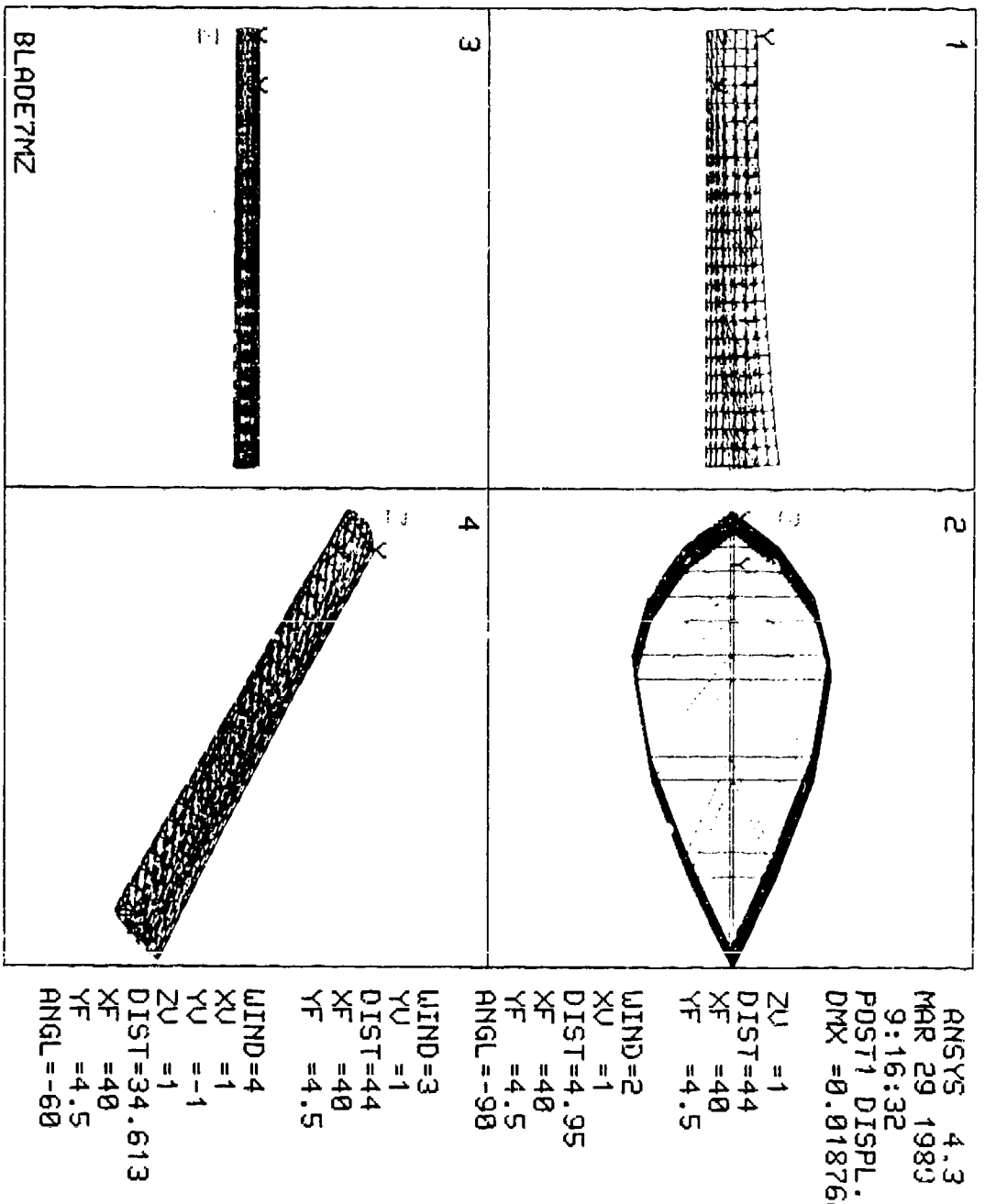

FIGURE 6.36

Blade Seven (Anisotropic) Under Bending Moment (Z)

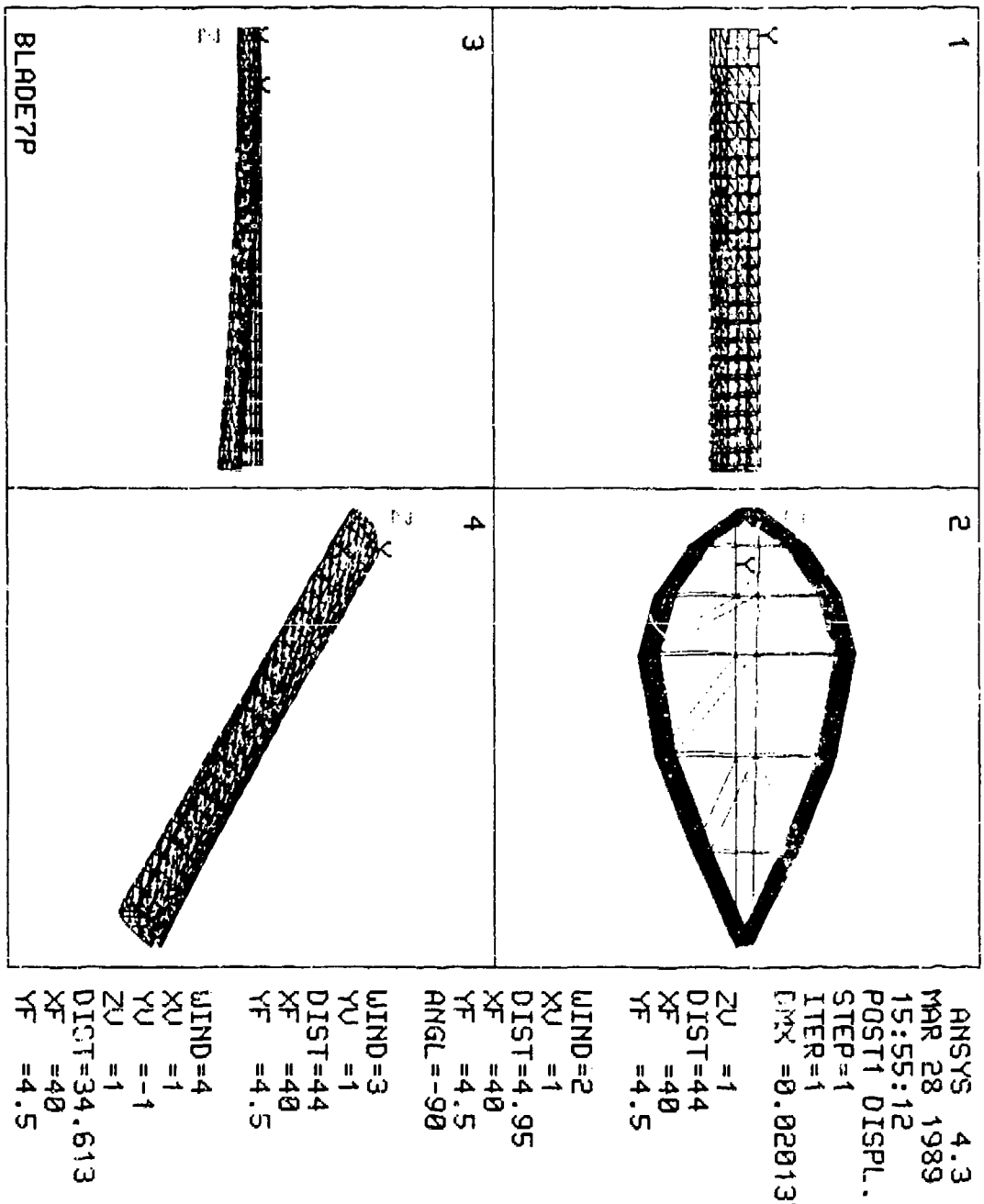

FIGURE 6.37

Blade Seven (Anisotropic) Under Axial Load

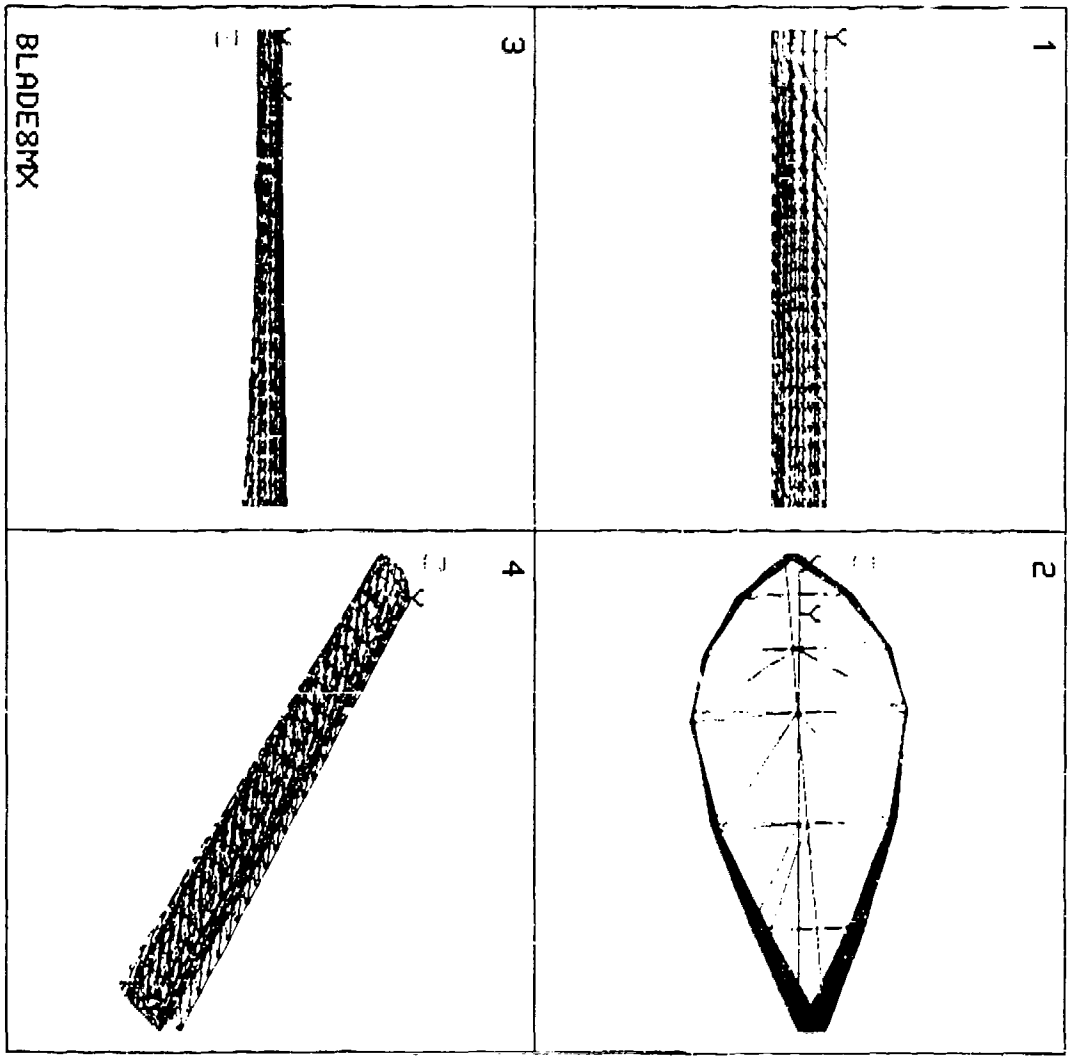

FIGURE 6.38

Blade Eight (Isotropic) Under Torsional Load

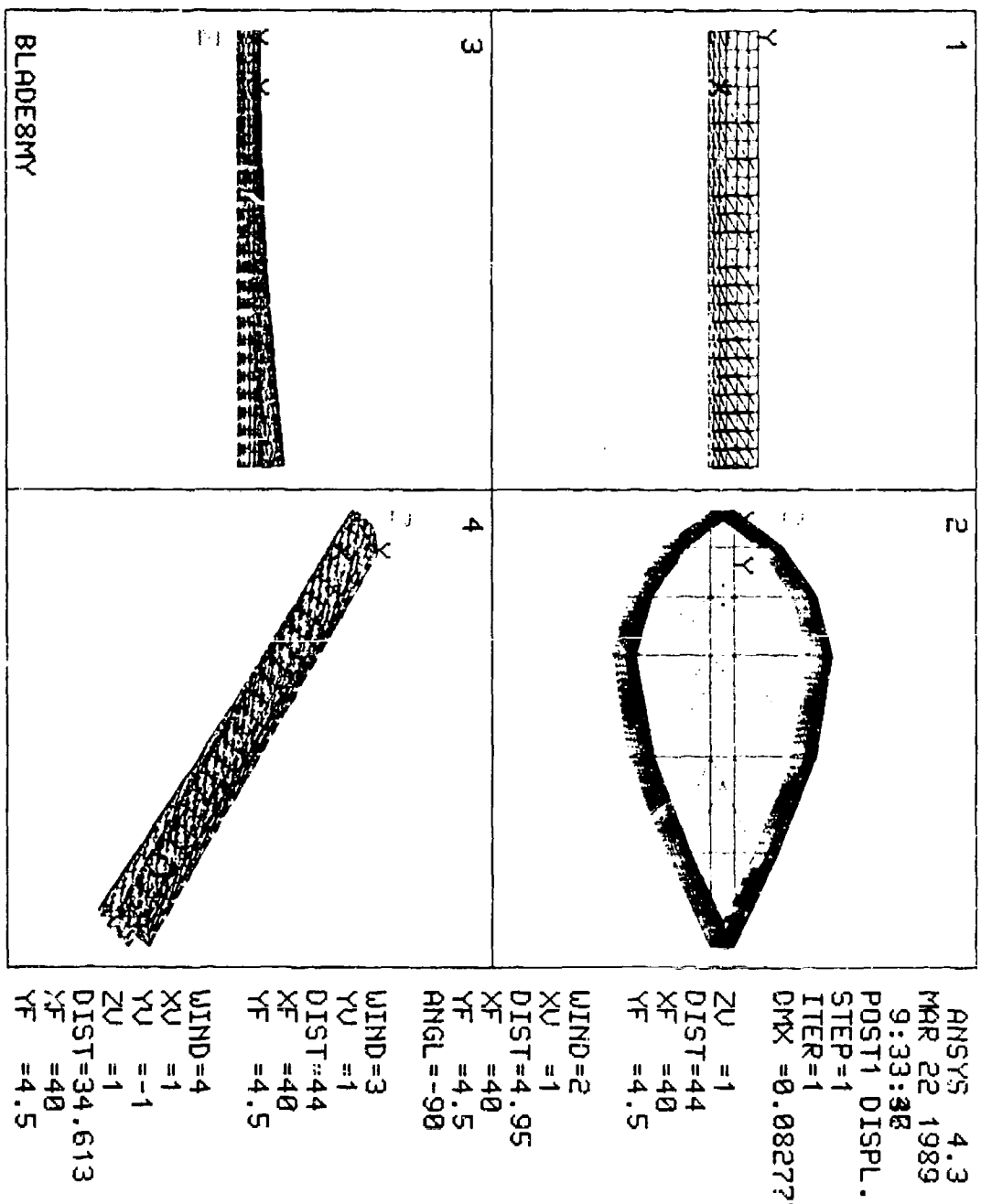

FIGURE 6.39

Blade Eight (Isotropic) Under Bending Moment (Y)

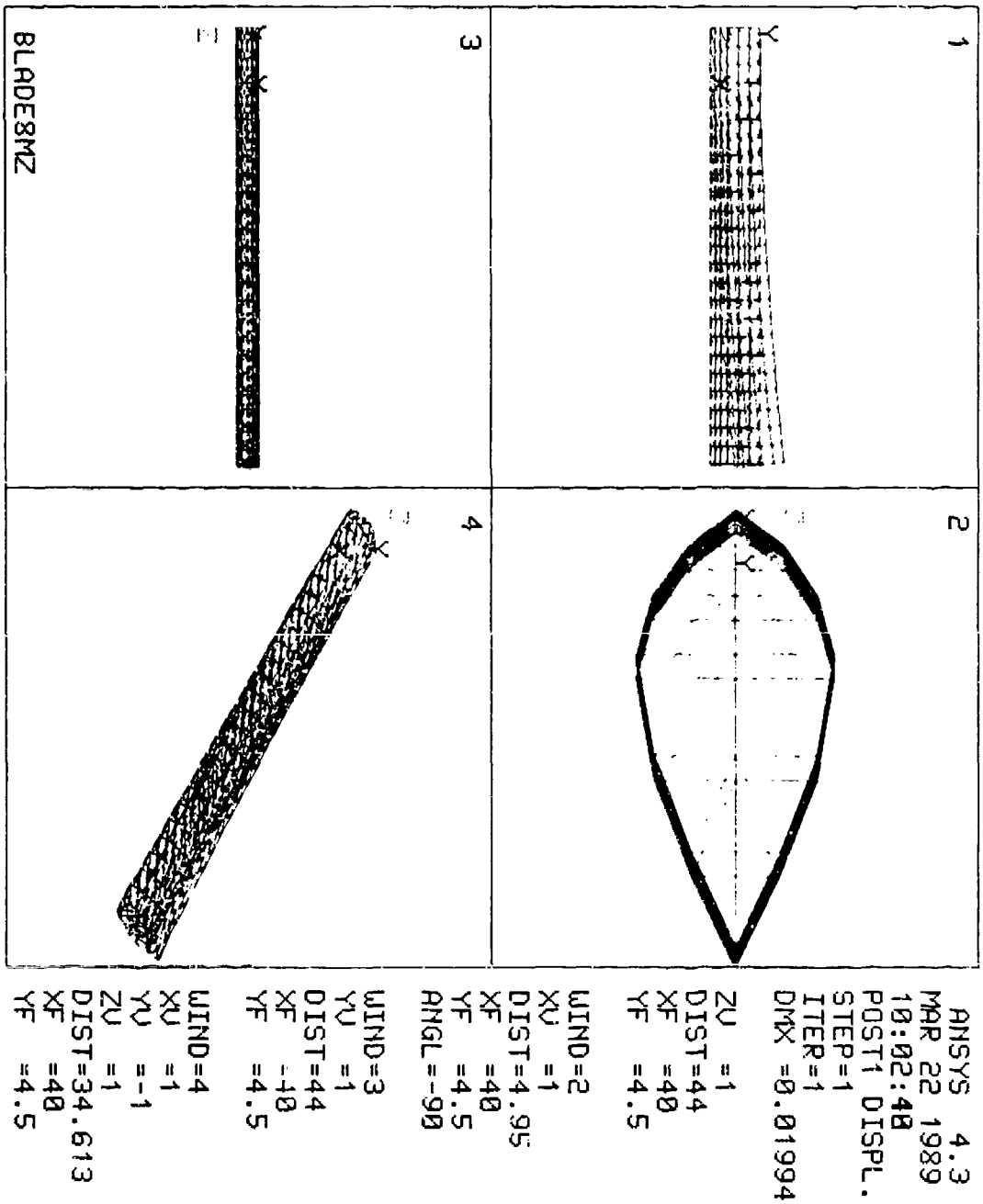

FIGURE 6.40

Blade Eight (Isotropic) Under Bending Moment (Z)

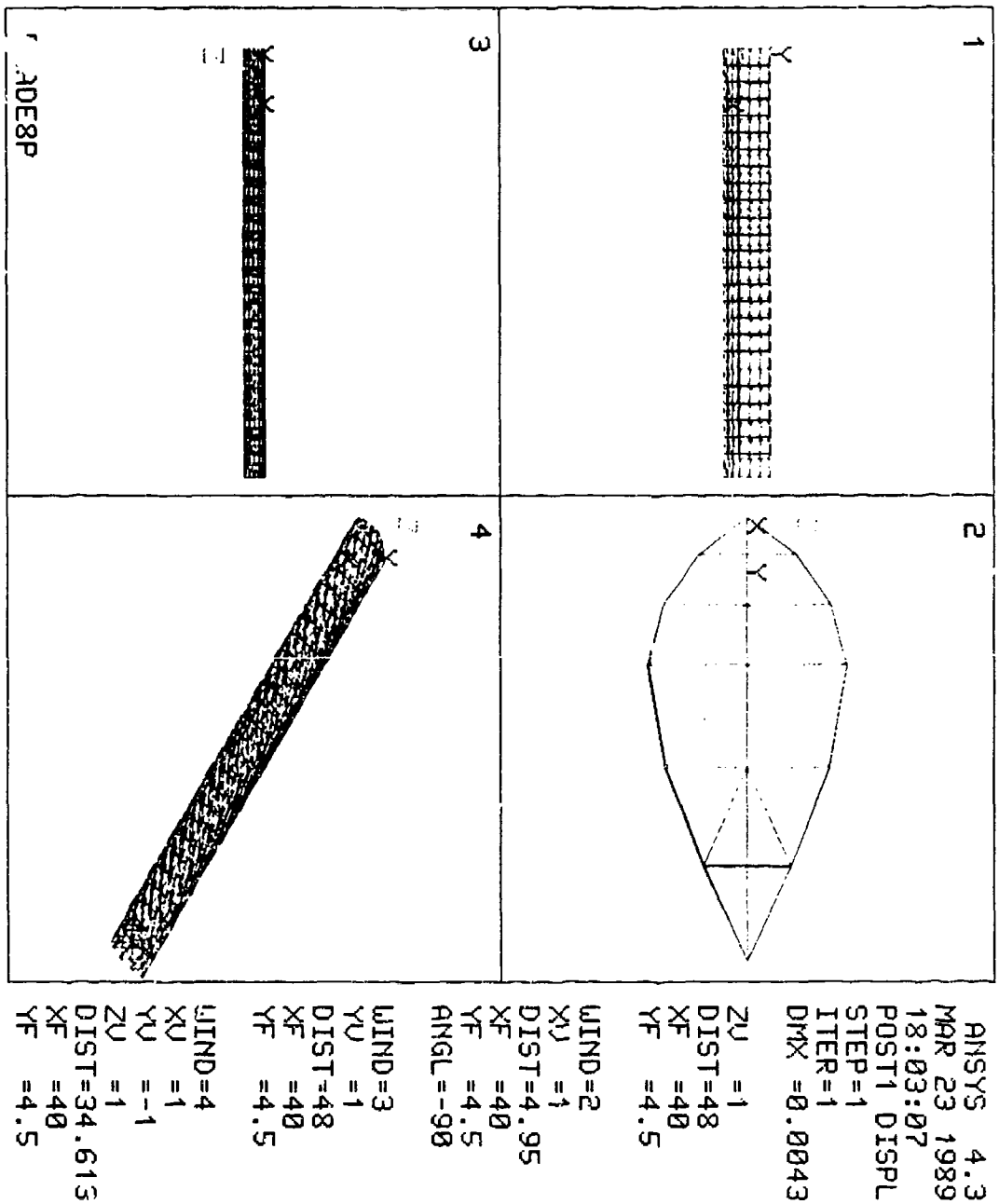

FIGURE 6.41

Blade Eight (Isotropic) Under Axial Load

Chapter Seven

Summary and Concluding Remarks

The advent of composite material construction in helicopter rotor blade design has opened new areas of research and development. In particular, the unique coupling properties afforded by anisotropic composites provide a potentially powerful new set of design variables for designing aeroelastic stability. The development of shell elements with anisotropic laminate capabilities which are incorporated into commercially available finite element packages makes this type of research possible.

Composites have better fatigue characteristics than metal and they permit the flexibility of tailoring the structural properties. One drawback of composite materials is that their structural characteristics, in particular the couplings of different bending modes, are not very well understood by a typical design engineer. Due to the complex directional nature of composite materials, the analysis of anisotropically laminated structures is complicated by the introduction of these elastic couplings. This is especially true in dynamic behavior since the elastic couplings have such a significant influence on characteristics like mode shape and frequency. Recent design practice has been to treat composites similarly to metals. This approach, however, does not permit the description of general composite lay-ups and its accuracy is questionable in view of the following facts [19]:

(a) The use of laminated composite materials for the blade structure results in significant shearing and warping deformations. These effects are far more pronounced for highly anisotropic composites than for metallic materials.

(b) The proper tailoring of composite lay-ups will result in elastic couplings, e.g., bending-twisting or extension-twisting couplings which are known to strongly influence the dynamic behavior and stability of the blade. Such couplings are not appropriately modeled with standard beam theories.

(c) In specific applications, the blade planform becomes wider, resulting again in increased shearing and warping deformations.

(d) Recent research shows that the torsional behavior, and the effects of pre-twist of the blade are accurately predicted only if out-of-plane warping of the cross-section is included.

In this research, the different stiffness coupling terms for a composite rotor blade were identified. These included the terms caused by bending-torsion and extension-torsion couplings of angle plies. It was shown that the ply lay-up and orientation has a substantial effect on the blade aeroelastic characteristics. It is concluded that the ply orientation angle and the ply thickness are suitable parametric variables for future studies aimed at assessing the influence of variations in structural properties which can in turn be used in the prediction of natural frequencies and aeroelastic stability.

The complex structural behavior of a rotor blade was modeled accurately. The following features were included: thin-walled cross-sections, proper scaling and material anisotropy. This resulted in an accurate modeling of the torsion, and coupled extension-twist behavior. While the undeformed blade geometry was accurate, the deformed geometry was somewhat deficient. The deformation was skewed at locations on the blade surface. This can be corrected by adding stiff ribs (similar to the end caps) throughout the length of the structure. Despite the fact that the geometries presented in this paper were rather simple, the formulation is applicable to complicated geometries.

Although we cannot increase the accuracy of predicted frequencies for the bending modes, which are basically uncoupled, we can greatly improve the prediction of the frequency of the torsional mode. This mode is elastically coupled and since there is an absence of off-diagonal coupling terms in the formulation of the equivalent engineering stiffnesses using beam theory, they must be predicted using lamination theory or determined experimentally.

In this research, the extension-twist terms were most pronounced. Potential applications of extension-twist coupling include the design of a tilt-rotor blade that would change twist as a function of rotor speed. Such a blade would be extremely useful on an aircraft such as the *V-22 OSPREY*. Besides the potentially positive aeroelastic benefits of twist, there are other useful applications of elastic coupling. These include the reduction or modification of structural vibration in rotor blade design. This is accomplished by building, into the blades, a natural aeroelastic compliance for vibration reduction [20].

To apply this model toward further analysis of elastic coupling, one would need a three-dimensional, non-linear beam element which includes shear and warping effects as well as a correct modeling of elastic couplings. This type of element is unavailable in ANSYS® and one would need to use a program such as MSC/NASTRAN®.

References

1. T.A. Weisshaar: *Aeroelastic Tailoring - Creative Uses of Unusual Materials.* AIAA-87-0976-CP, School of Aeronautics and Astronautics, Purdue University, Indiana (1987).

2. A.D. Stemple, S.W. Lee: *A Finite Element Model For Composite Beams Undergoing Large Deflection With Arbitrary Cross-Sectional Warping.* Department of Aerospace Engineering, University of Maryland, College Park, Maryland (1982).

3. R.C. Lake, M.W. Nixon: *A Preliminary Investigation of Finite-Element Modeling for Composite Rotor Blades.* Aerostructures Directorate, U.S. Army Aviation Research and Technology Activity - AVSCOM, NASA Langley Research Center, Virginia (1988).

4. O.A. Bauchau, C.H. Hong: *Finite Element Approach to Rotor Blade Modeling.* Department of Mechanic Engineering, Rensselaer Polytechnic Institute, New York (1985).

5. C. Hatch, A.R. Lee: *Determination of the Structural Properties of Helicopter Rotor Blades By Theoretical and Experimental Methods.* Royal Aircraft Establishment, Paper #67, Twelfth European Rotorcraft Forum, Farnborough, England (1986).

6. M.H. Shirk, T.J. Hertz, T.A. Weisshaar: *Aeroelastic Tailoring - Theory, Practice, Promise.* Journal of Aircraft, Vol. 23, No. 1, (1986).

7. A.R. Collar: *The First Fifty Years of Aeroelasticity.* Aerospace, Volume 5, No. 2, (1978).

8. H. Ashley: *The Constructive Uses of Aeroelasticity.* AIAA-80-0877, Department of Aeronautics and Astronautics, Stanford University, California (1982).

9. M.M. Munk: *Propeller Containing Diagonally Disposed Fibrous Material.* U.S. Patent 2,484,308,111 (1949).

10. F.H. Immen, R.L. Foye: *New Insights in Structural Design of Composite Rotor Blades for Helicopters.* Ames Research Center, U.S. Army R&T Laboratories, Moffett Field, California (1982).

11. R.R. Valisetty, L.W. Rehfield: *Simple Theoretical Models for Composite Rotor Blades*. NAG-1-398, School of Aerospace Engineering, Georgia Institute of Technology, Georgia (1984).

12. R.M. Jones: *Mechanics of Composite Materials*. Washington, D.C.: Scripta Book Company (1975).

13. F.B. Seely, J.O. Smith: *Advanced Mechanics of Materials*. Second Edition, New York: John Wiley and Sons, Inc. (1955)

14. J.M. Gere, S.P. Timoshenko: *Mechanics of Materials*. Second Edition, Boston, Massachusetts: PWS Publishing (1984).

15. J.M. Whitney: *Structural Analysis of Laminated Anisotropic Plates*. Lancaster, Pennsylvania: Technomic Publishing Company (1987).

16. C.H. Hong: *Aeroelastic Stability of Composite Rotor Blades in Hover*. University of Maryland, College Park, Maryland (1985).

17. PDA Engineering, Software Products Division: **PATRAN®** *User's Guide*. Version 2.1, Vol. I-II, PDA Engineering, California (1985).

18. G.J. DeSalvo, R.W. Gorman: **ANSYS®** *Engineering Analysis System User's Manual*. Version 4.3, Vol. I-II, Swanson Analysis Systems, Inc., Pennsylvania (1987).

19. O.A. Bauchau, B.S. Coffenberry, L.W. Rehfield: *A Comparison of Composite Rotor Blade Models with Experiments*. Department of Mechanical Engineering, Rensselaer Polytechnic Institute, New York (ND).

20. R.L. Bielawa: *Inclusion of a Generalized Anisotropic Beam Force-Deformation Relationship In Normal Mode Rotor Aeroelastic Analysis*. Department of Mechanical Engineering, Rensselaer Polytechnic Institute, New York (ND).

21. D.H. Allen, W.E. Haisler: *Introduction to Aerospace Structural Analysis*. New York: John Wiley & Sons (1985).

22. L. Nyhoff, S. Leestma: *FORTRAN 77 for Engineers and Scientist*. Second Edition, New York: Macmillan Publishing Company (1988).

23. I.H. Shames, C.L. Dym: *Energy and Finite Element Methods in Structural Mechanics*. Washington, D.C.: Hemisphere Publishing Corporation (1985)

24. B. Panda, I. Chopra: *Dynamics of Composite Rotor Blade in Forward Flight.* Center for the Rotorcraft Education and Research, Department of Aerospace Engineering, University of Maryland, College Park, Maryland (1985).

25. G. Hornung, D.W. Mathias, H. Rohrle: *Variation of Anisotropic Behavior in Structural Optimization.* Dornier GmbH, Friedrichshafen, Germany (1984).

26. M. Piening: *Effects of Anisotropic Design on the Static Aeroelasticity of a Swept Wing.* DFVLR, Institute for Structural Mechanics, Braunschweig, Germany (1985).

27. B. Hamilton, J. Peters, C. Callahan: *Optimal Design of an Advanced Composite Rotating Flexbeam.* Flight Technology Department, McDonnell Douglas Helicopter Company, Arizona (1988).

Appendix A

Laminate Analysis Program

```
      PROGRAM COMMAT  (INPUT,OUTPUT,TAPE5=INPUT,TAPE6=OUTPUT)
C
C     ***********-----*****************************************
C
C        COMPOSITE MATERIALS
C      LAMINATE ANALYSIS PROGRAM
C
C       PATRICK GRAHAM FORRESTER
C      UNIVERSITY OF VIRGINIA 1989
C
C          THESIS RESEARCH
C
C     ************************************************
C
C
C     THE PURPOSE OF THIS PROGRAM IS TO CALCUI ATE
C     THE LAMINATE PROPERTIES OF COMPOSITE MATERIAL
C     HELICOPTER BLADE MODELS GIVEN THE LAMINA
C     MATERIAL PROPERTIES OF GRAPHITE/EPOXY
C
C     ************************************************
C
      INTEGER IA,M,N,IAINV,IER
      INTEGER NOMAT,ANGLE,PLIES,LOAD,ILOAD,ITEMP,QUEST
      REAL S11(9),S12(9),S13(9),S22(9),S23(9),S33(9),S44(9),S55(9)
      REAL E11(9),E22(9),E33(9),G12(9),G23(9),G31(9),S66(9)
      REAL NU12(9),NU23(9),NU13(9),G13(9),RTHETA(9)
      DIMENSION D3(3,3),EPS3(3,9)
      INTEGER THETA(9),ISYM
      REAL Q11(9),Q12(9),Q22(9),Q66(9),QBAR11(9,9),QBAR12(9,9)
      REAL QBAR22(9,9),QBAR16(9,9),QBAR26(9,9),QBAR66(9,9)
      REAL EXX(9,9),EYY(9,9),EXY(9,9),NUXY(9,9),GXY(9,9)
      REAL ETAXYX(9,9),ETAXYY(9,9),KAP(3),H
      REAL NX,NY,NXY,MX,MY,MXY,DELTT,TEMP,TEMPN,TEMPM,ALAM(3)
      DIMENSION EPS1T(9,3),EPS1B(9,3),XST(9),YST(9),SSS(9)
      DIMENSION RMB(3),RNB(3),EPSB(3),EPSXB(9,3)
      DIMENSION ALP1(9),ALP2(9),ALP3(9),ALPX(9,9),ALPY(9,9),ALPXY(9,9)
      DIMENSION SIGXB(9,3),SIGXT(9,3),EPSXT(9,3),EPST(9,3),U(3,3)
      REAL KAPT(3),KAPB(3)
```

```
      DIMENSION EPSTH(3),DEL(9,3),NXX(9,3)
      REAL F1,F2,F6,F11,F12,F22,F66,BETA1(9,3),BETA2(9,3)
      DIMENSION EPST1(9,3),EPSTH1(9,3)
      DIMENSION RNT(3),RMT(3),SIG1T(9,3),SIG1B(9,3)
      REAL MIDEPX,MIDEPY,MIDEPXY,KAPX,KAPY,KAPXY
      DIMENSION X(6,6),P(3,3),T(3,3),R(6,6),PN(3),PM(3)
      REAL PI,C,S,TOL,WK1(12),WK2(6),S1(6),S2(3)
      REAL ETABXYX,ETABXYY,ETABXXY,ETABYXY,EBARX,EBARY
      DIMENSION A(6,6,9),B(6,6,9),E(3,3,9,9),D(3,3,9,9)
      DIMENSION MATN(9),ANGN(9),THICK(10),Z(11),D4(3,3),A4(3,3),B4(3,3)
      DIMENSION A1(3,3),B1(3,3),D1(3,3),A2(3,3),B2(3,3),D2(3,3),B5(3,3)
      DIMENSION EPS(3),RN(3),RM(3),P1(3),P2(3),A3(3,3),B3(3,3)
      DIMENSION SIG(3,9),EPS1(9,3),SIG1(9,3),SIG2(3,9),SIG3(3,9)
      DIMENSION SIGX(9,3),SIGY(3,9),SIGXY(3,9),EPS2(3,9)
      DIMENSION EPSX(9,3),EPSY(3,9),EPSXY(3,9),AA(3,3),BB(3,3),DD(3,3)
      DIMENSION ATEMP(6,6,9),CTEMP(3,3,9,9),T1(3,3,9),T2(3,3,9)
      OPEN (UNIT=6,FILE='RESULT')
C
C     .....ASSIGN INPUT DATA.....
C
      PI = 3.14159
      STHICK = 0.0
C
C     .....OBTAIN LAMINATE PARAMETERS.....
C
      WRITE(5,*) 'ENTER THE NUMBER OF DIFFERENT MATERIALS AND ANGLES'
      WRITE(5,*) 'AND THE NUMBER OF PLIES AND LOADS IN LAMINATE'
      READ (5,*)  NOMAT,ANGLE,PLIES,LOAD
C
      WRITE(5,*) 'IS THIS A SYMETRIC LAMINATE?  YES=0 NO=1'
      READ(5,*) ISYM
C
      WRITE(5,*) 'IS THERE THERMAL LOADING?  YES=0 NO=1'
      READ(5,*)  ITEMP
C
      WRITE(5,*) 'DO YOU KNOW NXX FOR FAILURE CRITERIA? YES=1 NO=0'
      READ(5,*) QUEST
C
C     .....OBTAIN VALUES OF ENGINEERING PARAMETERS .....
C
      DO 2 I=1,NOMAT
      WRITE(5,*) 'ENTER E11,E22 FOR MATERIAL NUMBER ',I
      READ(5,*)  E11(I),E22(I)
C
      WRITE(5,*) 'ENTER G12 FOR MATERIAL NUMBER ',I
      READ(5,*)  G12(I)
C
      WRITE(5,*) 'ENTER NU12,NU23 FOR MATERIAL NUMBER ', I
      READ(5,*)  NU12(I),NU23(I)
C
      WRITE(5,*) 'ENTER ALPHA1,ALPHA2 AND ALPHA3 FOR MATERIAL ',I
```

```
      READ(5,*) ALP1(I),ALP2(I),ALP3(I)
C
      WRITE(5,*) 'ENTER X SUB T, Y SUB T, S AND F12 FOR MATERIAL ',I
      READ(5,*) XST(I),YST(I),SSS(I),F12
C
      F1 = 0.0
      F2 = 0.0
      F6 = 0.0
      F11 = -1.0/(XST(I)**2)
      F22 = -1.0/(YST(I)**2)
      F66 = 1.0/(SSS(I)**2)
      E33(I) = E22(I)
      G13(I) = G12(I)
      G23(I) = E22(I)/(2.0*(1.0 + NU23(I)))
      NU13(I) = NU12(I)
    2 CONTINUE
      DO 3 I = 1,ANGLE
      WRITE(5,*) 'ENTER ANGLE NUMBER ', I
      READ(5,*) THETA(I)
      RTHETA(I) = PI/180.0 * THETA(I)
    3 CONTINUE
      DO 4 I = 1,PLIES
      WRITE(5,*) 'ENTER MATN,ANGN,THICK FOR PLY NUMBER ' ,I
      READ(5,*) MATN(I),ANGN(I),THICK(I)
C
      STHICK = STHICK + THICK(I)
    4 CONTINUE
C
      DO 5 I = 1,LOAD
      WRITE(5,*) 'DO YOU KNOW [N] AND [M]?  YES=0 NO=1'
      READ(5,*) ILOAD
      IF (ILOAD .EQ. 0) THEN
      WRITE(5,*) 'ENTER NX, NY AND NXY FOR LOADING CONDITION ',I
      READ(5,*) RN(1),RN(2),RN(3)
      WRITE(5,*) 'ENTER MX, MY AND MXY FOR LOADING CONDITION ',I
      READ(5,*) RM(1),RM(2),RM(3)
      ELSE
      WRITE(5,*) 'THAT MEANS YOU KNOW MIPLANE STRAINS AND CURVATURES'
      WRITE(5,*) 'ENTER EPSX, EPSY AND EPSXY FOR LOADING CONDITION ',I
      READ(5,*) EPS(1),EPS(2),EPS(3)
      WRITE(5,*) 'ENTER KAPX, KAPY AND KAPXY FOR LOADING CONDITION ',I
      READ(5,*) KAP(1),KAP(2),KAP(3)
      ENDIF
    5 CONTINUE
C
      IF (ITEMP .EQ. 1) GO TO  739
      WRITE(5,*) 'ENTER CHANGE IN TEMPERATURE'
      READ(5,*) DELTT
  739 CONTINUE
C
C
```

```
C     .....PERFORM COMPUTATIONS.....
C
      DO 6 I = 1,NOMAT
      S11(I) = 1.0/E11(I)
      S12(I) = -NU12(I)/E11(I)
      S22(I) = 1.0/E22(I)
      S33(I) = 1.0/E33(I)
      S44(I) = 1.0/G23(I)
      S13(I) = -NU13(I)/E11(I)
      S23(I) = -NU23(I)/E11(I)
      S55(I) = 1.0/G13(I)
      S66(I) = 1.0/G12(I)
C
C     .....CONSTRUCT THE COMPLIANCE MATRIX.....
C
C     .....SET THE INITIAL VALUES TO ZERO.....
C
      DO 1 K = 1,6
      DO 1 J = 1,6
      A(K,J,I) = 0.0
    1 CONTINUE
C
C     .....ESTABLISH NON-ZERO VALUES.....
C
      A(1,1,I) = S11(I)
      A(1,2,I) = S12(I)
      A(1,3,I) = S13(I)
      A(2,1,I) = S12(I)
      A(2,2,I) = S22(I)
      A(2,3,I) = S23(I)
      A(3,1,I) = S13(I)
      A(3,2,I) = S23(I)
      A(3,3,I) = S33(I)
      A(4,4,I) = S44(I)
      A(5,5,I) = S55(I)
      A(6,6,I) = S66(I)
C
      DO 21 K = 1,6
      DO 21 J = 1,6
   21 ATEMP(K,J,I) = A(K,J,I)
C
      DO 1000 K = 1,6
      DO 1000 J = 1,6
      X(K,J) = 0.0
 1000 CONTINUE
      X(1,1) = S11(I)
      X(1,2) = S12(I)
      X(1,3) = S13(I)
      X(2,1) = S12(I)
      X(2,2) = S22(I)
      X(2,3) = S23(I)
```

```
      X(3,1) = S13(I)
      X(3,2) = S23(I)
      X(3,3) = S33(I)
      X(4,4) = S44(I)
      X(5,5) = S55(I)
      X(6,6) = S66(I)
C
C     .....CALCULATE THE STIFFNESS MATRIX.....
C
      IA = 6
      IAINV = 6
      M = 6
      N = 6
      TOL = 0.0
C
      CALL LGINF (X,IA,M,N,TOL,R,IAINV,S1,WK1,IER)
C
      XY1 = R(1,1)
      XY2 = R(1,2)
      XY3 = R(1,3)
      XY4 = R(2,1)
      XY5 = R(2,2)
      XY6 = R(2,3)
      XY7 = R(3,1)
      XY8 = R(3,2)
      XY9 = R(3,3)
      XY10 = R(4,4)
      XY11 = R(5,5)
      XY12 = R(6,6)
      XY13 = 0.0
C
      DO 1001 K = 1,6
      DO 1001 J = 1,6
      B(K,J,I) = 0.0
 1001 CONTINUE
      B(1,1,I) = XY1
      B(1,2,I) = XY2
      B(1,3,I) = XY3
      B(2,1,I) = XY4
      B(2,2,I) = XY5
      B(2,3,I) = XY6
      B(3,1,I) = XY7
      B(3,2,I) = XY8
      B(3,3,I) = XY9
      B(4,4,I) = XY10
      B(5,5,I) = XY11
      B(6,6,I) = XY12
C
C     .....CALCULATE THE REDUCED STIFFNESS MATRIX WITH ROTATION.....
C
      Q11(I) = S22(I)/((S11(I)*S22(I)) - (S12(I)*S12(I)))
```

```
      Q12(I) = -S12(I)/((S11(I)*S22(I)) - (S12(I)*S12(I)))
      Q22(I) = S11(I)/((S11(I)*S22(I)) - (S12(I)*S12(I)))
      Q66(I) = 1.0/S66(I)
C
C     .....CONSTRUCT THE REDUCED STIFFNESS MATRIX WITH ROTATION.....
C
      DO 68 K = 1,ANGLE
C
C
      C = COS(RTHETA(K))
      S = SIN(RTHETA(K))
C
      QBAR11(I,K) = Q11(I)*(C*C*C*C) + 2.0*(Q12(I) +
     A  2.0*Q66(I))*(S*S)*(C*C) + Q22(I)*(S*S*S*S)
      QBAR12(I,K) = (Q11(I) + Q22(I) - 4.0*Q66(I))*(S*S)*(C*C) +
     A  Q12(I)*((S*S*S*S) + (C*C*C*C))
      QBAR22(I,K) = Q11(I)*(S*S*S*S) + 2.0*(Q12(I) + 2.0*Q66(I))*(S*S)
     A  *(C*C) + Q22(I)*(C*C*C*C)
      QBAR16(I,K) = (Q11(I) - Q12(I) - 2.0*Q66(I))*S*(C*C*C) + (Q12(I) -
     A  Q22(I) + 2.0*Q66(I)) *(S*S*S)*C
      QBAR26(I,K) = (Q11(I) - Q12(I) - 2.0*Q66(I))*(S*S*S)*C + (Q12(I) -
     A  Q22(I) + 2.0*Q66(I)) *S*(C*C*C)
      QBAR66(I,K) = (Q11(I) + Q22(I) - 2.0*Q12(I) - 2.0*Q66(I))*(S*S)
     A  *(C*C) + Q66(I)*((S*S*S*S) + (C*C*C*C))
C
C     .....CONSTRUCT THE REDUCED STIFFNESS MATRIX WITH ROTATION.....
C
      E(1,1,I,K) = QBAR11(I,K)
      E(1,2,I,K) = QBAR12(I,K)
      E(1,3,I,K) = QBAR16(I,K)
      E(2,1,I,K) = QBAR12(I,K)
      E(2,2,I,K) = QBAR22(I,K)
      E(2,3,I,K) = QBAR26(I,K)
      E(3,1,I,K) = QBAR16(I,K)
      E(3,2,I,K) = QBAR26(I,K)
      E(3,3,I,K) = QBAR66(I,K)
C
      DO 31 M = 1,3
      DO 31 J = 1,3
   31 CTEMP(M,J,I,K) = E(M,J,I,K)
C
C     .....CALCULATE THE REDUCED COMPLIANCE MATRIX.....
C
      P(1,1) = QBAR11(I,K)
      P(1,2) = QBAR12(I,K)
      P(1,3) = QBAR16(I,K)
      P(2,1) = QBAR12(I,K)
      P(2,2) = QBAR22(I,K)
      P(2,3) = QBAR26(I,K)
      P(3,1) = QBAR16(I,K)
      P(3,2) = QBAR26(I,K)
```

```
      P(3,3) = QBAR66(I,K)
C
C
      IA = 3
      IAINV = 3
      M = 3
      N = 3
      TOL = 0.0
C
      CALL LGINF(P,IA,M,N,TOL,T,IAINV,S2,WK2,IER)
C
      XYZ1 = T(1,1)
      XYZ2 = T(1,2)
      XYZ3 = T(1,3)
      XYZ4 = T(2,1)
      XYZ5 = T(2,2)
      XYZ6 = T(2,3)
      XYZ7 = T(3,1)
      XYZ8 = T(3,2)
      XYZ9 = T(3,3)
C
      D(1,1,I,K) = XYZ1
      D(1,2,I,K) = XYZ2
      D(1,3,I,K) = XYZ3
      D(2,1,I,K) = XYZ4
      D(2,2,I,K) = XYZ5
      D(2,3,I,K) = XYZ6
      D(3,1,I,K) = XYZ7
      D(3,2,I,K) = XYZ8
      D(3,3,I,K) = XYZ9
C
C     .....CALCULATE THE LAMINA ENGINEERING PARAMETERS.....
C
      EXX(I,K) = 1.0/(((1.0/E11(I))*(C*C*C*C)) + ((1.0/G12(I)) -
     A  (2.0*NU12(I)/E11(I)))
     B  *(S*S)*(C*C) + ((1.0/E22(I))*(S*S*S*S)))
      EYY(I,K) = 1.0/(((1.0/E11(I))*(S*S*S*S)) + ((1.0/G12(I)) -
     A  (2.0*NU12(I)/E11(I)))
     B  *(S*S)*(C*C) + ((1.0/E22(I))*(C*C*C*C)))
      NUXY(I,K) = EXX(I,K)*((NU12(I)/E11(I))*((S*S*S*S) + (C*C*C*C)) -
     A  ((1.0/E11(I)) +
     B  (1.0/E22(I)) - (1.0/G12(I)))*(S*S)*(C*C))
      GXY(I,K) = 1.0/((2.0*((2.0/E11(I)) + (2.0/E22(I)) +
     A  (4.0*NU12(I)/E11(I)) -
     B  (1.0/G12(I))))*((S*S)*(C*C)) + ((1.0/G12(I))*((S*S*S*S) +
     C  (C*C*C*C))))
      ETAXYX(I,K) = EXX(I,K)*(((2.0/E11(I)) + (2.0*NU12(I)/E11(I)) -
     A  (1.0/G12(I)))*S*(C*C*C) -
     B  ((2.0/E22(I)) + (2.0*NU12(I)/E11(I)) - (1.0/G12(I)))*(S*S*S)*C)
      ETAXYY(I,K) = EYY(I,K)*(((2.0/E11(I)) + (2.0*NU12(I)/E11(I)) -
     A  (1.0/G12(I)))*(S*S*S)*C
```

```
     B - ((2.0/E22(I)) + (2.0*NU12(I)/E11(I)) - (1.0/G12(I)))*S*(C*C*C))
  68 CONTINUE
C
   6 CONTINUE
C
C  ....CALCULATE THE [A], [B], AND [D] MATRICES.....
     DO 69 I = 1,3
     DO 69 J = 1,3
     A1(I,J) = 0.0
     B1(I,J) = 0.0
     D1(I,J) = 0.0
  69 CONTINUE
C
     Z(1) = - STHICK/2.0
C
     DO 70 I = 1,3
     DO 79 J = 1,3
     DO 72 K = 1,PLIES
     M = MATN(K)
     N = ANGN(K)
     Z(K + 1) = Z(K) + THICK(K)
C
     AT = E(I,J,M,N)*(Z(K+1) - Z(K))
     BT = E(I,J,M,N)*(Z(K+1)**2 - Z(K)**2)*(1.0/2.0)
     DT = E(I,J,M,N)*(Z(K+1)**3 - Z(K)**3)*(1.0/3.0)
C
     A1(I,J) = A1(I,J) + AT
     B1(I,J) = B1(I,J) + BT
     D1(I,J) = D1(I,J) + DT
  72 CONTINUE
  79 CONTINUE
  70 CONTINUE
C
     DO 909 I = 1,3
     DO 909 J = 1,3
     DD(I,J) = D1(I,J)
     AA(I,J) = A1(I,J)
     BB(I,J) = B1(I,J)
 909 CONTINUE
C
     DO 933 I = 1,ANGLE
     T1(1,1,I) = COS(RTHETA(I))**2
     T1(1,2,I) = SIN(RTHETA(I))**2
     T1(1,3,I) = COS(RTHETA(I))*SIN(RTHETA(I))
     T1(2,1,I) = T1(1,2,I)
     T1(2,2,I) = T1(1,1,I)
     T1(2,3,I) = -T1(1,3,I)
     T1(3,1,I) = T1(1,3,I)*2.0
     T1(3,2,I) = -T1(3,1,I)
     T1(3,3,I) = COS(RTHETA(I))**2 - SIN(RTHETA(I))**2
 933 CONTINUE
```

```
C
C
C   .....CALCULATE THE THERMAL COEFFICIENTS.....
C
      DO 332 J = 1,NOMAT
      DO 333 I = 1,ANGLE
      ALPX(J,I) = T1(1,1,I)*ALP1(J) + T1(1,2,I)*ALP2(J)
      ALPY(J,I) = T1(2,1,I)*ALP1(J) + T1(2,2,I)*ALP2(J)
      ALPXY(J,I) = T1(3,1,I)*ALP1(J) + T1(3,2,I)*ALP2(J)
  333 CONTINUE
      DO 4000 I=1,4
      WRITE (6,555) ALPX(1,I)
      WRITE (6,555) ALPY(1,I)
      WRITE (6,555) ALPXY(1,I)
  555 FORMAT (5X,4E11.5)
 4000 CONTINUE
  332 CONTINUE
C
      DO 334 L = 1,PLIES
      J=MATN(L)
      K=ANGN(L)
      EPST(L,1) = ALPX(J,K)*DELTT
      EPST(L,2) = ALPY(J,K)*DELTT
      EPST(L,3) = ALPXY(J,K)*DELTT
  334 CONTINUE
      DO 9000 I = 1, PLIES
 9000 WRITE (6,55) EPST(I,1),EPST(I,2),EPST(I,3)
      Z(1) = -STHICK/2.0
C
      DO 335 L = 1,PLIES
      J = MATN(L)
      K = ANGN(L)
      DO 336 I = 1,3
      TEMP = E(I,1,J,K)*EPST(L,1)
     A    + E(I,2,J,K)*EPST(L,2) + E(I,3,J,K)*EPST(L,3)
      TEMPN = TEMP*(Z(L+1) - Z(L))
      TEMPM = TEMP*(Z(L+1)**2-Z(L)**2)/2.0
      RNT(I) = RNT(I) + TEMPN
      RMT(I) = RMT(I) + TEMPM
  336 CONTINUE
  335 CONTINUE
      CALL INVRS(A1,A2)
C
C
C   ....CALCULATE THE LAMINATE COEFFICIENT OF THERMAL EXPANSION.....
C
      IF (ISYM .EQ. 1) GO TO 921
      DO 444 I = 1,3
      ALAM(I) = (A2(I,1)*RNT(1) + A2(I,2)*RNT(2) + A2(I,3)*RNT(3))
     A   *(1.0/DELTT)
  444 CONTINUE
```

```
 921 CONTINUE
C
C
C  ...INVERT THE A1 MATRIX TO USE FOR LAMINATE ENGINEERING PARAMETERS..
C
    CALL INVRS(A1,A2)
C
C  .....INVERT THE B1 MATRIX AND THE D1 MATRIX FOR CALCULATIONS.....
C
C
C  ....CALCULATE THE LAMINATE ENGINEERING PARAMETERS.....
C
    IF (ISYM .EQ. 1) GO TO 200
    EBARX = 1.0/(STHICK * A2(1,1))
    EBARY = 1.0/(STHICK * A2(2,2))
    GBARXY = 1.0/(STHICK * A2(3,3))
    NUBARXY = -A2(1,2)/A2(1,1)
    ETABXYX = A2(1,3)/A2(1,1)
    ETABXYY = A2(2,3)/A2(2,2)
    ETABXXY = A2(1,3)/A2(3,3)
    ETABYXY = A2(2,3)/A2(3,3)
 200 CONTINUE
C
    IF (ILOAD .EQ. 0) GO TO 600
C
C
C  .....COMPUTE [M] AND [N] GIVEN MIDPLANE STRAINS AND CURVATURES....
C
    CALL MPLY(A1,EPS,P1,3,3,1)
    CALL MPLY(B1,KAP,P2,3,3,1)
    CALL PLUS(P1,P2,PN,3,1)
    CALL MPLY(B1,EPS,P1,3,3,1)
    CALL MPLY(D1,KAP,P2,3,3,1)
    CALL PLUS(P1,P2,PM,3,1)
    GO TO 300
 600 CONTINUE
C
C  ...COMPUTE THE MIDPLANE STRAINS AND CURVATURES GIVEN [M] AND [N]....
C
    IF (ISYM .EQ.0) THEN
    CALL INVRS(A1,A3)
    CALL INVRS(D1,D2)
    DO 400 I = 1,3
    DO 401 J = 1,3
    B3(I,J) = 0
    B4(I,J) = 0
 401 CONTINUE
 400 CONTINUE
    ELSE
    CALL INVRS(A1,A4)
    CALL MPLY(A4,B1,B2,3,3,3)
```

```
      DO 402 I = 1,3
      DO 403 J = 1,3
      B2(I,J) = -B2(I,J)
  403 CONTINUE
  402 CONTINUE
C
      CALL MPLY(B1,A4,B5,3,3,3)
      CALL MPLY(B1,B2,D3,3,3,3)
      CALL PLUS(D1,D3,D4,3,3)
      CALL INVRS(D4,D2)
      CALL MPLY(B2,D2,B3,3,3,3)
      CALL MPLY(B3,B5,D3,3,3,3)
      CALL MINUS(A4,D3,A3,3,3)
      CALL MPLY(D2,B5,B4,3,3,3)
      DO 404 I = 1,3
      DO 405 J = 1,3
      B4(I,J) = -B4(I,J)
  405 CONTINUE
  404 CONTINUE
      ENDIF
C
      CALL MPLY(A3,RN,P1,3,3,1)
      CALL MPLY(B3,RM,P2,3,3,1)
      CALL PLUS(P1,P2,EPS,3,1)
      CALL MPLY(B4,RN,P1,3,3,1)
      CALL MPLY(D2,RM,P2,3,3,1)
      CALL PLUS(P1,P2,KAP,3,1)
C
C ...CALCULATE MIDPLANE STRAINS AND CURVATURES WITH THERMAL LOADS...
C
      CALL MPLY(A2,RNT,P1,3,3,1)
      CALL MPLY(B3,RMT,P2,3,3,1)
      CALL PLUS(P1,P2,EPSTH,3,1)
      CALL MPLY(B4,RNT,P1,3,3,1)
      CALL MPLY(D2,RMT,P2,3,3,1)
      CALL PLUS(P1,P2,KAPT,3,1)
C
C ..CALCULATE MIDPLANE STRAINS AND CURVATURES WITH
C     MECHANICAL AND THERMAL LOADING.....
C
      DO 408 I = 1,3
      RNB(I) = RN(I) + RNT(I)
      RMB(I) = RM(I) + RMT(I)
  408 CONTINUE
C
      CALL MPLY(A2,RNB,P1,3,3,1)
      CALL MPLY(B3,RMB,P2,3,3,1)
      CALL PLUS(P1,P2,EPSB,3,1)
      CALL MPLY(B4,RNB,P1,3,3,1)
      CALL MPLY(D2,RMB,P2,3,3,1)
      CALL PLUS(P1,P2,KAPB,3,1)
```

```
C
 300 CONTINUE
C
C  ....CALCULATE THE STRESSES IN EACH PLY IN THE X-Y DIRECTION....
C
      DO 900  L = 1,PLIES
      DO 901  J = 1,3
      H = (Z(L+1)-Z(L))/2.0 + Z(L)
      WRITE (6,55) H
      EPSX(L,J) = EPS(J) + H*KAP(J)
      EPSXT(L,J) = EPSTH(J) + H*KAPT(J)
      EPSXB(L,J) = EPSB(J) + H*KAPB(J)
      EPST1(L,J) = EPSXT(L,J) - EPST(L,J)
      EPSTH1(L,J) = EPSXB(L,J) - EPST(L,J)
  901 CONTINUE
  900 CONTINUE
      DO 9001 I=1,PLIES
      WRITE (6,55) EPSXT(I,1),EPSXT(I,2),EPSXT(I,3)
 9001 CONTINUE
      DO 9002 I =1,PLIES
      WRITE (6,55) EPST1(I,1),EPST1(I,2),EPST1(I,3)
 9002 CONTINUE
      WRITE (6,55) RNT(1),RNT(2),RNT(3)
      WRITE (6,55) EPSTH(1),EPSTH(2),EPSTH(3)
      WRITE (6,55) KAPT(1),KAPT(2),KAPT(3)
C
      DO 701 I = 1,PLIES
      K = ANGN(I)
      J = MATN(I)
      DO 703 L = 1,3
      SIGX(I,L) = E(L,1,J,K)*EPSX(I,1) + E(L,2,J,K)*EPSX(I,2) +
     A  E(L,3,J,K)*EPSX(I,3)
      SIGXT(I,L) = E(L,1,J,K)*EPST1(I,1) + E(L,2,J,K)*EPST1(I,2) +
     A  E(L,3,J,K)*EPST1(I,3)
      SIGXB(I,L) = E(L,1,J,K)*EPSTH1(I,1) + E(L,2,J,K)*EPSTH1(I,2) +
     A  E(L,3,J,K)*EPSTH1(I,3)
  703 CONTINUE
  701 CONTINUE
C
C  ....CALCULATE THE STRESSES IN THE 1-2 DIRECTION.....
C
      DO 932 I = 1,ANGLE
      T1(1,1,I) = COS(RTHETA(I))**2
      T1(1,2,I) = SIN(RTHETA(I))**2
      T1(1,3,I) = COS(RTHETA(I))*SIN(RTHETA(I))
      T1(2,1,I) = T1(1,2,I)
      T1(2,2,I) = T1(1,1,I)
      T1(2,3,I) = -T1(1,3,I)
      T1(3,1,I) = -T1(1,3,I)*2.0
      T1(3,2,I) = -T1(3,1,I)
      T1(3,3,I) = COS(RTHETA(I))**2 - SIN(RTHETA(I))**2
```

```
 932 CONTINUE
C
      DO 963  L = 1,PLIES
      K = ANGN(L)
      DO 964  I = 1,3
      EPS1(L,I) = T1(I,1,K)*EPSX(L,1) + T1(I,2,K)*EPSX(L,2)
     A   + T1(I,3,K)*EPSX(L,3)
      EPS1T(L,I) = T1(I,1,K)*EPSXT(L,1) + T1(I,2,K)*EPSXT(L,2)
     A  + T1(I,3,K)*EPSXT(L,3)
      EPS1B(L,I) = T1(I,1,K)*EPSXB(L,1) + T1(I,2,K)*EPSXB(L,2)
     A  + T1(I,3,K)*EPSXB(L,3)
 964 CONTINUE
 963 CONTINUE
C
      DO 705  I = 1,PLIES
      K = MATN(I)
      SIG1(I,1) = Q11(K)*EPS1(I,1) + Q12(K)*EPS1(I,2)
      SIG1(I,2) = Q12(K)*EPS1(I,1) + Q22(K)*EPS1(I,2)
      SIG1(I,3) = Q66(K)*EPS1(I,3)
      SIG1T(I,1) = Q11(K)*EPS1T(I,1) + Q12(K)*EPS1T(I,2)
      SIG1T(I,2) = Q12(K)*EPS1T(I,1) + Q22(K)*EPS1T(I,2)
      SIG1T(I,3) = Q66(K)*EPS1T(I,3)
C
      SIG1B(I,1) = Q11(K)*EPS1B(I,1) + Q12(K)*EPS1B(I,2)
      SIG1B(I,2) = Q12(K)*EPS1B(I,1) + Q22(K)*EPS1B(I,2)
      SIG1B(I,3) = Q66(K)*EPS1B(I,3)
 705 CONTINUE
C
C
C
C     .....DISPLAY ALL DATA OBTAINED.....
C
      PRINT *, 'THIS IS A LAMINATE COMPOSITE MATERIAL PROGRAM'
      PRINT *, ' '
      PRINT *, ' '
      PRINT *, ' '
      PRINT *, 'THERE IS ', NOMAT,' TYPE OF MATERIAL'
      PRINT *, ' '
      PRINT *, 'THERE ARE ',ANGLE,' DIFFERENT ANGLES IN THIS LAMINATE'
      PRINT *, ' '
      DO 210 I = 1,ANGLE
      PRINT *, ' '
      PRINT *, 'ROTATION ',I,' EQUALS ',THETA(I),' DEGREES'
 210 CONTINUE
      PRINT *, ' '
      PRINT *, ' '
      IF (ITEMP .EQ. 1) GO TO 1111
      PRINT *, 'THERE ARE THERMAL EFFECTS IN THIS LAMINATE'
      PRINT *,' '
      PRINT *, ' '
1111 CONTINUE
```

```
      DO 201 I = 1,NOMAT
      PRINT *, 'THE ENGINEERING PARAMETERS FOR MATERIAL ',I,' ARE:'
      PRINT *, ' '
      PRINT *, '    E11      E22      G12      NU12 '
      PRINT *, ' '
      WRITE (6,52)  E11(I),E22(I),G12(I),NU12(I)
   52 FORMAT (3E11.5,1F5.2)
  201 CONTINUE
      PRINT *, ' '
      PRINT *, ' '
      DO 202 I = 1,NOMAT
      PRINT *, ' '
      PRINT *, 'ORTHOTROPIC COMPLIANCE MATRIX FOR MATERIAL ',I
      PRINT *, ' '
      DO 10 J = 1,6
   10 WRITE (6,50) (A(J,K,I), K = 1,6)
   50 FORMAT (5X, 6E11.5)
      PRINT *, ' '
  202 CONTINUE
      PRINT *, ' '
      DO 203 I = 1,NOMAT
      PRINT *, ' '
      PRINT *, 'ORTHOTROPIC STIFFNESS MATRIX FOR MATERIAL ',I
      PRINT *, ' '
      DO 11 J = 1,6
   11 WRITE (6,50) (B(J,K,I), K = 1,6)
      PRINT *, ' '
  203 CONTINUE
      PRINT *, ' '
      DO 204  I = 1,NOMAT
      DO 205  K = 1,ANGLE
      PRINT *, ' '
      PRINT *, 'THE REDUCED STIFFNESS MATRIX FOR MATERIAL ', I
      PRINT *, 'AND ROTATION ', K, ' IS:'
      PRINT *, ' '
      DO 12 J = 1,3
   12 WRITE(6,51) (E(J,M,I,K), M=1,3)
   51 FORMAT (5X,3E11.5)
      PRINT *, ' '
  205 CONTINUE
  204 CONTINUE
      PRINT *, ' '
C
      DO 206  I = 1,NOMAT
      DO 207  K = 1,ANGLE
      PRINT *, ' '
      PRINT *, 'THE REDUCED COMPLIANCE MATRIX FOR MATERIAL ', I
      PRINT *, 'AND ROTATION ', K, ' IS:'
      PRINT *, ' '
      DO 13 J = 1,3
   13 WRITE(6,51) (D(J,M,I,K), M = 1,3)
```

```
      PRINT *, ' '
  207 CONTINUE
  206 CONTINUE
      PRINT *, ' '
      PRINT *, ' '
C
      DO 208 I = 1,NOMAT
      DO 209 K = 1,ANGLE
      PRINT *, ' '
      PRINT *, 'THE LAMINA ENGINEERING PARAMETERS FOR MATERIAL ',I
      PRINT *, 'AND ROTATION ',K,' ARE:'
      PRINT *, ' '
      PRINT *, '  EXX    EYY    NUXY   GXY  ETAXYX  ETAXYY'
      PRINT *, ' '
      WRITE(6,53) EXX(I,K),EYY(I,K),NUXY(I,K),GXY(I,K),ETAXYX(I,K),
     A ETAXYY(I,K)
   53 FORMAT (2E11.5,F5.2,E11.5,2F6.3)
      PRINT *, ' '
  209 CONTINUE
  208 CONTINUE
      PRINT *, ' '
      IF (ISYM .EQ. 1) GO TO 800
      PRINT *, ' '
      PRINT *, 'THE LAMINATE ENGINEERING PARAMETERS ARE:'
      PRINT *, ' '
      PRINT *, 'EBARX   EBARY   GBARXY   NUBARXY  ETABXYX  ETABXYY
     AETABXXY  ETABYXY'
      PRINT *, ' '
      WRITE(6,54) EBARX,EBARY,GBARXY,NUBARXY,ETABXYX,ETABXYY,ETABXXY,
     A ETABYXY
   54 FORMAT (3E9.3,F5.2,4E10.4)
      PRINT *, ' '
      GO TO 801
C
  800 CONTINUE
      PRINT *, 'THERE ARE NO LAMINATE ENGINEERING PARAMETERS'
      PRINT *, ' '
  801 CONTINUE
      PRINT *, 'THE LAMINATE COEFFICIENTS OF THERMAL EXPANSION ARE: '
      PRINT *, ' '
      DO 88 I = 1,3
      WRITE (6,58) ALAM(I)
   58 FORMAT (5X,3E11.5)
   88 CONTINUE
      PRINT *, ' '
      PRINT *, ' '
      PRINT *, 'THE [A] MATRIX FOR THE LAMINATE IS'
      PRINT *, ' '
      DO 211  I = 1,3
  211 WRITE (6,51) (AA(I,J), J=1,3)
      PRINT *, ' '
```

```
      PRINT *, ' '
      PRINT *, 'THE [B] MATRIX FOR THE LAMINATE IS'
      PRINT *, ' '
      DO 212  I = 1,3
  212 WRITE (6,51) (BB(I,J),  J = 1,3)
      PRINT *, ' '
      PRINT *, 'THE [D] MATRIX FOR THE LAMINATE IS'
      PRINT *, ' '
      DO 213 I=1,3
  213 WRITE (6,51) (DD(I,J), J=1,3)
      PRINT *, ' '
      PRINT *, ' '
      PRINT *, 'THE MECHANICAL STRESSES IN THE X-Y DIRECTION ARE'
      PRINT *, ' '
      DO 214 I = 1,PLIES
      PRINT *, 'IN PLY ',I ,':'
      WRITE (6,55) (SIGX(I,J), J=1,3)
  214 CONTINUE
      PRINT *, ' '
      PRINT *, 'THE THERMAL STRESSES IN THE X-Y DIRECTION ARE'
      PRINT *, ' '
      DO 218 I = 1,PLIES
      PRINT *, 'IN PLY ',I,':'
      WRITE (6,55) (SIGXT(I,J), J=1,3)
  218 CONTINUE
      PRINT *, ' '
      PRINT *, 'THE THERMAL AND MECHANICAL STRESSES '
      PRINT *, '      IN THE X-Y DIRECTION'
      PRINT *, ' '
      DO 219 I = 1, PLIES
      PRINT *, 'IN PLY ',I,':'
      WRITE (6,55) (SIGXB(I,J), J=1,3)
  219 CONTINUE
      PRINT *, ' '
   55 FORMAT (10X,3E11.5)
      PRINT *, ' '
      PRINT *, ' '
      PRINT *, 'THE MECHANICAL STRESSES IN THE 1-2 DIRECTION ARE'
      PRINT *, ' '
      DO 215  I = 1,PLIES
      PRINT *, 'IN PLY ',I ,':'
      WRITE (6,55) (SIG1(I,J),J=1,3)
  215 CONTINUE
      PRINT *, ' '
      PRINT *, 'THE THERMAL STRESSES IN THE 1-2 DIRECTION ARE'
      PRINT *, ' '
      DO 220 I = 1,PLIES
      PRINT *, 'IN PLY ',I,':'
      WRITE (6,55) (SIG1T(I,J),J=1,3)
  220 CONTINUE
      PRINT *, ' '
```

```
      PRINT *, 'THE THERMAL AND MECHANICAL STRESSES '
      PRINT *, '     IN THE 1-2 DIRECTION '
      PRINT *, ' '
      DO 221 I = 1,PLIES
      PRINT *, 'IN PLY ',I,':'
      WRITE (6,55) (SIG1B(I,J),J=1,3)
  221 CONTINUE
      PRINT *, ' '
      PRINT *,' '
      IF (ILOAD .EQ. 0) GO TO 775
      PRINT *, ' '
      PRINT *, 'THE RESULTANT FORCES AND MOMENTS ARE'
      PRINT *, ' '
      PRINT *, '   [N]       [M]'
      DO 216 I = 1,3
  216 WRITE (6,57) PN(I),PM(I)
   57 FORMAT (F7.2,5X,F7.2)
      PRINT *, ' '
      GO TO 776
  775 CONTINUE
      PRINT *, ' '
      PRINT *, 'THE RESULTANT MIDPLANE STRAINS AND CURVATURES ARE'
      PRINT *, ' '
      PRINT *, 'STRAINS     CURVATURES'
      PRINT *, ' '
      DO 217 I = 1,3
  217 WRITE (6,56) EPS(I),KAP(I)
   56 FORMAT (E11.5,5X,E11.5)
  776 CONTINUE
C
      PRINT *, ' '
      PRINT *, ' '
      PRINT *, 'THE RESULTS OF THE MAX STRESS FAILURE CRITERION'
      PRINT *, ' '
      IF (QUEST .EQ. 1) GO TO 2000
      DO 2001 I = 1, PLIES
      PRINT *, 'THE FORCE RESULTANT TO PRODUCE FIRST PLY FAIL'
      PRINT *, ' '
      PRINT *, 'FOR PLY ', I,':'
 2001 WRITE (6,55) (NXX(I,J), J=1,3)
      GO TO 2002
 2000 CONTINUE
      PRINT *, 'THE CHANGE IN TEMPERATURE TO PRODUCE
     A  FIRST PLY FAILURE IS'
      PRINT *, ' '
      DO 2003 I = 1,PLIES
      PRINT *, 'FOR PLY ',I,':'
 2003 WRITE (6,55) (DEL(I,J), J=1,3)
 2002 CONTINUE
      PRINT *,' '
      PRINT *, ' '
```

```
      WRITE (6,55) EPST1(1,1),EPSTH(1),KAPT(1)
      WRITE (6,55) EPSXT(1,1),EPST(1,1),ALPX(1,1)
      WRITE (6,55) T2(1,2,1),ALP2(1),DELTT
      WRITE (6,55) RNT(1),RMT(1),TEMPN
      PRINT *, ' '
      DO 3000 I = 1, PLIES
      WRITE (6,55) (ALPX(I,J),J=1,3)
      WRITE (6,55) (EPST(I,J),J=1,3)
      WRITE (6,55) (ALPY(I,J),J=1,3)
 3000 CONTINUE
      PRINT *, ' '
C
      STOP
      END
C*************** ************************************************
C
C     .....SUBROUTINE TO INVERT A 3 BY 3 MATRIX.....
C
      SUBROUTINE INVRS(U,V)
C
      DIMENSION U(3,3), A(3,3), V(3,3)
      DET1 = U(2,2)*U(3,3)-U(2,3)*U(3,2)
      DET2 = U(2,1)*U(3,3)-U(2,3)*U(3,1)
      DET3 = U(2,1)*U(3,2)-U(2,2)*U(3,1)
      DET = U(1,1)*DET1-U(1,2)*DET2+U(1,3)*DET3
C
      A(1,1) = U(2,2)*U(3,3)-U(2,3)*U(3,2)
      A(1,2) = (U(1,2)*U(3,3)-U(1,3)*U(3,2))*(-1.0)
      A(1,3) = U(1,2)*(2,3)-U(1,3)*U(2,2)
      A(2,1) = (U(2,1)*U(3,3)-U(2,3)*U(3,1))*(-1.0)
      A(2,2) = U(1,1)*U(3,3)-U(1,3)*U(3,1)
      A(2,3) = (U(1,1)*U(2,3)-U(1,3)*U(2,1))*(-1.0)
      A(3,1) = U(2,1)*U(3,2)-U(2,2)*U(3,1)
      A(3,2) = (U(1,1)*U(3,2)-U(1,2)*U(3,1))*(-1.0)
      A(3,3) = U(1,1)*U(2,2)-U(1,2)*U(2,1)
C
      DO 20, I = 1,3
        DO 10,  J = 1,3
          V(I,J) = A(I,J)/DET
   10 CONTINUE
   20 CONTINUE
      RETURN
      END
C
C*****************************************************************
C
      SUBROUTINE MPLY(U,V,T,M,K,N)
C
      DIMENSION U(M,K),V(K,N),T(M,N)
      DO 20,  I = 1,M
      DO 20,  J = 1,N
```

```
      T(I,J) = 0.0
      DO 20, L = 1,K
      T1 = U(I,L)*V(L,J)
      T(I,J) = T(I,J) + T1
   20 CONTINUE
      RETURN
      END


C
C*********************************************************************
C
      SUBROUTINE PLUS(U,V,T,K,L)
C
      DIMENSION U(K,L),V(K,L),T(K,L)
      DO 5, I = 1,K
      DO 5, J = 1,L
      T(I,J) = 0.0
    5 CONTINUE
      DO 10, I = 1,K
      DO 10, J = 1,L
      T(I,J) = U(I,J) + V(I,J)
   10 CONTINUE
      RETURN
      END
C
C*********************************************************************
C
      SUBROUTINE MINUS(U,V,T,K,L)
C
      DIMENSION U(K,L),V(K,L),T(K,L)
      DO 5, I = 1,K
      DO 5 J = 1,L
      T(I,J) = 0.0
    5 CONTINUE
      DO 10, I = 1,K
      DO 10, J = 1,L
      T(I,J) = U(I,J) - V(I,J)
   10 CONTINUE
      RETURN
      END
```

Appendix B

Session File

B.1 Log In

```
>PATRAN2
>4107
>GO
>1
```

B.2 Model Generation

```
>1
>1
>GR,1
>GR,8,TR,0/9/0
>VIEW
>1
>30,30,30
>GR,4,,0/3/0
>GR,2,,0,.6,.8
>GR,3,,0,1.1,1.3
>GR,5,,0,1.6,1.6
>GR,6,,0,2.1,1.8
>GR,7,,0,4,1.9
>GR,9,,0,6.6,1.1
>LI,1,FIT,,1/2/3/5/6/4
>LI,2,TR,80,1
>LI,3,FIT,,4/7/9/8
>LI,4.TR,80,3
>PA,1,2L,,1,2
>PA,2,2L,,3,4
>PA,3,MI,Z,1
>PA,4,MI,Z,2
>SET,LABE,OFF
>END
```

B.3 Node Generation

```
>2
>1
>1
>SET,CPLOT,ON
>GF,PA1,,4/25
>GF,PA2,,4/25
```

```
>GF,PA3,,25/4
>GF,PA4,,25/4
```

B.4 Material Property Definition

```
>PMAT,10,ORT,56.3E6,2(1.1E6),.41,.45,.00801,,2.2E6,
>.5E6,2.2E6,.5E-6,2(6.5E-6)
>PMAT,30,ISO,.67E6,,.36,,25E-6
>DATA,15,.6,.4,1,1,2,2,1
>PMAT,50,HAL,D15,10/30
>PMAT,100/107,LAMS,4(.015),0/30/15/90,4(50)
>END
```

B.5 Element Mesh Generation

```
>2
>1
>CF,PA1T4,TRI3/53,T1
>END
```

B.6 Equivalencing

```
>SET,CPLOT,OFF
>3
>N
>2
>1
>N
END
```

B.7 Force and Constraint Application

```
>SET,PH1,OFF
>4
>1
>DF,PA1,FORCE,100,1,ED2
>DF,PA2,FORCE,100,1,ED2
>DF,PA3,FORCE,100,1,ED1
>DF,PA4,FORCE,100,1,ED1
>DF,PA1,D,/0/0///,1,N4/100
>END
```

B.8 Model Optimization

```
>7
>5
>3
>2
>END
```

B.9 Material Property Assignment

```
>5
>1
```

```
>PF,PA1T4,TRI/3/53,1,106
>END
```

B.10 ANSYS Interface

```
>8
>5
>3
>1
>1
>'
>BLADE1
>Y
>Y
>2
>2
>5
>6
```

Appendix C

Equation Solution Program

```
      PROGRAM CALC
C
C     ****************************************************
C     *
C     *          PROGRAM CALC
C     *
C     *        PATRICK GRAHAM FORRESTER
C     *       UNIVERSITY OF VIRGINIA 1989
C     *          THESIS RESEARCH
C     *
C     ****************************************************
C
C
C     THIS PROGRAM IS DESIGNED TO READ THE DISPLACEMENT INFORMATION
C     PROUCED BY ANSYS.43A FOR 24 NODES OF THE COMPOSITE BLADE
C     MODEL AND USE IT TO CALCULATE THE CHANGE IN DISPLACEMENT
C     OVER THE LENGTH OF THE BLADE AND THEN SOLVE THE CLASSICAL
C     BEAM EQUATIONS.
C
C     ****************************************************
C
      REAL UX1,UX2,UY1,UY2,UZ1,UZ2
      REAL UX(2,100),UY(2,100),UZ(2,100)
      REAL INT,SLOPE
      REAL Y1,Y2,Z1,Z2,L1,L2,T1,T2
      REAL BETA(100),PHI(100),PSI(100),U(100)
      REAL UXNOT(100),UYNOT(100),UZNOT(100)
      REAL BETAP(100),PHIP(100),PSIP(100),UP(100)
      DIMENSION A(4,4,12),B(4),X(4)
      INTEGER BLADES,NODES,LOADS
      REAL H,C,ZETA(100)
      OPEN (UNIT=12,FILE='NEWDATA',STATUS='OLD')
      OPEN (UNIT=13,FILE='RES5',STATUS='NEW')
C
C     .....ASSIGN INPUT DATA.....
C
      H = 3.33333
      C = 9.0
      NODES = 2
```

```
      BLADES = 1
      LOADS = 4
C
C     .....READ IN NODAL DISPLACEMENTS FROM ANSYS.....
C
C      1 = LEADING EDGE NODE
C      2 = LEADING EDGE NODE
C
      DO 1 K = 1,BLADES
      DO 9 L = 1,LOADS
      DO 2 J = 1,3*NODES
C
      T1 = 9.0
      T2 = 0.0
      L1 = 0.0
      L2 = 0.0
C
      READ(12,*) UX1,UY1,UZ1,UX2,UY2,UZ2
C
      UX(1,J) = UX1
      UY(1,J) = UY1
      UZ(1,J) = UZ1
      UX(2,J) = UX2
      UY(2,J) = UY2
      UZ(2,J) = UZ2
C
C     .....CALCULATE ZETA FOR ISOTROPIC MODEL.....
C
      IF (K .NE. 1) GO TO 2
      IF (L .NE. 1) GO TO 2
C
      Y1 = L1 + UY1
      Y2 = T1 + UY2
      Z1 = L2 + UZ1
      Z2 = T2 + UZ2
C
      SLOPE = (Y1 - Y2)/(Z1 - Z2)
      INT = (Y1 - (Z1/SLOPE))
      ZETA(J) = INT/C
C
    2 CONTINUE
C
C
C     .....CALCULATE DISPLACEMENTS AND ROTATIONS.....
C
C     .....CALCULATE ALL BETA FOR MODEL.....
C
      DO 3 J = 1,6
      BETA(J) = -(UZ(1,J) - UZ(2,J))/C
    3 CONTINUE
C
```

```
C   .....CALCULATE ALL PHI FOR MODEL.....
C
    DO 4 J = 1,6
    UZNOT(J) = UZ(1,J)*(1 - ZETA(J)) + UZ(2,J)*(ZETA(J))
    UYNOT(J) = UY(1,J)*(1 - ZETA(J)) + UY(2,J)*(ZETA(J))
    UXNOT(J) = UX(1,J)*(1 - ZETA(J)) + UX(2,J)*(ZETA(J))
  4 CONTINUE
C
    PHI(1) = (UZNOT(3) - UZNOT(2))/H
    PHI(2) = (UZNOT(2) - UZNOT(1))/H
    PHI(3) = (UZNOT(6) - UZNOT(5))/H
    PHI(4) = (UZNOT(5) - UZNOT(4))/H
C
C   .....CALCULATE ALL PSI FOR MODEL.....
C
C
    PSI(1) = (UYNOT(3) - UYNOT(2))/H
    PSI(2) = (UYNOT(2) - UYNOT(1))/H
    PSI(3) = (UYNOT(6) - UYNOT(5))/H
    PSI(4) = (UYNOT(5) - UYNOT(4))/H
C
C
C   .....CALCULATE THE FIRST DERIVATIVE WRT X.....
C
    BETAP(1) = (BETA(3) - BETA(1))/(2*H)
    BETAP(2) = (BETA(6) - BETA(4))/(2*H)
C
    PHIP(1) = (PHI(1) - PHI(2))/H
    PHIP(2) = (PHI(3) - PHI(4))/H
C
    PSIP(1) = (PSI(1) - PSI(2))/H
    PSIP(2) = (PSI(3) - PSI(4))/H
C
    UP(1) = (UXNOT(3) - UXNOT(1))/(2*H)
    UP(2) = (UXNOT(6) - UXNOT(4))/(2*H)
C
    DO 30 J = 1,NODES
C
C   .....IDENTIFY LOADS AND DISPLACEMENTS.....
C
    X(1) = 1000
    X(2) = 1000
    X(3) = 1000
    X(4) = 1000
C
    B(1) =  BETAP(J)
    B(2) =  PHIP(J)
    B(3) =  PSIP(J)
    B(4) =  UP(J)
C
C   .....SOLVE THE EQUATION MATRIX.....
```

```
C
      DO 99 I = 1,4
      A(I,L,J) = B(I)/X(L)
   99 CONTINUE
C
C     .....WRITE THE COLUMN SOLUTION FOR FUTURE USE.....
C
      WRITE(13,*)
      WRITE(13,*) 'NUMBER ',L,' COLUMN FOR SECTION: ',J,',', ' BLADE: ',
     A   K
      WRITE(13,*)
      DO 6 I = 1,4
      WRITE(13,666) A(I,L,J)
    6 CONTINUE
  666 FORMAT (15X,1E15.6)
C
C     .....BUILD THE MATRIX FOR EACH NODE.....
C
   30 CONTINUE
    9 CONTINUE
      DO 11 J = 1,NODES
      WRITE(13,*)
      WRITE (13,*) 'MATRIX FOR SECTION: ',J,'.', ' BLADE: ',K
      WRITE(13,*)
      DO 10 I = 1,4
      WRITE (13,667) A(I,1,J), A(I,2,J), A(I,3,J), A(I,4,J)
   10 CONTINUE
   11 CONTINUE
  667 FORMAT (12X,4E14.6)
      DO 300 J = 1,6
      WRITE (13,669) ZETA(J)
  669 FORMAT (2X,1E14.6)
  300 CONTINUE
    1 CONTINUE
      STOP
      END
```

Appendix D

Sample ANSYS Input File

```
C*** PREP7 INPUT PRODUCED BY "PATANS" VERSION 1.7B

C*** 06-FEB-89  16:28: 9

/TITLE, BLADE2MZ
/NOPR

C*** NODAL COORDINATE DEFINITION

N,   1, 0.0000000  , 0.0000000  , 0.0000000
N,   2, 0.0000000  , 0.7652769  , 0.9910634
N,   3, 0.0000000  , 1.788908   , 1.688653
N,   4, 0.0000000  , 3.000000   , 2.000000
N,   5, 3.333333   , 0.0000000  , 0.0000000
N,   6, 3.333333   , 0.7652769  , 0.9910634
N,   7, 3.333333   , 1.788908   , 1.688653
N,   8, 3.333333   , 3.000000   , 2.000000
N,   9, 6.666666   , 0.0000000  , 0.0000000
N,  10, 6.666666   , 0.7652769  , 0.9910634
N,  11, 6.666666   , 1.788908   , 1.688653
N,  12, 6.666666   , 3.000000   , 2.000000
N,  13, 10.00000   , 0.0000000  , 0.0000000
N,  14, 10.00000   , 0.7652769  , 0.9910634
N,  15, 10.00000   , 1.788908   , 1.688653
N,  16, 10.00000   , 3.000000   , 2.000000
N,  17, 13.33333   , 0.0000000  , 0.0000000
N,  18, 13.33333   , 0.7652769  , 0.9910634
N,  19, 13.33333   , 1.788908   , 1.688653
N,  20, 13.33333   , 3.000000   , 2.000000
N,  21, 16.66666   , 0.0000000  , 0.0000000
N,  22, 16.66666   , 0.7652769  , 0.9910634
N,  23, 16.66666   , 1.788908   , 1.688653
N,  24, 16.66666   , 3.000000   , 2.000000
N,  25, 20.00000   , 0.0000000  , 0.0000000
N,  26, 20.00000   , 0.7652769  , 0.9910634
N,  27, 20.00000   , 1.788908   , 1.688653
N,  28, 20.00000   , 3.000000   , 2.000000
N,  29, 23.33333   , 0.0000000  , 0.0000000
N,  30, 23.33333   , 0.7652769  , 0.9910634
```

```
N,   31,  23.33333  ,  1.788908  ,  1.688653
N,   32,  23.33333  ,  3.000000  ,  2.000000
N,   33,  26.66666  ,  0.0000000 ,  0.0000000
N,   34,  26.66666  ,  0.7652769 ,  0.9910634
N,   35,  26.66666  ,  1.788908  ,  1.688653
N,   36,  26.66666  ,  3.000000  ,  2.000000
N,   37,  30.00000  ,  0.0000000 ,  0.0000000
N,   38,  30.00000  ,  0.7652769 ,  0.9910634
N,   39,  30.00000  ,  1.788908  ,  1.688653
```

-THRU-

```
N,  301,  79.99998  ,  .7652769  ,  0.0000000
N,  302,  79.99998  ,  1.788908  ,  0.0000000
N,  303,  79.99998  ,  3.000000  ,  0.0000000
N,  304,  79.99998  ,  5.085196  ,  0.0000000
N,  305,  79.99998  ,  7.079720  ,  0.0000000
N,  306,  0.000000  ,  .7652769  ,  0.0000000
N,  307,  0.000000  ,  1.788908  ,  0.0000000
N,  308,  0.000000  ,  3.000000  ,  0.0000000
N,  309,  0.000000  ,  5.085196  ,  0.0000000
N,  310,  0.000000  ,  7.079720  ,  0.0000000
```

C*** ELEMENT LIBRARY DEFINITION

```
ET,   1,  53,   0,   0,   8,   0,   0,   0
```

C*** ELEMENT CONNECTIVITY DEFINITION

```
TYPE,   1 $MAT,   106 $REAL,   1

E,  106,  103,  252,  252
E,  102,  103,  106,  106
E,  252,  254,  106,  106
E,  254,  252,  251,  251
E,  101,  102,  105,  105
E,  106,  105,  102,  102
E,  109,  106,  254,  254
E,  105,  106,  109,  109
E,  251,  253,  254,  254
E,  253,  251,  178,  178
E,  256,  254,  253,  253
E,  254,  256,  109,  109
```

-THRU-

```
E,   89,   93,  245,  245
E,  245,  248,  249,  249
E,  248,  245,   93,   93
E,   99,   98,   94,   94
E,   93,   94,   98,   98
```

```
E,  98,  97,  93,  93
E,  93,  97, 248, 248

TYPE,  1 $MAT,  106 $REAL,  2

E,   1,   2, 306, 306
E,   2,   3, 307, 307
E,   2, 307, 306, 306
E,   3,   4, 307, 307
E,   4, 308, 307, 307
E,   4, 101, 308, 308
E, 101, 309, 308, 308
E, 101, 102, 309, 309
E, 102, 310, 309, 309
E, 102, 103, 310, 310
E,   1, 306, 176, 176
E, 306, 307, 176, 176
E, 307, 177, 176, 176
E, 307, 308, 178, 178
E, 307, 178, 177, 177
E, 308, 309, 251, 251
E, 308, 251, 178, 178
E, 309, 310, 252, 252
E, 309, 252, 251, 251
E, 310, 103, 252, 252
E,  97,  98, 301, 301
E,  98, 302, 301, 301
E,  98,  99, 302, 302
E,  99, 100, 302, 302
E, 100, 303, 302, 302
E, 100, 173, 303, 303
E, 173, 304, 303, 303
E, 173, 174, 304, 304
E, 174, 305, 304, 304
E, 174, 175, 305, 305
E,  97, 301, 248, 248
E, 301, 302, 248, 248
E, 248, 302, 249, 249
E, 302, 250, 249, 249
E, 302, 303, 250, 250
E, 303, 299, 250, 250
E, 303, 304, 299, 299
E, 304, 305, 300, 300
E, 304, 300, 299, 299
E, 305, 175, 300, 300

C*** REAL CONSTANT DEFINITION

R , 1,.015,50,0,.015,50,30
RMORE,.015,50,15,.015,50,90
RMORE,.015,50,90,.015,50,15
```

```
RMORE,.015,50,30,.015,50,0
R , 2,.3,106,90,.3,106,0
RMORE,.3,106,90,.3,106,0
RMORE,.3,106,90,.3,106,0
RMORE,.3,106,90,.3,106,0

C*** MATERIAL DEFINITION

ALPX,  30, 0.2500000E-05
EX ,  30, 670000.0
NUXY,  30, 0.3600000
GXY ,  30, 246323.5
DENS,  50, 1.000000
ALPX,  50, 0.5157655E-06$ALPY,  50,-0.2215747E-06$ALPZ,  50,-0.2215593E-06
EX ,  50, 0.1920000E+08$EY ,  50, 1560000.  $EZ ,  50, 1560000.
NUXY,  50, 0.1950000E-01$NUYZ,  50, 0.2100000  $NUXZ,  50, 0.801000E-02
GXY ,  50, 820000.0
DENS,  106, 1.000000
ALPX,  106, 0.4391691E-06$ALPY,  106, 0.4441189E-06$ALPZ,  106,-0.4642736E-06
EX ,  106, 91963000.  $EY ,  106, 61118000.  $EZ ,  106, 61118000.
NUXY,  106, 01.051700E-01$NUYZ,  106, 2.400697E-01$NUXZ,  106, 01.051700E-01
GXY ,  106, 8381000.

C*** LOADS AND CONSTRAINTS DEFINITION

KTEMP, 0
DDEL,ALL $FDEL,ALL $NTDEL,ALL
TEDEL, 1,99999 $TDEL,1,99999 $EPDEL,1,99999,1,1 $RP6,,,,1
F ,  303,MZ , 1000.00
D ,  1,ALL , 0.0000000
D ,  2,ALL , 0.0000000
D ,  3,ALL , 0.0000000
D ,  4,ALL , 0.000000
D ,  101,ALL , 0.000000
D ,  102,ALL , 0.000000
D ,  103,ALL , 0.000000
D ,  176,ALL , 0.000000
D ,  177,ALL , 0.000000
D ,  178,ALL , 0.000000
D ,  251,ALL , 0.000000
D ,  252,ALL , 0.000000
LWRITE
/GOPR
```

Appendix E

Sample ANSYS Output File

GEOMETRY STORED FOR 310 NODES 616 ELEMENTS
TITLE= BLADE5MX
***** POST1 NODAL DISPLACEMENT LISTING *****

LOAD STEP 1 ITERATION= 1 SECTION= 1
TIME= 0.00000 LOAD CASE= 1

THE FOLLOWING X,Y,Z DISPLACEMENTS ARE IN NODAL COORDINATES

NODE	UX	UY	UZ	ROTX	ROTY	ROTZ
1	0.2283E-06	-0.1450E-06	0.2482	-0.8246E-01	-0.2335E-06	0.1792E-06
2	-0.1302E-06	0.8199E-01	0.1849	-0.8043E-01	-0.2723E-06	0.6654E-07
3	-0.2755E-06	0.1397	0.1002	-0.8131E-01	-0.1494E-06	-0.1079E-06
4	-0.6522E-07	0.1654	-0.3092E-07	-0.6561E-01	-0.1118E-07	-0.2450E-06
5	0.7092E-06	0.2541E-04	0.2487	-0.8299E-01	-0.2331E-03	0.7063E-04
6	-0.6694E-04	0.8227E-01	0.1852	-0.8298E-01	-0.7047E-03	0.1428E-02
7	-0.9195E-04	0.1400	0.1005	-0.8255E-01	-0.3136E-03	0.1129E-02
8	-0.8979E-04	0.1658	0.3806E-04	-0.8374E-01	0.3925E-02	0.1229E-01
9	-0.7112E-06	0.1869E-04	0.2495	-0.8311E-01	-0.2254E-03	-0.1435E-04
10	-0.1100E-03	0.8234E-01	0.1859	-0.8304E-01	-0.3756E-03	0.1526E-03
11	-0.1601E-03	0.1402	0.1009	-0.8306E-01	-0.4591E-03	0.4760E-03
12	-0.1681E-03	0.1661	0.2943E-03	-0.8301E-01	-0.4955E-03	0.1485E-02

***** POST1 NODAL DISPLACEMENT LISTING *****

LOAD STEP 1 ITERATION= 1 SECTION= 1
TIME= 0.00000 LOAD CASE= 1

THE FOLLOWING X,Y,Z DISPLACEMENTS ARE IN NODAL COORDINATES

NODE	UX	UY	UZ	ROTX	ROTY	ROTZ
13	0.6165E-06	0.3206E-07	0.2503	-0.8328E-01	-0.2781E-03	-0.2460E-05
14	-0.1491E-03	0.8250E-01	0.1866	-0.8324E-01	-0.2747E-03	0.9224E-04
15	-0.2319E-03	0.1405	0.1014	-0.8320E-01	-0.2429E-03	0.2577E-03
16	-0.2510E-03	0.1664	0.6454E-03	-0.8317E-01	-0.7682E-04	0.6402E-03
17	0.2653E-05	-0.9957E-05	0.2513	-0.8344E-01	-0.3180E-03	-0.1159E-05
18	-0.1889E-03	0.8265E-01	0.1875	-0.8340E-01	-0.2912E-03	0.5352E-04
19	-0.3011E-03	0.1408	0.1021	-0.8336E-01	-0.2565E-03	0.1227E-03
20	-0.3316E-03	0.1667	0.1171E-02	-0.8332E-01	-0.1905E-03	0.2422E-03
21	0.4029E-05	-0.1126E-04	0.2525	-0.8359E-01	-0.3570E-03	0.1469E-05
22	-0.2279E-03	0.8280E-01	0.1885	-0.8356E-01	-0.3235E-03	0.4998E-04
23	-0.3685E-03	0.1411	0.1030	-0.8352E-01	-0.2786E-03	0.9272E-04
24	-0.4111E-03	0.1670	0.1821E-02	-0.8349E-01	-0.2149E-03	0.1447E-03

***** POST1 NODAL DISPLACEMENT LISTING *****

LOAD STEP 1 ITERATION= 1 SECTION= 1
TIME= 0.00000 LOAD CASE= 1

THE FOLLOWING X,Y,Z DISPLACEMENTS ARE IN NODAL COORDINATES

NODE	UX	UY	UZ	ROTX	ROTY	ROTZ
25	0.4624E-05	-0.7447E-05	0.2537	-0.8373E-01	-0.3962E-03	0.2056E-05
26	-0.2664E-03	0.8295E-01	0.1896	-0.8371E-01	-0.3598E-03	0.4692E-04
27	-0.4349E-03	0.1413	0.1039	-0.8368E-01	-0.3133E-03	0.8112E-04
28	-0.4901E-03	0.1673	0.2605E-02	-0.8365E-01	-0.2551E-03	0.1086E-03
29	0.4668E-05	-0.1461E-05	0.2551	-0.8388E-01	-0.4353E-03	0.2056E-05
30	-0.3048E-03	0.8311E-01	0.1909	-0.8387E-01	-0.3975E-03	0.4624E-04
31	-0.5009E-03	0.1416	0.1051	-0.8384E-01	-0.3501E-03	0.7815E-04
32	-0.5689E-03	0.1677	0.3519E-02	-0.8382E-01	-0.2934E-03	0.9716E-04
33	0.4400E-05	0.4874E-05	0.2566	-0.8404E-01	-0.4744E-03	0.1770E-05
34	-0.3435E-03	0.8327E-01	0.1923	-0.8402E-01	-0.4360E-03	0.4609E-04
35	-0.5669E-03	0.1419	0.1063	-0.8400E-01	-0.3882E-03	0.7698E-04
36	-0.6475E-03	0.1680	0.4564E-02	-0.8398E-01	-0.3325E-03	0.9279E-04

***** POST1 NODAL DISPLACEMENT LISTING *****

LOAD STEP 1 ITERATION= 1 SECTION= 1
TIME= 0.00000 LOAD CASE= 1

THE FOLLOWING X,Y,Z DISPLACEMENTS ARE IN NODAL COORDINATES

NODE	UX	UY	UZ	ROTX	ROTY	ROTZ
37	0.3976E-05	0.1064E-04	0.2583	-0.8419E-01	-0.5135E-03	0.1403E-05
38	-0.3824E-03	0.8343E-01	0.1938	-0.8417E-01	-0.4750E-03	0.4610E-04
39	-0.6330E-03	0.1421	0.1077	-0.8416E-01	-0.4269E-03	0.7657E-04
40	-0.7260E-03	0.1683	0.5740E-02	-0.8414E-01	-0.3716E-03	0.9114E-04
41	0.3478E-05	0.1542E-04	0.2600	-0.8435E-01	-0.5528E-03	0.1028E-05
42	-0.4215E-03	0.8359E-01	0.1955	-0.8433E-01	-0.5142E-03	0.4609E-04
43	-0.6993E-03	0.1424	0.1092	-0.8431E-01	-0.4659E-03	0.7641E-04
44	-0.8046E-03	0.1686	0.7045E-02	-0.8430E-01	-0.4108E-03	0.9045E-04
45	0.2941E-05	0.1901E-04	0.2619	-0.8450E-01	-0.5922E-03	0.6627E-06
46	-0.4607E-03	0.8374E-01	0.1973	-0.8449E-01	-0.5535E-03	0.4603E-04
47	-0.7658E-03	0.1427	0.1108	-0.8447E-01	-0.5051E-03	0.7633E-04
48	-0.8832E-03	0.1689	0.8481E-02	-0.8445E-01	-0.4499E-03	0.9017E-04

***** POST1 NODAL DISPLACEMENT LISTING *****

LOAD STEP 1 ITERATION= 1 SECTION= 1
TIME= 0.00000 LOAD CASE= 1

THE FOLLOWING X,Y,Z DISPLACEMENTS ARE IN NODAL COORDINATES

NODE	UX	UY	UZ	ROTX	ROTY	ROTZ
49	0.2374E-05	0.2132E-04	0.2640	-0.8466E-01	-0.6316E-03	0.3082E-06
50	-0.5001E-03	0.8390E-01	0.1992	-0.8464E-01	-0.5929E-03	0.4592E-04
51	-0.8323E-03	0.1429	0.1125	-0.8463E-01	-0.5443E-03	0.7631E-04
52	-0.9618E-03	0.1692	0.1005E-01	-0.8461E-01	-0.4890E-03	0.9007E-04
53	0.1777E-05	0.2224E-04	0.2662	-0.8482E-01	-0.6711E-03	-0.4259E-07
54	-0.5395E-03	0.8406E-01	0.2012	-0.8480E-01	-0.6324E-03	0.4579E-04
55	-0.8990E-03	0.1432	0.1144	-0.8479E-01	-0.5837E-03	0.7634E-04

56 -0.1040E-02 0.1696 0.1174E-01-0.8477E-01-0.5280E-03 0.9007E-04
57 0.1153E-05 0.2168E-04 0.2685 -0.8498E-01-0.7106E-03-0.3972E-06
58 -0.5790E-03 0.8422E-01 0.2034 -0.8496E-01-0.6721E-03 0.4571E-04
59 -0.9656E-03 0.1435 0.1164 -0.8494E-01-0.6231E-03 0.7649E-04
60 -0.1119E-02 0.1699 0.1357E-01-0.8493E-01-0.5670E-03 0.9021E-04

***** POST1 NODAL DISPLACEMENT LISTING *****

LOAD STEP 1 ITERATION= 1 SECTION= 1
TIME= 0.00000 LOAD CASE= 1

THE FOLLOWING X,Y,Z DISPLACEMENTS ARE IN NODAL COORDINATES

NODE UX UY UZ ROTX ROTY ROTZ
61 0.5119E-06 0.1953E-04 0.2709 -0.8514E-01-0.7504E-03-0.8223E-06
62 -0.6186E-03 0.8437E-01 0.2057 -0.8512E-01-0.7120E-03 0.4583E-04
63 -0.1032E-02 0.1437 0.1186 -0.8510E-01-0.6628E-03 0.7702E-04
64 -0.1198E-02 0.1702 0.1552E-01-0.8508E-01-0.6060E-03 0.9064E-04
65 -0.1224E-06 0.1570E-04 0.2735 -0.8530E-01-0.7898E-03-0.8985E-06
66 -0.6581E-03 0.8453E-01 0.2082 -0.8528E-01-0.7525E-03 0.4681E-04
67 -0.1099E-02 0.1440 0.1209 -0.8526E-01-0.7031E-03 0.7868E-04
68 -0.1276E-02 0.1705 0.1761E-01-0.8525E-01-0.6448E-03 0.9202E-04
69 -0.6993E-06 0.1005E-04 0.2762 -0.8545E-01-0.8353E-03-0.5314E-05
70 -0.6975E-03 0.8468E-01 0.2107 -0.8544E-01-0.7974E-03 0.4924E-04
71 -0.1166E-02 0.1443 0.1233 -0.8543E-01-0.7456E-03 0.8369E-04
72 -0.1355E-02 0.1708 0.1982E-01-0.8541E-01-0.6838E-03 0.9619E-04

***** POST1 NODAL DISPLACEMENT LISTING *****

LOAD STEP 1 ITERATION= 1 SECTION= 1
TIME= 0.00000 LOAD CASE= 1

THE FOLLOWING X,Y,Z DISPLACEMENTS ARE IN NODAL COORDINATES

NODE UX UY UZ ROTX ROTY ROTZ
73 -0.1168E-05 0.2545E-05 0.2790 -0.8561E-01-0.8485E-03 0.1495E-04
74 -0.7365E-03 0.8483E-01 0.2134 -0.8560E-01-0.8374E-03 0.6572E-04
75 -0.1232E-02 0.1445 0.1258 -0.8559E-01-0.7914E-03 0.1001E-03
76 -0.1434E-02 0.1711 0.2216E-01-0.8557E-01-0.7233E-03 0.1095E-03
77 -0.1141E-05-0.7248E-05 0.2819 -0.8577E-01-0.9971E-03-0.6374E-04
78 -0.7748E-03 0.8498E-01 0.2163 -0.8576E-01-0.9716E-03 0.7177E-04
79 -0.1298E-02 0.1448 0.1285 -0.8575E-01-0.8764E-03 0.1399E-03
80 -0.1512E-02 0.1715 0.2464E-01-0.8573E-01-0.7690E-03 0.1493E-03
81 -0.1250E-07-0.1645E-04 0.2850 -0.8594E-01-0.8935E-03 0.2113E-04
82 -0.8125E-03 0.8514E-01 0.2192 -0.8593E-01-0.8052E-03 0.1593E-03
83 -0.1363E-02 0.1451 0.1313 -0.8591E-01-0.8318E-03 0.2522E-03
84 -0.1591E-02 0.1718 0.2724E-01-0.8589E-01-0.7812E-03 0.2726E-03

***** POST1 NODAL DISPLACEMENT LISTING *****

LOAD STEP 1 ITERATION= 1 SECTION= 1
TIME= 0.00000 LOAD CASE= 1

THE FOLLOWING X,Y,Z DISPLACEMENTS ARE IN NODAL COORDINATES

NODE UX UY UZ ROTX ROTY ROTZ
85 0.3426E-05-0.1887E-04 0.2882 -0.8510E-01-0.8927E-03 0.1602E-03

```
 86 -0.8497E-03 0.8529E-01 0.2223   -0.8609E-01-0.1473E-02 0.3925E-03
 87 -0.1428E-02 0.1453   0.1342   -0.8609E-01-0.1834E-02 0.9139E-03
 88 -0.1668E-02 0.1721   0.2998E-01-0.8601E-01-0.1229E-02 0.8389E-03
 89  0.9019E-05-0.1026E-05 0.2916   -0.8623E-01-0.9567E-03-0.6209E-04
 90 -0.8862E-03 0.8544E-01 0.2256   -0.8629E-01-0.1727E-02 0.2659E-03
 91 -0.1491E-02 0.1456   0.1373   -0.8616E-01-0.9865E-03 0.7199E-03
 92 -0.1744E-02 0.1724   0.3280E-01-0.8626E-01 0.5281E-03 0.1162E-03
 93  0.8251E-05 0.3780E-04 0.2951   -0.8635E-01-0.1197E-02 0.4802E-03
 94 -0.9152E-03 0.8552E-01 0.2290   -0.8624E-01-0.2103E-02 0.6081E-03
 95 -0.1555E-02 0.1459   0.1404   -0.8695E-01 0.1485E-02-0.1051E-02
 96 -0.1833E-02 0.1728   0.3575E-01-0.8549E-01-0.4080E-02 0.9093E-02

     ***** POST1 NODAL DISPLACEMENT LISTING *****

LOAD STEP    1 ITERATION=    1 SECTION=  1
TIME=  0.00000       LOAD CASE=  1

THE FOLLOWING X,Y,Z DISPLACEMENTS ARE IN NODAL COORDINATES

NODE    UX       UY       UZ       ROTX     ROTY     ROTZ
 97  0.1600E-05 0.4343E-04 0.2986   -0.8676E-01-0.9476E-03 0.5884E-06
 98 -0.9377E-03 0.8575E-01 0.2324   -0.8880E-01-0.9475E-03 0.4544E-06
 99 -0.1599E-02 0.1461   0.1439   -0.8790E-01-0.9473E-03-0.2643E-07
100 -0.1893E-02 0.1730   0.3913E-01-0.1040   -0.9469E-03-0.9950E-07
101  0.4105E-06 0.1363   -0.1725   -0.5966E-01 0.2545E-06-0.1400E-06
102 -0.6052E-07 0.7385E-01-0.3375   -0.7488E-01 0.4199E-06 0.3117E-06
103 -0.1633E-05 0.1145E-05-0.4963   -0.7847E-01 0.2525E-06 0.8813E-06
104 -0.5301E-04 0.1365   -0.1727   -0.8408E-01 0.6142E-02 0.7814E-02
105 -0.1845E-04 0.7431E-01-0.3371   -0.8262E-01 0.2739E-02 0.2078E-02
106 -0.1708E-04 0.8081E-04-0.4967   -0.8438E-01 0.1691E-02-0.3974E-03
107 -0.1082E-03 0.1368   -0.1729   -0.8296E-01 0.3590E-04 0.3608E-02
108 -0.4432E-04 0.7400E-01-0.3386   -0.8302E-01-0.4169E-04 0.2629E-02

     ***** POST1 NODAL DISPLACEMENT LISTING *****

LOAD STEP    1 ITERATION=    1 SECTION=  1
TIME=  0.00000       LOAD CASE=  1

THE FOLLOWING X,Y,Z DISPLACEMENTS ARE IN NODAL COORDINATES

NODE    UX       UY       UZ       ROTX     ROTY     ROTZ
 109  0.1211E-05 0.6931E-04-0.4975   -0.8247E-01-0.6907E-03 0.6106E-03
 110 -0.1729E-03 0.1371   -0.1727   -0.8311E-01 0.5550E-03 0.1316E-02
 111 -0.7552E-04 0.7434E-01-0.3384   -0.8311E-01 0.9901E-03 0.1157E-02
 112  0.4388E-05 0.4588E-04-0.4981   -0.8328E-01 0.6848E-03-0.4932E-03
 113 -0.2345E-03 0.1373   -0.1725   -0.8329E-01 0.2957E-04 0.5057E-03
 114 -0.1083E-03 0.7442E-01-0.3386   -0.8328E-01 0.1907E-03 0.5795E-03
 115  0.2945E-05 0.3405E-04-0.4985   -0.8328E-01-0.5128E-04 0.2282E-03
 116 -0.2987E-03 0.1376   -0.1722   -0.8345E-01-0.5216E-04 0.2193E-03
 117 -0.1429E-03 0.7456E-01-0.3386   -0.8344E-01 0.8841E-04 0.2242E-03
 118  0.1851E-05 0.2615E-04-0.4988   -0.8344E-01 0.1137E-03-0.1347E-04
 119 -0.3638E-03 0.1378   -0.1718   -0.8362E-01-0.1374E-03 0.1229E-03
 120 -0.1784E-03 0.7469E-01-0.3385   -0.8360E-01-0.2461E-04 0.1071E-03

     ***** POST1 NODAL DISPLACEMENT LISTING *****

LOAD STEP    1 ITERATION=    1 SECTION=  1
```

TIME= 0.00000 LOAD CASE= 1

THE FOLLOWING X,Y,Z DISPLACEMENTS ARE IN NODAL COORDINATES

NODE	UX	UY	UZ	ROTX	ROTY	ROTZ
121	0.6841E-06	0.2160E-04	-0.4990	-0.8359E-01	0.2737E-04	0.1387E-04
122	-0.4292E-03	0.1381	-0.1712	-0.8378E-01	-0.1878E-03	0.9022E-04
123	-0.2142E-03	0.7482E-01	-0.3383	-0.8376E-01	-0.8478E-04	0.6258E-04
124	-0.1328E-06	0.1914E-04	-0.4991	-0.8373E-01	-0.5041E-05	0.3202E-05
125	-0.4946E-03	0.1383	-0.1705	-0.8394E-01	-0.2321E-03	0.7927E-04
126	-0.2500E-03	0.7496E-01	-0.3379	-0.8391E-01	-0.1341E-03	0.4766E-04
127	-0.7424E-06	0.1797E-04	-0.4990	-0.8389E-01	-0.4690E-04	0.1786E-05
128	-0.5599E-03	0.1386	-0.1697	-0.8410E-01	-0.2735E-03	0.7555E-04
129	-0.2857E-03	0.7510E-01	-0.3374	-0.8407E-01	-0.1775E-03	0.4253E-04
130	-0.1231E-05	0.1769E-04	-0.4988	-0.8404E-01	-0.8667E-04	0.7756E-06
131	-0.6250E-03	0.1389	-0.1687	-0.8426E-01	-0.3137E-03	0.7419E-04
132	-0.3213E-03	0.7524E-01	-0.3367	-0.8423E-01	-0.2185E-03	0.4078E-04

***** POST1 NODAL DISPLACEMENT LISTING *****

LOAD STEP 1 ITERATION= 1 SECTION= 1
TIME= 0.00000 LOAD CASE= 1

THE FOLLOWING X,Y,Z DISPLACEMENTS ARE IN NODAL COORDINATES

NODE	UX	UY	UZ	ROTX	ROTY	ROTZ
133	-0.1659E-05	0.1812E-04	-0.4984	-0.8420E-01	-0.1264E-03	0.3820E-06
134	-0.6900E-03	0.1391	-0.1676	-0.8442E-01	-0.3532E-03	0.7363E-04
135	-0.3568E-03	0.7538E-01	-0.3359	-0.8439E-01	-0.2584E-03	0.4014E-04
136	-0.2055E-05	0.1918E-04	-0.4979	-0.8436E-01	-0.1660E-03	0.2365E-06
137	-0.7549E-03	0.1394	-0.1663	-0.8458E-01	-0.3923E-03	0.7336E-04
138	-0.3921E-03	0.7553E-01	-0.3350	-0.8455E-01	-0.2978E-03	0.3989E-04
139	-0.2435E-05	0.2080E-04	-0.4973	-0.8452E-01	-0.2054E-03	0.2574E-06
140	-0.8196E-03	0.1397	-0.1650	-0.8474E-01	-0.4312E-03	0.7326E-04
141	-0.4274E-03	0.7567E-01	-0.3339	-0.8470E-01	-0.3369E-03	0.3982E-04
142	-0.2810E-05	0.2298E-04	-0.4965	-0.8467E-01	-0.2448E-03	0.3855E-06
143	-0.8843E-03	0.1399	-0.1635	-0.8489E-01	-0.4698E-03	0.7335E-04
144	-0.4626E-03	0.7581E-01	-0.3328	-0.8486E-01	-0.3758E-03	0.3987E-04

***** POST1 NODAL DISPLACEMENT LISTING *****

LOAD STEP 1 ITERATION= 1 SECTION= 1
TIME= 0.00000 LOAD CASE= 1

THE FOLLOWING X,Y,Z DISPLACEMENTS ARE IN NODAL COORDINATES

NODE	UX	UY	UZ	ROTX	ROTY	ROTZ
145	-0.3190E-05	0.2570E-04	-0.4957	-0.8483E-01	-0.2841E-03	0.5941E-06
146	-0.9490E-03	0.1402	-0.1619	-0.8505E-01	-0.5082E-03	0.7379E-04
147	-0.4978E-03	0.7595E-01	-0.3314	-0.8502E-01	-0.4144E-03	0.4012E-04
148	-0.3577E-05	0.2898E-04	-0.4947	-0.8499E-01	-0.3234E-03	0.8722E-06
149	-0.1014E-02	0.1404	-0.1601	-0.8521E-01	-0.5461E-03	0.7522E-04
150	-0.5330E-03	0.7610E-01	-0.3300	-0.8517E-01	-0.4528E-03	0.4086E-04
151	-0.3965E-05	0.3286E-04	-0.4935	-0.8514E-01	-0.3628E-03	0.1226E-05
152	-0.1078E-02	0.1407	-0.1582	-0.8537E-01	-0.5833E-03	0.7951E-04
153	-0.5683E-03	0.7624E-01	-0.3284	-0.8533E-01	-0.4906E-03	0.4298E-04
154	-0.4324E-05	0.3733E-04	-0.4922	-0.8530E-01	-0.4021E-03	0.1685E-05

155 -0.1143E-02 0.1410 -0.1562 -0.8552E-01-0.6186E-03 0.9233E-04
156 -0.6036E-03 0.7638E-01-0.3267 -0.8548E-01-0.5270E-03 0.4911E-04

***** POST1 NODAL DISPLACEMENT LISTING *****

LOAD STEP 1 ITERATION= 1 SECTION= 1
TIME= 0.00000 LOAD CASE= 1

THE FOLLOWING X,Y,Z DISPLACEMENTS ARE IN NODAL COORDINATES

NODE UX UY UZ ROTX ROTY ROTZ
157 -0.4588E-05 0.4231E-04-0.4908 -0.8545E-01-0.4415E-03 0.2323E-05
158 -0.1209E-02 0.1412 -0.1541 -0.8568E-01-0.6475E-03 0.1286E-03
159 -0.6392E-03 0.7652E-01-0.3249 -0.8563E-01-0.5590E-03 0.6612E-04
160 -0.4638E-05 0.4761E-04-0.4893 -0.8560E-01-0.4809E-03 0.3361E-05
161 -0.1275E-02 0.1415 -0.1518 -0.8584E-01-0.6600E-03 0.2362E-03
162 -0.6754E-03 0.7666E-01-0.3229 -0.8579E-01-0.5799E-03 0.1185E-03
163 -0.4264E-05 0.5270E-04-0.4876 -0.8575E-01-0.5221E-03 0.3852E-05
164 -0.1343E-02 0.1417 -0.1494 -0.8598E-01-0.6383E-03 0.5498E-03
165 -0.7129E-03 0.7681E-01-0.3208 -0.8596E-01-0.5539E-03 0.2543E-03
166 -0.3085E-05 0.5658E-04-0.4858 -0.8591E-01-0.5570E-03 0.1756E-04
167 -0.1412E-02 0.1420 -0.1468 -0.8627E-01 0.1229E-03 0.1113E-02
168 -0.7539E-03 0.7698E-01-0.3185 -0.8612E-01-0.5036E-03 0.7403E-03

***** POST1 NODAL DISPLACEMENT LISTING *****

LOAD STEP 1 ITERATION= 1 SECTION= 1
TIME= 0.00000 LOAD CASE= 1

THE FOLLOWING X,Y,Z DISPLACEMENTS ARE IN NODAL COORDINATES

NODE UX UY UZ ROTX ROTY ROTZ
169 -0.4994E-06 0.5641E-04-0.4839 -0.8607E-01-0.6280E-03-0.3022E-04
170 -0.1483E-02 0.1424 -0.1438 -0.8449E-01-0.2202E-02 0.8340E-02
171 -0.7818E-03 0.7748E-01-0.3153 -0.8615E-01-0.7363E-03 0.2577E-02
172 0.1782E-05 0.3875E-04-0.4817 -0.8660E-01-0.4814E-03-0.1184E-03
173 -0.1559E-02 0.1425 -0.1412 -0.1097 -0.9461E-03 0.1274E-07
174 -0.8446E-03 0.7725E-01-0.3137 -0.9442E-01-0.9461E-03 0.3650E-06
175 -0.1149E-06 0.4381E-04-0.4797 -0.9037E-01-0.9464E-03 0.2743E-06
176 0.3240E-06-0.8199E-01 0.1849 -0.7589E-01-0.1797E-06 0.1829E-06
177 0.1916E-06 0.[illegible]7 0.1002 -0.7287E-01-0.5586E-07 0.2508E-06
178 -0.1525E-06-0.1654 0.2653E-06-0.4791E-01 0.1620E-06 0.2933E-06
179 0.6537E-04-0.8227E-01 0.1852 -0.8329E-01-0.8238E-03-0.8916E-03
180 0.9284E-04-0.1400 0.1004 -0.8350E-01-0.9032E-03-0.2492E-02

***** POST1 NODAL DISPLACEMENT LISTING *****

LOAD STEP 1 ITERATION= 1 SECTION= 1
TIME= 0.00000 LOAD CASE= 1

THE FO[illegible]OWING X,Y,Z DISPLACEMENTS ARE IN NODAL COORDINATES

NODE UX UY UZ ROTX ROTY ROTZ
181 0.1018E-03-0.1659 -0.3114E-03-0.8462E-01 0.1070E-02-0.3890E-02
182 0.1133E-03-0.8239E-01 0.1858 -0.8314E-01-0.2151E-03-0.4507E-04
183 0.1698E-03-0.1403 0.1007 -0.8300E-01-0.1638E-03-0.2147E-04
184 0.1834E-03-0.1661 0.2506E-03-0.8280E-01-0.3647E-03-0.1335E-03

185 0.1559E-03-0.8255E-01 0.1866 -0.8329E-01-0.2526E-03-0.5205E-04
186 0.2425E-03-0.1406 0.1013 -0.8317E-01-0.2132E-03-0.1017E-03
187 0.2593E-03-0.1664 0.7082E-03-0.8301E-01-0.1247E-03-0.1559E-03
188 0.1965E-03-0.8269E-01 0.1875 -0.8342E-01-0.2907E-03-0.4630E-04
189 0.3095E-03-0.1408 0.1021 -0.8332E-01-0.2480E-03-0.7179E-04
190 0.3349E-03-0.1667 0.1248E-02-0.8324E-01-0.1838E-03-0.8376E-04
191 0.2354E-03-0.8282E-01 0.1885 -0.8355E-01-0.3271E-03-0.4274E-04
192 0.3743E-03-0.1411 0.1030 -0.8349E-01-0.2795E-03-0.7275E-04

***** POST1 NODAL DISPLACEMENT LISTING *****

LOAD STEP 1 ITERATION= 1 SECTION= 1
TIME= 0.00000 LOAD CASE= 1

THE FOLLOWING X,Y,Z DISPLACEMENTS ARE IN NODAL COORDINATES

NODE UX UY UZ ROTX ROTY ROTZ
193 0.4120E-03-0.1670 0.1892E-02-0.8344E-01-0.2122E-03-0.8890E-04
194 0.2735E-03-0.8296E-01 0.1896 -0.8370E-01-0.3628E-03-0.4235E-04
195 0.4390E-03-0.1413 0.1040 -0.8366E-01-0.3138E-03-0.7360E-04
196 0.4900E-03-0.1673 0.2660E-02-0.8363E-01-0.2504E-03-0.8878E-04
197 0.3115E-03-0.8310E-01 0.1909 -0.8385E-01-0.3995E-03-0.4284E-04
198 0.5042E-03-0.1416 0.1051 -0.8383E-01-0.3502E-03-0.7496E-04
199 0.5684E-03-0.1676 0.3559E-02-0.8381E-01-0.2894E-03-0.9007E-04
200 0.3497E-03-0.8325E-01 0.1923 -0.8401E-01-0.4373E-03-0.4361E-04
201 0.5698E-03-0.1418 0.1063 -0.8399E-01-0.3880E-03-0.7606E-04
202 0.6472E-03-0.1680 0.4590E-02-0.8397E-01-0.3291E-03-0.9094E-04
203 0.3881E-03-0.8340E-01 0.1938 -0.8417E-01-0.4758E-03-0.4433E-04
204 0.6359E-03-0.1421 0.1077 -0.8415E-01-0.4267E-03-0.7684E-04

***** POST1 NODAL DISPLACEMENT LISTING *****

LOAD STEP 1 ITERATION= 1 SECTION= 1
TIME= 0.00000 LOAD CASE= 1

THE FOLLOWING X,Y,Z DISPLACEMENTS ARE IN NODAL COORDINATES

NODE UX UY UZ ROTX ROTY ROTZ
205 0.7262E-03-0.1683 0.5754E-02-0.8414E-01-0.3690E-03-0.9156E-04
206 0.4267E-03-0.8355E-01 0.1955 -0.8433E-01-0.5149E-03-0.4491E-04
207 0.7023E-03-0.1424 0.1092 -0.8431E-01-0.4660E-03-0.7735E-04
208 0.8053E-03-0.1686 0.7051E-02-0.8430E-01-0.4090E-03-0.9197E-04
209 0.4655E-03-0.8371E-01 0.1973 -0.8449E-01-0.5543E-03-0.4538E-04
210 0.7689E-03-0.1426 0.1108 -0.8447E-01-0.5057E-03-0.7767E-04
211 0.8845E-03-0.1689 0.8481E-02-0.8445E-01-0.4491E-03-0.9222E-04
212 0.5044E-03-0.8386E-01 0.1992 -0.8464E-01-0.5939E-03-0.4576E-04
213 0.8357E-03-0.1429 0.1125 -0.8463E-01-0.5455E-03-0.7786E-04
214 0.9638E-03-0.1692 0.1005E-01-0.8461E-01-0.4892E-03-0.9234E-04
215 0.5433E-03-0.8402E-01 0.2012 -0.8480E-01-0.6337E-03-0.4606E-04
216 0.9025E-03-0.1431 0.1144 -0.8478E-01-0.5855E-03-0.7793E-04

***** POST1 NODAL DISPLACEMENT LISTING *****

LOAD STEP 1 ITERATION= 1 SECTION= 1
TIME= 0.00000 LOAD CASE= 1

THE FOLLOWING X,Y,Z DISPLACEMENTS ARE IN NODAL COORDINATES

NODE	UX	UY	UZ	ROTX	ROTY	ROTZ
217	0.1043E-02	-0.1695	0.1174E-01	-0.8477E-01	-0.5293E-03	-0.9234E-04
218	0.5822E-03	-0.8417E-01	0.2034	-0.8496E-01	-0.6735E-03	-0.4628E-04
219	0.9694E-03	-0.1434	0.1164	-0.8494E-01	-0.6257E-03	-0.7790E-04
220	0.1122E-02	-0.1698	0.1357E-01	-0.8493E-01	-0.5695E-03	-0.9223E-04
221	0.6212E-03	-0.8433E-01	0.2057	-0.8511E-01	-0.7135E-03	-0.4641E-04
222	0.1036E-02	-0.1437	0.1186	-0.8510E-01	-0.6659E-03	-0.7776E-04
223	0.1202E-02	-0.1701	0.1554E-01	-0.8508E-01	-0.6096E-03	-0.9199E-04
224	0.6602E-03	-0.8449E-01	0.2082	-0.8527E-01	-0.7534E-03	-0.4641E-04
225	0.1103E-02	-0.1439	0.1209	-0.8525E-01	-0.7061E-03	-0.7742E-04
226	0.1281E-02	-0.1705	0.1764E-01	-0.8524E-01	-0.6496E-03	-0.9162E-04
227	0.6992E-03	-0.8464E-01	0.2108	-0.8542E-01	-0.7944E-03	-0.4662E-04
228	0.1170E-02	-0.1442	0.1233	-0.8541E-01	-0.7468E-03	-0.7718E-04

***** POST1 NODAL DISPLACEMENT LISTING *****

LOAD STEP 1 ITERATION= 1 SECTION= 1
TIME= 0.00000 LOAD CASE= 1

THE FOLLOWING X,Y,Z DISPLACEMENTS ARE IN NODAL COORDINATES

NODE	UX	UY	UZ	ROTX	ROTY	ROTZ
229	0.1361E-02	-0.1708	0.1987E-01	-0.8540E-01	-0.6896E-03	-0.9133E-04
230	0.7381E-03	-0.8480E-01	0.2135	-0.8557E-01	-0.8305E-03	-0.4507E-04
231	0.1237E-02	-0.1445	0.1259	-0.8556E-01	-0.7847E-03	-0.7546E-04
232	0.1440E-02	-0.1711	0.2224E-01	-0.8556E-01	-0.7284E-03	-0.9046E-04
233	0.7765E-03	-0.8496E-01	0.2163	-0.8571E-01	-0.8870E-03	-0.5491E-04
234	0.1303E-02	-0.1447	0.1286	-0.8572E-01	-0.8360E-03	-0.8137E-04
235	0.1519E-02	-0.1714	0.2473E-01	-0.8573E-01	-0.7731E-03	-0.9701E-04
236	0.8141E-03	-0.8512E-01	0.2193	-0.8586E-01	-0.8836E-03	-0.5124E-04
237	0.1368E-02	-0.1450	0.1314	-0.8587E-01	-0.8260E-03	-0.6253E-04
238	0.1598E-02	-0.1717	0.2737E-01	-0.8591E-01	-0.7836E-03	-0.6628E-04
239	0.8512E-03	-0.8530E-01	0.2224	-0.8601E-01	-0.1085E-02	-0.1141E-03
240	0.1431E-02	-0.1453	0.1343	-0.8597E-01	-0.1064E-02	-0.1831E-03

***** POST1 NODAL DISPLACEMENT LISTING *****

LOAD STEP 1 ITERATION= 1 SECTION= 1
TIME= 0.00000 LOAD CASE= 1

THE FOLLOWING X,Y,Z DISPLACEMENTS ARE IN NODAL COORDINATES

NODE	UX	UY	UZ	ROTX	ROTY	ROTZ
241	0.1677E-02	-0.1720	0.3014E-01	-0.8593E-01	-0.9888E-03	-0.3213E-03
242	0.8882E-03	-0.8548E-01	0.2255	-0.8630E-01	-0.9774E-03	-0.2885E-03
243	0.1486E-02	-0.1456	0.1373	-0.8614E-01	-0.5754E-03	-0.2268E-03
244	0.1757E-02	-0.1723	0.3306E-01	-0.8710E-01	-0.3391E-03	0.9434E-03
245	0.9283E-03	-0.8566E-01	0.2289	-0.8598E-01	-0.2814E-02	-0.1298E-02
246	0.1563E-02	-0.1460	0.1403	-0.8540E-01	-0.4198E-02	-0.4295E-02
247	0.1827E-02	-0.1727	0.3641E-01	-0.7997E-01	-0.2706E-02	-0.6971E-02
248	0.9401E-03	-0.8566E-01	0.2324	-0.9340E-01	-0.9474E-03	0.6722E-06
249	0.1600E-02	-0.1460	0.1439	-0.9656E-01	-0.9466E-03	0.9592E-06
250	0.1894E-02	-0.1729	0.3913E-01	-0.1226	-0.9467E-03	0.4926E-06
251	-0.3625E-06	-0.1363	-0.1725	-0.4332E-01	0.2258E-06	0.1503E-06
252	-0.7122E-06	-0.7385E-01	-0.3375	-0.6374E-01	0.3074E-06	0.3940E-06

***** POST1 NODAL DISPLACEMENT LISTING *****

LOAD STEP 1 ITERATION= 1 SECTION= 1
TIME= 0.00000 LOAD CASE= 1

THE FOLLOWING X,Y,Z DISPLACEMENTS ARE IN NODAL COORDINATES

NODE	UX	UY	UZ	ROTX	ROTY	ROTZ
253	0.6955E-04	-0.1370	-0.1714	-0.8863E-01	0.2908E-02	-0.4036E-02
254	0.9713E-05	-0.7479E-01	-0.3357	-0.8870E-01	0.2344E-02	-0.1802E-02
255	0.9650E-04	-0.1370	-0.1722	-0.8215E-01	-0.2142E-03	-0.7699E-03
256	0.3763E-04	-0.7413E-01	-0.3380	-0.8196E-01	0.3014E-03	-0.8906E-03
257	0.1603E-03	-0.1372	-0.1723	-0.8305E-01	0.1546E-03	-0.1641E-03
258	0.6870E-04	-0.7437E-01	-0.3381	-0.8351E-01	0.2934E-03	-0.4028E-03
259	0.2250E-03	-0.1374	-0.1723	-0.8324E-01	-0.4686E-04	-0.7246E-04
260	0.1034E-03	-0.7444E-01	-0.3384	-0.8335E-01	0.8070E-04	-0.5995E-04
261	0.2919E-03	-0.1376	-0.1721	-0.8344E-01	-0.8589E-04	-0.6043E-04
262	0.1389E-03	-0.7455E-01	-0.3385	-0.8350E-01	0.1094E-04	-0.4276E-04
263	0.3589E-03	-0.1378	-0.1717	-0.8362E-01	-0.1380E-03	-0.6539E-04
264	0.1752E-03	-0.7467E-01	-0.3385	-0.8363E-01	-0.4341E-04	-0.3166E-04

***** POST1 NODAL DISPLACEMENT LISTING *****

LOAD STEP 1 ITERATION= 1 SECTION= 1
TIME= 0.00000 LOAD CASE= 1

THE FOLLOWING X,Y,Z DISPLACEMENTS ARE IN NODAL COORDINATES

NODE	UX	UY	UZ	ROTX	ROTY	ROTZ
265	0.4256E-03	-0.1381	-0.1712	-0.8379E-01	-0.1837E-03	-0.6974E-04
266	0.2113E-03	-0.7479E-01	-0.3382	-0.8377E-01	-0.9073E-04	-0.3551E-04
267	0.4919E-03	-0.1383	-0.1705	-0.8395E-01	-0.2275E-03	-0.7280E-04
268	0.2473E-03	-0.7493E-01	-0.3379	-0.8392E-01	-0.1344E-03	-0.3786E-04
269	0.5578E-03	-0.1386	-0.1697	-0.8411E-01	-0.2698E-03	-0.7448E-04
270	0.2831E-03	-0.7507E-01	-0.3374	-0.8407E-01	-0.1765E-03	-0.3951E-04
271	0.6235E-03	-0.1388	-0.1687	-0.8427E-01	-0.3110E-03	-0.7530E-04
272	0.3186E-03	-0.7520E-01	-0.3367	-0.8423E-01	-0.2174E-03	-0.4032E-04
273	0.6890E-03	-0.1391	-0.1676	-0.8442E-01	-0.3515E-03	-0.7559E-04
274	0.3540E-03	-0.7534E-01	-0.3359	-0.8439E-01	-0.2575E-03	-0.4060E-04
275	0.7543E-03	-0.1394	-0.1663	-0.8458E-01	-0.3916E-03	-0.7557E-04
276	0.3892E-03	-0.7548E-01	-0.3350	-0.8455E-01	-0.2972E-03	-0.4056E-04

***** POST1 NODAL DISPLACEMENT LISTING *****

LOAD STEP 1 ITERATION= 1 SECTION= 1
TIME= 0.00000 LOAD CASE= 1

THE FOLLOWING X,Y,Z DISPLACEMENTS ARE IN NODAL COORDINATES

NODE	UX	UY	UZ	ROTX	ROTY	ROTZ
277	0.8196E-03	-0.1396	-0.1650	-0.8474E-01	-0.4314E-03	-0.7539E-04
278	0.4244E-03	-0.7562E-01	-0.3339	-0.8470E-01	-0.3366E-03	-0.4032E-04
279	0.8847E-03	-0.1399	-0.1635	-0.8490E-01	-0.4709E-03	-0.7510E-04
280	0.4595E-03	-0.7576E-01	-0.3328	-0.8486E-01	-0.3758E-03	-0.3996E-04
281	0.9499E-03	-0.1401	-0.1618	-0.8506E-01	-0.5103E-03	-0.7477E-04
282	0.4946E-03	-0.7590E-01	-0.3314	-0.8502E-01	-0.4147E-03	-0.3951E-04
283	0.1015E-02	-0.1404	-0.1601	-0.8522E-01	-0.5494E-03	-0.7443E-04
284	0.5297E-03	-0.7603E-01	-0.3300	-0.8518E-01	-0.4536E-03	-0.3902E-04
285	0.1080E-02	-0.1406	-0.1582	-0.8538E-01	-0.5884E-03	-0.7423E-04

286 0.5647E-03-0.7617E-01-0.3284 -0.8534E-01-0.4924E-03-0.3857E-04
287 0.1145E-02-0.1409 -0.1562 -0.8554E-01-0.6273E-03-0.7438E-04
288 0.6000E-03-0.7630E-01-0.3267 -0.8550E-01-0.5312E-03-0.3843E-04

***** POST1 NODAL DISPLACEMENT LISTING *****

LOAD STEP 1 ITERATION= 1 SECTION= 1
TIME= 0.00000 LOAD CASE= 1

THE FOLLOWING X,Y,Z DISPLACEMENTS ARE IN NODAL COORDINATES

NODE UX UY UZ ROTX ROTY ROTZ
289 0.1210E-02-0.1411 -0.1540 -0.8571E-01-0.6650E-03-0.7816E-04
290 0.6354E-03-0.7644E-01-0.3249 -0.8565E-01-0.5700E-03-0.3984E-04
291 0.1276E-02-0.1414 -0.1517 -0.8587E-01-0.7005E-03-0.8176E-04
292 0.6713E-03-0.7657E-01-0.3229 -0.8581E-01-0.6080E-03-0.4673E-04
293 0.1341E-02-0.1417 -0.1493 -0.8600E-01-0.7395E-03-0.1918E-03
294 0.7079E-03-0.7670E-01-0.3208 -0.8598E-01-0.6324E-03-0.8570E-04
295 0.1409E-02-0.1419 -0.1468 -0.8665E-01-0.5437E-03 0.2074E-04
296 0.7463E-03-0.7686E-01-0.3185 -0.8612E-01-0.6250E-03-0.2036E-03
297 0.1474E-02-0.1422 -0.1440 -0.8189E-01-0.1004E-02-0.3559E-02
298 0.7778E-03-0.7702E-01-0.3161 -0.8481E-01-0.6506E-03-0.9445E-03
299 0.1559E-02-0.1424 -0.1412 -0.1262 -0.9464E-03-0.1304E-06
300 0.8449E-03-0.7716E-01-0.3137 -0.1056 -0.9461E-03-0.1230E-06

***** POST1 NODAL DISPLACEMENT LISTING *****

LOAD STEP 1 ITERATION= 1 SECTION= 1
TIME= 0.00000 LOAD CASE= 1

THE FOLLOWING X,Y,Z DISPLACEMENTS ARE IN NODAL COORDINATES

NODE UX UY UZ ROTX ROTY ROTZ
301 0.1193E-05 0.4347E-04 0.2324 -0.9610E-01-0.9475E-03 0.5418E-06
302 0.7784E-06 0.4367E-04 0.1439 0.1118 -0.9471E-03 0.4921E-06
303 0.3327E-06 0.4374E-04 0.3913E-01-0.1697 -0.9470E-03 0.3550E-06
304 0.1994E-06 0.4378E-04-0.1412 -0.1215 -0.9462E-03 0.3686E-06
305 0.1605E-06 0.4377E-04-0.3137 -0.1031 -0.9462E-03 0.2380E-06
306 0.1155E-06-0.1835E-06 0.1849 -0.7325E-01-0.2278E-06 0.1110E-06
307 0.3081E-07-0.8591E-07 0.1002 -0.5778E-01-0.1545E-06 0.5496E-07
308 0.0000 0.0000 0.0000 0.0000 0.0000 0.0000
309 0.2274E-08 0.3168E-06-0.1725 -0.4793E-01 0.2268E-06 0.7406E-07
310 -0.4158E-06 0.7867E-06-0.3375 -0.6611E-01 0.3620E-06 0.3978E-06

MAXIMUMS
NODE 250 100 124 303 104 8
VALUE 0.1894E-02 0.1730 -0.4991 -0.1697 0.6142E-02 0.1229E-01